Large-Deviation Theory Approach to Systems with Orientational Order: Results for Two and Three Dimensional Liquid Crystals

By

Eleftherios Mainas

B.S., Chemistry, University of Athens, Greece, 2017

M.A., Chemistry, Brown University, U.S.A., 2019

Submitted in partial fulfillment of the requirements for the Degree of Doctor of Philosophy in the Department of Chemistry at Brown University

PROVIDENCE, RHODE ISLAND

October 2023

This dissertation by Eleftherios Mainas is accepted in its present form by the Department of Chemistry as satisfying the dissertation requirement for the degree of Doctor of Philosophy.

Date _____ _____

Richard Stratt, Advisor

Recommended to the Graduate Council

Date _____ _____

Brenda Rubenstein, Reader

Date _____ _____

Brad Marston, Reader

Approved by the Graduate Council

Date _____ _____

Thomas A. Lewis, Dean of the Graduate School

Curriculum Vitae

Education

2018–2023 Ph.D., Chemistry
Brown University (Providence, RI, USA)

2018-2019
M.A., Chemistry
Brown University (Providence, RI, USA)

2013–2017
B.Sc., Chemistry
National and Kapodistrian University of Athens (Athens, Greece)

Publications

Mainas, E. and Stratt, R. (2023). Exceptionally large fluctuations in orientational order: The lessons of large-deviation theory for liquid crystalline systems. (Manuscript under preparation).

Mainas, E., *et al.* (2020). Coating of magnetic nanoparticles affects their interactions with model cell membranes. Biochimica et Biophysica Acta (BBA) - General Subjects, Volume 1864, Issue 11, November 2020.

Teaching

September 2019–May 2023

Teaching Assistant, *Chemistry*, (Brown University, Providence, Rhode Island, U.S.A.) Courses: "Physical Chemistry: Quantum Chemistry", "Physical Chemistry: Thermodynamics and Statistical Mechanics", "Equilibrium, Rate, and Structure Lab"

Awards and Fellowships

AHEPA Mavroyannis Scholar for the 2022-2023 academic year

Acknowledgments

In September 2018, I moved to Providence with the goal of pursuing a Ph.D. at Brown University. After a span of five years, filled with numerous ideas, equations, and lines of computer code, this wonderful journey has now reached its conclusion. Brown University's environment could not have been more welcoming and intellectually stimulating, and I could not have made a better decision in choosing my supervisor, Richard Stratt. A true master of his craft, Professor Stratt shaped my scientific thinking and showed me how to effectively communicate complex ideas. His belief in my abilities never wavered, even when I doubted myself, and he consistently encouraged me to develop and present my own derivations, calculations, and ideas. Without his guidance, I would not have been equipped to solve the challenging problems presented in this thesis. After all, there is no Edmond Dantès without Abbe Faria, and no D'Artagnan without Athos. I am also deeply grateful for the guidance and support provided by my committee members, Brenda Rubenstein and Brad Marston. Professor Rubenstein's expertise in simulations, and Professor Marston's insights into classical physics, have been indispensable to my research. Additionally, their mentorship has been instrumental in helping me navigate the various phases of my Ph.D. milestones. Lastly, I would like to acknowledge Yichen Chai and Dawei Si for their friendship and kind help with various research-related issues.

Contents

List of Figures

List of Tables

Abstract of "Large-Deviation Theory Approach to Systems with Orientational Order: Results for Two and Three Dimensional Liquid Crystals", by Eleftherios Mainas, Ph.D., Brown University, August 2023

Problems like describing the extent of order in isotropic liquid crystals, the extend of magnetization in magnetic systems and finding polymer end-to-end distances, can be described in terms of the probability distributions of collective molecular orientations. However, standard statistical mechanical methods for evaluating these distributions fail when large fluctuations become important, as they do close to the isotropic/nematic transition. Moreover, it is even difficult to extract quantitative details on large fluctuation behavior from simulations because of numerical noise. Using **large-deviation theory**, we described an approach to computing expressions for these probability distributions that can make use of simulation information to accurately compute even the large fluctuation limit of these distributions. Large-deviation theory can be shown to connect the applied field/orientational-order parameter equation of state to the desired probability distribution. The key is to think about the limiting extremes of the system's response to an applied field. When the field is weak, the central-limit theorem applies, but in the presence of a strong field, individual rotors feel a mean-field from the rest of the system. We show that simple Pade' interpolation between these limits generates a form for the equation of state that leads to a way of generating accurate orientational probability distributions from simulation.

"What I cannot create I do not understand"

—Richard Feynman

CHAPTER 1

Introduction

1.1 Liquid crystals and the Isotropic/Nematic phase transition

Nature is much more diverse and interesting than the simple trichotomy "gas-liquid-solid" that is presented in high school chemistry. For example, there is a plethora of intermediate states of matter that lie between the perfect solid crystal and the isotropic liquid [23, Chapter 1]. These states of matter are given the, perhaps peculiar, name "liquid crystals", since they flow like ordinary liquids but have optical properties similar to crystals. Many anisotropic organic molecules (See figure 1.1), minerals and even viruses that possess anisotropic shapes (in the sense that they are not spherical) have the ability to form liquid crystals states of matter [50, Chapter 1].

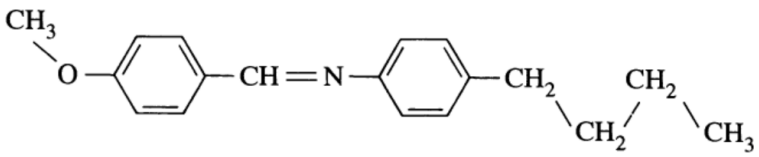

Figure 1.1: N-(p-methoxybenzylidene)-p-butylaniline (MBBA) forms the nematic liquid crystal phase. It was synthesized in 1969 [34] and is nematic from 20^o to 47^o at atmospheric pressure. Figure is taken from [23, p. 3].

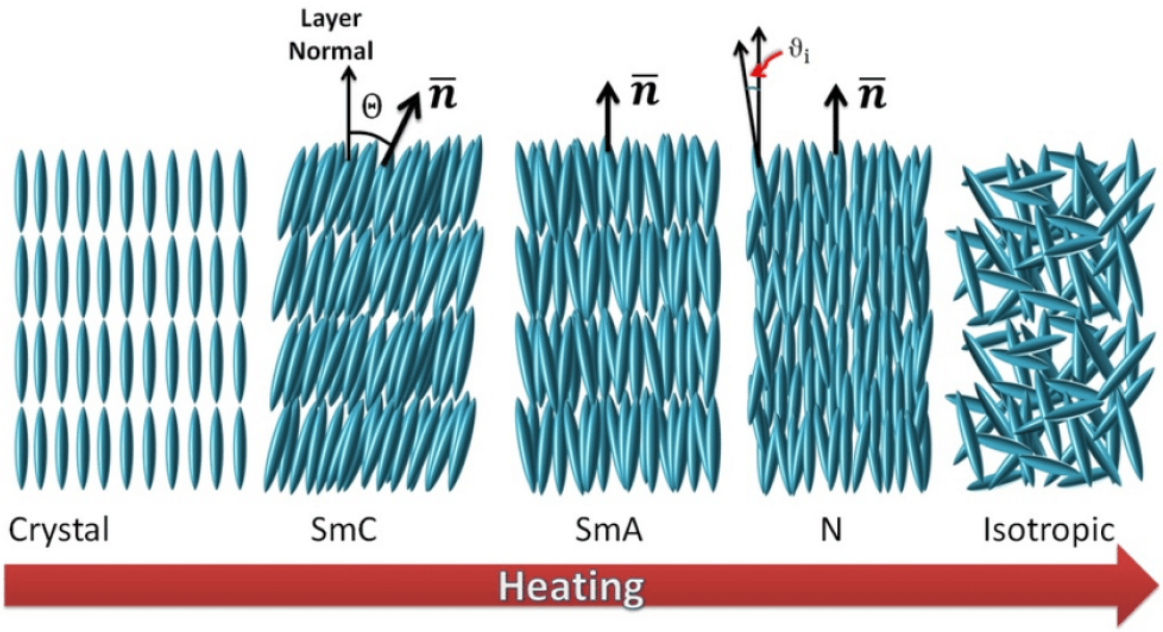

Figure 1.2: Figure is taken from [14].

In figure 1.2 we can see a variety of phases that one would stumble upon heating a perfect solid crystal of ellipsoidal molecules. There are the so-called smectic phases, where there is long orientational order and at the same time, the molecules form layers (long translational order between center-of-masses of the molecules). Then there is the nematic phase where there is only long orientational order, and finally the isotropic liquid with no translational or orientational order. In this study we shall focus on the isotropic phase and the nematic phase and we shall investigate how a system of perfect disorder behaves as it approaches the neighboring nematic phase.

A vast number of experiments has been conducted in order to study the pre-transitional behavior of isotropic liquid crystals close to the isotropic/nematic coexistence line (See for example [43], [42], [57], [44], [58], [53], [54], [8], [56], [55]). It has been experimentally observed that there is a very slow orientational relaxation next to the I/N transition in the isotropic phase. This slow relaxation is attributed to the formation of nematic droplets inside the isotropic phase [56] which are known as pseudo-nematic domains and have a correlation length ξ that is very large. The Landau-De Gennes theory [12] gives the

temperature dependence of ξ,

$$\xi(T) = \xi_0 \left(\frac{T^*}{T - T^*} \right)^{1/2} \tag{1.1}$$

where ξ_0 is a molecular scale and T^* is the critical temperature that is actually bellow the isotropic/nematic transition temperature T_{NI} so the system never gets to T^* because it transitions to the nematic phase first. A cartoon picture of the domains can be seen in figure 1.3.

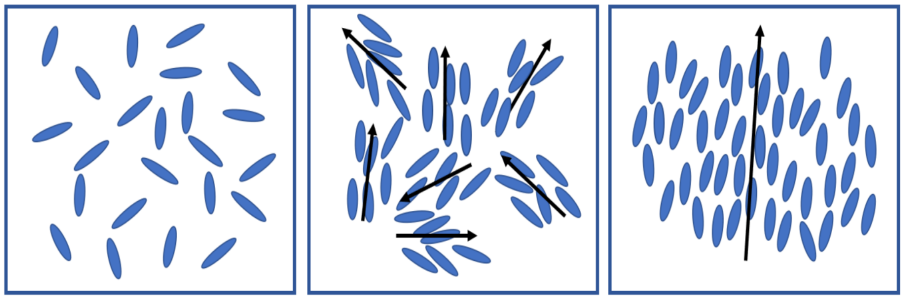

Figure 1.3: In the middle we can see the formation of domains, right before the system transitions to the nematic phase.

Locally the system has nematic ordering (pseudo-nematic domains) but globally the orientations of the domains cancel each other out giving macroscopically isotropic order.

1.2 Orientational order parameter

We describe the transition between phases with different orientational symmetry via an orientational order parameter. This way we can differentiate between an isotropic and a nematic phase. The order parameter of choice needs to mark a clear difference between a probability distribution along $\pm\hat{n}$ and some other random macroscopic direction. The two pieces of information needed to specify nematic ordering is the extend of ordering and the director and can be defined simultaneously in terms of a real, symmetric and traceless

second-rank tensor $\mathcal{Q}$ [12],

$$\mathcal{Q} = \frac{1}{N}\sum_{j=1}^{N}\frac{1}{D-1}(D\,\hat{\Omega}_j\hat{\Omega}_j - \mathbf{1}) \tag{1.2}$$

with N the number of molecules, D the dimensionality of the system and $\mathbf{1}$ the unit matrix. The object $\hat{\Omega}_j\hat{\Omega}_j$ is called a dyadic product and is used in order to build the second-rank tensor $\mathcal{Q}$ from the molecular orientations. For two vectors $\hat{a} = (a_x, a_y)$ and $\hat{b} = (b_x, b_y)$ the dyadic product is defined as,

$$(\hat{a}\hat{b})_{\mu\nu} = a_\mu b_\nu, \quad \hat{a}\hat{b} = \begin{pmatrix} a_x b_x & a_x b_y \\ a_y b_x & a_y b_y \end{pmatrix} \tag{1.3}$$

The molecular orientation vector $\hat{\Omega}_j$ is the unit vector that goes through the long axis of the anisotropic molecule (See figure 1.4),

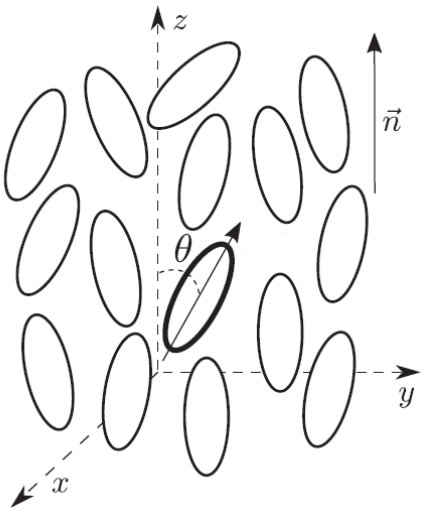

Figure 1.4: Definition of the angle θ for a system of anisotropic molecules. The image is taken from [2]

We define the angle θ_j of some molecule as,

$$\cos\theta_j = \hat{\Omega}_j \cdot \hat{z} \tag{1.4}$$

where $\hat{z}$ is some arbitrary macroscopic axis. The definition of the angle θ_j does not depend on the choice of the axis. In other words if we rotate all the orientations $\hat{\Omega}_j$ around some arbitrary angle, the tensor $\mathcal{Q}$ will not be affected. In a simulation we usually choose $\hat{z}$ to be some edge of the simulation box. The definition of $\mathcal{Q}$ in equation 1.2 is very useful for computer simulations and we can sum up all the important properties of the tensor,

$$\mathcal{Q} = \mathcal{Q}^T \tag{1.5}$$

$$Tr\mathcal{Q} = \frac{1}{N}\sum_{j}^{N}(D\,Tr(\hat{\Omega}_j\hat{\Omega}_j) - Tr(\mathbf{1})) = \frac{1}{N}\sum_{j}^{N}(D(1) - D) = 0 \tag{1.6}$$

Property 1.5 guarantees that the tensor can always be written in a diagonal form while property 1.6 ensures that the average order will be zero for a macroscopically isotropic phase (We used $Tr(\hat{a}\hat{b}) = Tr(\hat{a}\cdot\hat{b})$). The definition of $\mathcal{Q}$ is suitable for computer simulations of liquid crystal models (See for example [41] and [18]) because the director $\hat{n}$ is not known beforehand. Also, it is important to mention that $\mathcal{Q}$ measures the orientational ordering of the entire system of N molecules; it is a global measure and is defined for each configuration of a computer simulation. Direct diagonalization of the tensor for each configuration gives us the (instantaneous) largest eigenvalue s (the scalar order parameter) with the corresponding eigenvector $\hat{n}$,

$$\mathcal{Q}\hat{n} = s\hat{n} \tag{1.7}$$

$$s = \frac{1}{N}\sum_{j=1}^{N}\frac{D\left(\hat{\Omega}_j\cdot\hat{n}\right)^2 - 1}{D-1} = \frac{1}{N}\sum_{j=1}^{N}\frac{D\cos^2\theta_j - 1}{D-1}, \quad 0 \le s \le 1 \tag{1.8}$$

It is convenient to use s because it is a scalar quantity and we can utilize it to quantify the extend of nematic order in some liquid crystal simulation. For a perfectly isotropic system the average value $\langle\cos^2\theta_j\rangle = D^{-1}$ and $\langle s\rangle = 0$. For a perfectly ordered system we have $\langle\cos^2\theta_j\rangle = 1$ and $\langle s\rangle = 1$. A macroscopic sample of liquid crystal molecules in the isotropic phase will obviously have zero order $\langle s\rangle = 0$ (as will $\langle\mathcal{Q}\rangle = 0$) and

the probability distribution $p(s)$ will be a delta function (as will $P(\mathcal{Q})$). In computer simulations however, we study finite systems and $p(s)$ is not trivial anymore. We expect the probability distribution to fluctuate and these fluctuations are exactly what we wish to study. More specifically we will look at the N dependence of $p(s)$ in the isotropic phase close to the I/N transition.

1.3 Probability distribution fluctuations

The fundamental distinction between thermodynamic variables is extensive-intensive [7, Chapter 2]. Extensive variables depend on the number of molecules N of the system and intensive variables do not. The nematic order parameter $N\mathcal{Q}$ is an extensive property and its probability distribution will also depend on the size of the system. For a finite sample of isotropic liquid crystal molecules there is a non-trivial probability distribution (We start from the probability density of the tensor and in later chapters we will show the connection with $p(s)$),

$$P(\mathcal{Q}), \int P(\mathcal{Q}) d\mathcal{Q} = 1 \tag{1.9}$$

that fluctuates. It is precisely these fluctuations that we wish to study as they contain important molecular information. Especially in computer "experiments" we are able to simulate small numbers of molecules efficiently and calculate $P(\mathcal{Q})$ for different N values. This way, we can numerically probe the fluctuations of the highly non-trivial $P(\mathcal{Q})$ in order to quantify nematic order inside an intrinsically isotropic medium.

The study of fluctuations can be traced back to Einstein [17] where he studied thermal fluctuations in the context of Brownian motion. In the context of liquid crystals, we may express the probability of observing a fluctuation as a function of the excess free energy of domain formation $\Delta F(\mathcal{Q}) = F(\mathcal{Q}) - F_0$,

$$P(\mathcal{Q}) \sim \exp\left(-\beta \Delta F(\mathcal{Q})\right) \tag{1.10}$$

where $\beta = 1/(k_B T)$ and F_0 a constant. In the vicinity of the critical point $\Delta F(\mathcal{Q})$ becomes flat and the probability of observing high $\mathcal{Q}$ fluctuations increases. Before we proceed to the Landau-de Gennes answer for $\Delta F(\mathcal{Q})$ we need mention some important mathematical facts about $\Delta F(\mathcal{Q})$.

The free energy $\Delta F(\mathcal{Q})$ will not depend on the choice of the axis and so it will only be a function of the so-called "absolute rotational invariants (ARI's)" of the tensor $\mathcal{Q}$ [25]. These objects are invariant with respect to similarity transformations $\mathcal{R}$,

$$\mathcal{Q} \to \mathcal{R}^T \mathcal{Q} \mathcal{R} \tag{1.11}$$

and are thus functions of

$$Tr((\mathcal{R}^T \mathcal{Q} \mathcal{R})^n) = Tr(\mathcal{Q}^n), \quad n = 1, 2, 3... \tag{1.12}$$

However, all traces of power n can be expressed as polynomials of the first three [29, p. 194], which means that for $D = 3$ the only ARI's are,

$$Tr(\mathcal{Q}^2), \quad Tr(\mathcal{Q}^3) \tag{1.13}$$

In the case of $D = 2$ the only ARI is $Tr(\mathcal{Q}^2)$. The traditional approach to $F(\mathcal{Q})$ has to do with the Landau-De Gennes theory of the isotropic/nematic phase transition. It is a phenomenological picture that assumes an analytic $F(\mathcal{Q})$. For three-dimensional liquid crystals the theory [12] is based on a power series expansion of the free energy in powers of the traces,

$$F(\mathcal{Q}) = F_0 + \frac{1}{2} A(T)\, Tr(\mathcal{Q}^2) + B(T) \frac{1}{3}\, Tr(\mathcal{Q}^3) + C(T) \frac{1}{4}\, Tr(\mathcal{Q}^2)^2 + ... \tag{1.14}$$

where there is no external field term and $Tr(\mathcal{Q}) = 0$ from the definition of $\mathcal{Q}$ (See property in 1.6). For small values of $Tr(\mathcal{Q}^2)$ and when $Tr(\mathcal{Q}^2) >> Tr(\mathcal{Q}^3)$ (this makes sense as

$Tr(\mathcal{Q}^3)$ corresponds to fluctuations perpendicular to the director and they are small as we will see in the discussion section) the conventional Landau approach to the isotropic phase predicts,

$$F(\mathcal{Q}) \approx F_0 + \frac{1}{2}A(T)Tr(\mathcal{Q}^2) \tag{1.15}$$

$$P(\mathcal{Q}) \sim \exp\left(-\frac{1}{2}\beta A(T)\, Tr(\mathcal{Q}^2)\right) \tag{1.16}$$

a gaussian profile of the probability distribution [12]. However, this is precisely the approach that we do not wish to take since when the system is in the pre-transitional region, fluctuations are large and the power series in equation 1.14 is inadequate. The goal of this thesis is to go beyond the gaussian probability distribution and capture the divergence of the free energy. Firstly, we will show how this gaussian picture can be derived rigorously from random matrix theory methods and that it is a consequence of the central-limit theorem in statistics. Then, we will go beyond the central-limit theory with the help of large-deviation theory [60]; a solid mathematical framework that systematically studies random variables with strong fluctuations. Right at the point where the Landau-De Gennes picture fails and the fluctuations grow, we will use large-deviation theory to accurately calculate $P(\mathcal{Q})$ (and $p(s)$).

1.4 The Gay-Berne model - Phase diagram in two- and three dimensions

In molecular dynamics simulations we wish to reproduce the characteristics of molecules that form isotropic and nematic liquid crystal phases. As we already have discussed, these are organic molecules with ellipsoidal shapes and short-range non-bonded interactions. To capture simultaneously the steric effects and the non-bonded interactions that are non-Coulombic in nature we use the Gay-Berne [22] potential, a generalization of the more common Lennard-Jones potential. The Gay-Berne potential energy $U^* = U/\epsilon_0$ is a

function of the distance between the two center-of-masses $r^* = r/\sigma_0$, $r = |\hat{\mathbf{r}}|$ as well as the orientations $\hat{\Omega}_i, \hat{\Omega}_j$ of the interacting molecules,

$$U^* = 4\epsilon^{\nu}\epsilon'^{\mu}\left[\left(\frac{1}{r^* - \sigma + 1}\right)^{12} - \left(\frac{1}{r^* - \sigma + 1}\right)^{6}\right] \tag{1.17}$$

$$\epsilon = \left[1 - \chi^2\left(\hat{\Omega}_i \cdot \hat{\Omega}_j\right)^2\right]^{-\frac{1}{2}} \tag{1.18}$$

$$\epsilon' = 1 - \frac{\chi'}{2}\left[\frac{\left(\hat{\mathbf{r}} \cdot \hat{\Omega}_i + \hat{\mathbf{r}} \cdot \hat{\Omega}_j\right)^2}{1 + \chi'\left(\hat{\Omega}_i \cdot \hat{\Omega}_j\right)} + \frac{\left(\hat{\mathbf{r}} \cdot \hat{\Omega}_i - \hat{\mathbf{r}} \cdot \hat{\Omega}_j\right)^2}{1 - \chi'\left(\hat{\Omega}_i \cdot \hat{\Omega}_j\right)}\right] \tag{1.19}$$

$$\sigma = 1 - \frac{\chi}{2}\left[\frac{\left(\hat{\mathbf{r}} \cdot \hat{\Omega}_i + \hat{\mathbf{r}} \cdot \hat{\Omega}_j\right)^2}{1 + \chi\left(\hat{\Omega}_i \cdot \hat{\Omega}_j\right)} + \frac{\left(\hat{\mathbf{r}} \cdot \hat{\Omega}_i - \hat{\mathbf{r}} \cdot \hat{\Omega}_j\right)^2}{1 - \chi\left(\hat{\Omega}_i \cdot \hat{\Omega}_j\right)}\right]^{-\frac{1}{2}} \tag{1.20}$$

where χ and χ' are the anisotropy parameters and are defined as,

$$\chi = \frac{\left(\sigma_{\parallel}/\sigma_{\perp}\right)^2 - 1}{\left(\sigma_{\parallel}/\sigma_{\perp}\right)^2 + 1} \tag{1.21}$$

$$\chi' = \frac{\left(\epsilon_{ss}/\epsilon_{ee}\right)^{1/\mu} - 1}{\left(\epsilon_{ss}/\epsilon_{ee}\right)^{1/\mu} + 1} \tag{1.22}$$

We use standard Gay-Berne parameters [13] that have been extensively used in liquid crystal studies,

$$\frac{\epsilon_{ss}}{\epsilon_{ee}} = 5, \quad \epsilon_{ss} = \frac{5}{3}\epsilon_0, \quad \frac{\sigma_{\parallel}}{\sigma_{\perp}} = 3, \quad \sigma_{\parallel} = 3\sigma_0, \quad \mu = 2, \quad \nu = 1 \tag{1.23}$$

where the quantity $\epsilon_{ss}/\epsilon_{ee}$ is the ratio of the depth of the potential well when two molecules are placed side-to-side to that when two molecules are placed end-to-end and the quantity $\sigma_{\parallel}/\sigma_{\perp}$ is the ratio of the major axis of the Gay-Berne molecule to the minor axis. In figure 1.5 we show the potential energy as a function of the intermolecular distance.

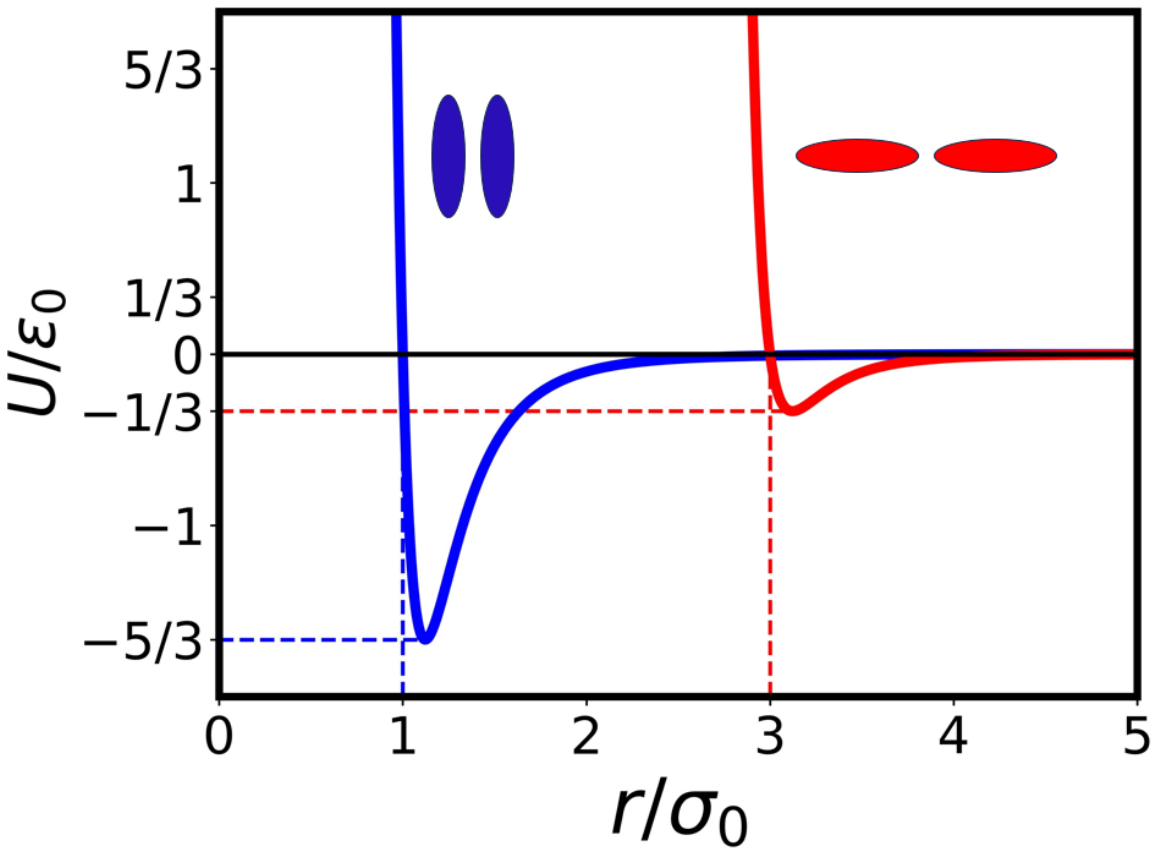

Figure 1.5: The two extreme limits of the Gay-Berne potential. When the two interacting molecules approach side-to-side (blue curve) and end-to-end (red curve). When they approach side-to-side they can get 3 times as close and it is 5 times more energetically favorable as compared to the end-to-end approach.

In the case of spherical symmetry $\chi = 0$ and $\chi' = 0$ we recover the standard Lennard-Jones curve,

$$U^* = 4\left[\left(\frac{1}{r^*}\right)^{12} - \left(\frac{1}{r^*}\right)^{6}\right] \tag{1.24}$$

where of course there is no nematic phase. Nematic order rises due to the anisotropic shapes of the molecules [14] as it was shown early on for molecules with $\sigma_{\|}/\sigma_{\perp} >> 1$ by Onsager [49]. In standard terminology [6] the Gay-Berne model we will use is,

$$\mathrm{GB}(\sigma_{\|}/\sigma_{\perp}, \epsilon_{ss}/\epsilon_{ee}, \mu, \nu) = \mathrm{GB}(3, 5, 2, 1) \tag{1.25}$$

While that model is not unique we will use it throughout this study because the 2D [36]

and 3D [13] phase diagrams of that model have been extensively studied and mapped out.

The phase-diagram (See figure 1.7) is given in terms of the reduced temperature $T^* = (k_B T)/\epsilon_0$ and the reduced density $\rho^* = \rho\sigma_0^D$, two- dimensions $D = 2$ (grey-blue region in figure) and three-dimensions $D = 3$ (white and red regions in figure) respectively. In this study the control parameter driving the system to different regions of the phase diagram, is the density ρ^* and the temperature will be set equal to $T^* = 1$ (dotted line in figure) for all simulations. The three-dimensional conditions that correspond to the deep-isotropic/nematic/pre-transitional isotropic have been worked out in previous work [63]. The deep isotropic density is $\rho^* = 0.280$, the pre-transitional is $\rho^* = 0.300$ and the pre-transitional extremely close to the nematic phase is $\rho^* = 0.304$. These three conditions can be seen as red dots in figure 1.7. All these different thermodynamic conditions will be used in order to evaluate the accuracy of different approached to the probability distribution of the nematic order parameter in finite isotropic systems. For two-dimensional ($D = 2$ systems, we performed our own analysis (see figure 1.6) and calculated $\langle s \rangle$ for different densities in order to find which one is a good candidate for to the deep-isotropic and which one works as a pre-transitional. We found that for $N = 800$, $\langle s \rangle$ changes significantly around $\rho^* \approx 0.30$ which is consistent with other $D = 2$ studies (See [36], [37] and [6]). This is also consistent with figure 1.7 where the nematic phase in $D = 2$ (blue region) stabilizes for smaller ρ^* compared to $D = 3$ (red region).

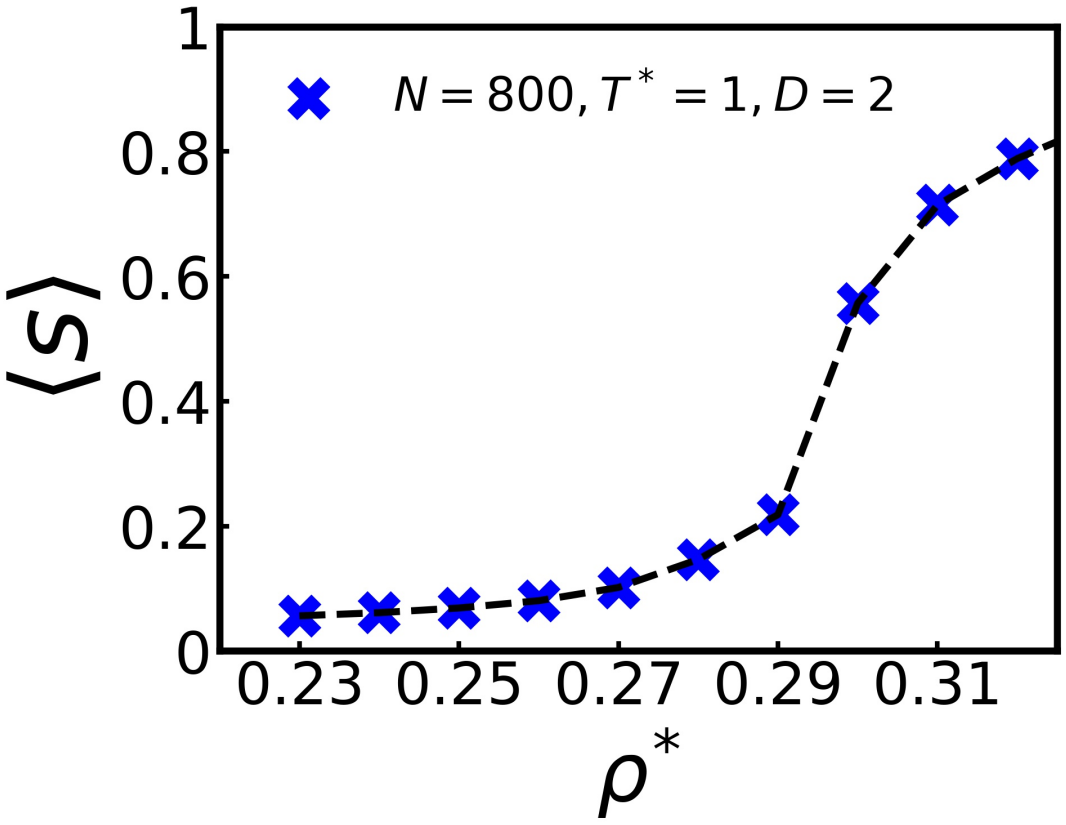

Figure 1.6: The average order parameter versus the density. Each cross consists of 10^5 configurations of the GB(3, 5, 2, 1) produced via Molecular Dynamics simulation with $T^* = 1$ and $N = 800$ in two dimensions $D = 2$.

The density $\rho^* = 0.230$ was chosen as the deep-isotropic density with weak fluctuations and the density $\rho^* = 0.285$ was chosen as the pre-transitional isotropic density with strong fluctuations. These conditions can be seen as blue x's in figure 1.7.

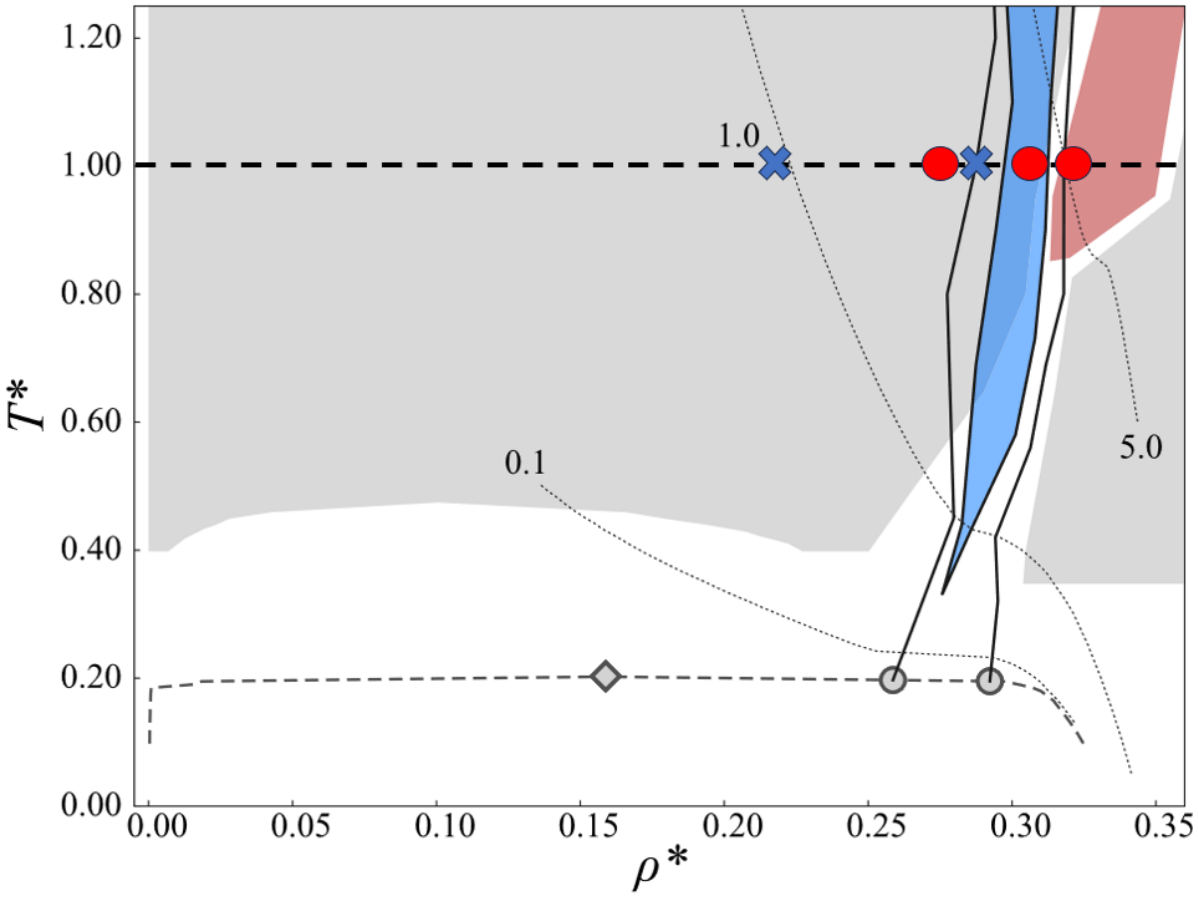

Figure 1.7: A superposition of the phase diagrams in three- and two-dimensions. The three-dimensional isotropic phase is the white region and the nematic is the red. The two-dimensional isotropic is the grey and the nematic is the blue. The dotted line corresponds to $T^* = 1$ which is the temperature used for all the simulations in the thesis. The three red circles correspond to the three different density conditions we used for the three-dimensional systems ($\rho^* = 0.280, \rho^* = 0.300$ and $\rho^* = 0.304$). The two blue x's correspond to the two different densities ($\rho^* = 0.230$ and $\rho^* = 0.285$) used in two-dimensional simulations. Original figure is taken from [6].

1.5 A note on the two-dimensional GB(3, 5, 2, 1) model

The true nature of the phase transition in two-dimensions is slightly more convoluted. In fact, it would be probably wiser to use the word quasi-nematic instead of nematic. There is evidence [37] that in two-dimensions, because of the Mermin-Wagner theorem [46], thermal fluctuations destabilize long-range order and for large enough systems the

nematic phase will eventually vanish. It has been found that the transition is of the Kosterlitz-Thouless type between an isotropic phase where orientational correlations decay exponentially and a quasi-nematic phase where the correlations decay as a power law. The underlying mechanism that drives the transition is the binding and unbinding of disclinations [37]. Nevertheless, in our study we cannot tell the difference between nematic and quasi-nematic because we work with small systems who still show significant nematic order (See figure 1.6) and we shall keep using the word "nematic" for two-dimensions as well. Moreover it is impossible to distinguish between different underlying geometries (like the topological defects) with the order parameter we are using. The tensor $\mathcal{Q}$ is a global measure of the orientational order and not a local measure as it contains molecular information but it does not contain spatial information.

CHAPTER 2

Statistical mechanical lessons from the random flight problem in 3D

The problem of a random flight dates back to the beginning of the 20th century [16] and is a useful platform to introduce all the fundamental ideas that will be used in the thesis. As the name suggests, a random flight consist of a sequence of uncorrelated steps of unit length with orientations $\hat{\Omega}_j$ in three-dimensional ($D = 3$) space. An interesting question that one can ask is the following: What is the probability density of the sum of all the steps; the end-to-end distance? In other words, how likely is the random flight to return to the origin or stray off completely after an x number of steps? We can answer this question exactly and also showcase possible approximations as the number of steps N gets larger. Exactly solvable models like the random flight can provide insight and guidance in order to tackle the more complicated case of interacting Gay-Berne molecules.

2.1 Random flight in three dimensions

Imagine that we have a sequence of N steps of length d. The unit orientation of each step l is defined as,

$$\hat{\Omega}_l = \begin{pmatrix} \cos\phi_l \sin\theta_l \\ \sin\phi_l \sin\theta_l \\ \cos\theta_l \end{pmatrix}, \quad l = 1, ..., N \tag{2.1}$$

and the angles ϕ and θ are measured with respect to some arbitrary macroscopic axis.

$$\cos\theta_l = \hat{\Omega}_l \cdot \hat{z} \tag{2.2}$$

The axis $\hat{z}$ can point anywhere in space. The natural way of characterising how much the flight has progressed since its initiation is by measuring the distance between the tail of $\hat{\Omega}_1$ and the head of $\hat{\Omega}_N$ vectors. This is called the end-to-end distance and it is simply the sum of all the steps with length d,

$$\mathbf{R} = d\sum_{l=1}^{N} \hat{\Omega}_l, \quad R = |\mathbf{R}| = \sqrt{R_1^2 + R_2^2 + R_3^3} \tag{2.3}$$

For $N \to \infty$ we expect $\langle \mathbf{R} \rangle = \mathbf{0}$ but when we have a finite N we expect a non-vanishing average and $P(\mathbf{R})$ to fluctuate. Equivalently we can define a scalar reduced end-to-end distance r that is intensive,

$$r = \frac{|\mathbf{R}|}{|\mathbf{R}|_{max}} = \frac{R}{Nd} \tag{2.4}$$

and goes from $\langle r \rangle = 0$ (steps in random directions) to $\langle r \rangle = 1$ when all the steps are in the same direction. What is the typical size of a random flight that consists of a finite number of steps? Before we even begin our analysis we can look at the root-mean-square

or r in a similar manner to s in liquid crystals and examine the limiting cases,

$$\sqrt{\langle r^2 \rangle} = \sqrt{\frac{1}{N^2} \sum_{l,l'=1}^{N} \langle \hat{\Omega}_l \cdot \hat{\Omega}'_l \rangle} = \begin{cases} 1/\sqrt{N}, & \text{random steps} \\ 1, & \text{fully extended} \end{cases}$$

These two limiting behaviors will provide valuable insight into the formulation approximations to the probability distribution as we will see later on.

2.2 Exact probability distribution

We wish to calculate $P(\mathbf{R})$ and for this simple model the exact answer can be given in terms of integrals. By using the delta function representation of the probability,

$$P(\mathbf{R}) = \left\langle \delta(\mathbf{R} - d \sum_{l=1}^{N} \hat{\Omega}_l) \right\rangle \tag{2.5}$$

where

$$\langle f(\theta, \phi) \rangle = \frac{\int_0^{2\pi} \int_0^{\pi} f(\theta, \phi) \sin\theta d\theta d\phi}{\int_0^{2\pi} \int_0^{\pi} \sin\theta d\theta d\phi} \tag{2.6}$$

The Fourier representation of the delta function yields,

$$P(\mathbf{R}) = \frac{1}{(2\pi)^3} \int d\mathbf{k} e^{i\mathbf{k}\cdot\mathbf{R}} \psi^N(k) \tag{2.7}$$

$$\psi^N(k) = \left(\frac{\sin(kd)}{(kd)} \right)^N \tag{2.8}$$

where $\psi(k)$ is the characteristic function of a single step and can be written as an N product because the steps are uncorrelated. This is the reason why the random flight problem is easy. Moreover, $\psi(k)$ is a spherically symmetric function as it only depends on the magnitude of the imaginary field k. It is straightforward to see that the exact answer

is the following integral,

$$P(\mathbf{R}) = \frac{1}{2\pi^2 R}\int_0^\infty k\sin(kR)\psi^N(k)dk \tag{2.9}$$

This answer dates back to Lord Rayleigh [20]. It is a cumbersome integral answer that is not very useful for numerical calculations. However, we are interested in exploring the limiting behaviors of $P(\mathbf{R})$ as N gets larger.

2.3 Central-limit theorem, small fluctuations around the origin

For very small chains $P(\mathbf{R})$ might be useful but as we go to larger N values the integral is difficult to compute. Thus, very early on, various large-N approximations were of great importance for practical calculations. The central-limit theorem is the easiest one to use and it holds for very small fluctuations of the flight around its origin. This corresponds to very small values of k and allows for the use of simple Taylor series. The gaussian density is a result of expanding $\psi(k)$ up to a second power of the field k and then taking the limit as $N \to \infty$,

$$\psi^N(k) \overset{\text{k}\to 0}{\approx} \left(1 - \frac{d^2k^2}{6}\right)^N \tag{2.10}$$

$$\lim_{N\to\infty}\psi^N(k) = \lim_{N\to\infty}\left(1 - \frac{d^2k^2}{6}\right)^N = \exp\left(-N\frac{d^2k^2}{6}\right) \tag{2.11}$$

and by integrating with the low-field characteristic function we get the expected gaussian density

$$P(\mathbf{R}) \sim \exp\left(-N\frac{3}{2}r^2\right), \quad r \to 0 \tag{2.12}$$

This makes sense because if we wait long enough it will probably be found where we left it. This is very intuitive and is a result of the central-limit theorem in statistics.

It is very interesting to think of the random flight as extremely simple model of a non-

interacting polymer of N links and draw numerous parallels with the polymer literature. Imagine that each step is a stiff link where at the two ends of the link lies some atom. Atoms do not interact and the polymer each link is free to rotate in space. The variable r represents the size of the polymer in the same way that it worked for the size of the random flight. With that picture in mind we can now re-examine the density and notice that it has the form,

$$P(\mathbf{R}) \sim \exp\left[-NI(r)\right] \tag{2.13}$$

where

$$I(r) = \frac{3}{2}r^2 \tag{2.14}$$

being the elastic free energy for small deformations. Furthermore, this elastic free energy is related to the entropic force of the ideal chain [51]. For small deformations the entropic force τ is the gradient of the free energy with respect to R,

$$\tau(R) = \frac{\partial I(r)}{\partial r}\frac{\partial r}{\partial R} = \frac{3k_BT}{N^2d^2}R \tag{2.15}$$

and for the entire chain we recover the well-known expression for the total force $T(R)$ on the chain,

$$T(R) = N\tau(R) = \frac{3k_BT}{Nd^2}R \tag{2.16}$$

where $\frac{3k_BT}{Nd^2}$ is called the entropic spring constant (See [51, p. 72] and the form of 2.15 is reminiscent of Hooke's law for ideal chains; A linear relation between the applied force per step τ and the extension R of the chain.

The relation between τ and R is known in classical thermodynamics as an equation of state and it relates the extensive order parameter R of the problem to the conjugate intensive force variable τ. For small fluctuations is takes a linear form and we will see that this will be the case for all of the systems considered in this thesis. Moreover, we do work reversibly in the system by applying an external force quasi-statically. This way the

system remains in equilibrium and the reversible work we do is equal to the difference in free energy. This is the **reversible work theorem** [7, Chapter 4-5] from classical thermodynamics and is at the heart of this thesis. The reversible work theorem is written as,

$$I(r) = \beta\Delta f(r) = -w_{rev} = \int_A^B \tau(r')dr' \tag{2.17}$$

where $\beta\Delta f(r) = \beta f(r) - \beta f_0$ is the difference in free energy between states A and B. The constant βf_0 can be ignored as it does not affect the calculations and the integral is written as $I(r) = \int_0^r \tau(r')dr'$. The probability density is related to the free energy in the usual manner,

$$P(\mathbf{R}) \sim \exp\left(-N\beta f(r)\right) = \exp\left[-N\int_0^r 3r'dr'\right] \tag{2.18}$$

We will derive all of this results in the context of large-deviation theory and we will use them extensively in order to create approximations to probability distributions that are too complicated to be derived analytically. Finally we test whether our expression recovers the correct result for $\sqrt{\langle r^2\rangle}$. We can multiply equation 2.12 with the surface element of a three-dimensional sphere in order to get the spherical probability distribution,

$$P(r) \sim r^2 \exp\left(-\frac{3N}{2}r^2\right) \tag{2.19}$$

and verify that the second moment is correct,

$$\sqrt{\langle r^2\rangle} = \frac{1}{\sqrt{N}} \tag{2.20}$$

We see that for very small deformations r and large number of steps N the the random flight will be anticipated to be found at the origin. In the language of ideal chains that means that we apply a very weak entropic force to the polymer and it extends very little.

2.4 Complete alignment limit

What happens when the extension of the polymer is large? Or in the case of the random flight how could we describe the probability of the flight to be found very far from the origin? This statistical fluctuation might be rare and thus very hard to compute in a computer simulation. However, extreme value statistics provides a very rigorous method of studying these large fluctuations:: the saddle point approximation. The gaussian density was derived because we assumed that fluctuations in k (and thus in r) are small but when this is not true the gaussian is very inaccurate and the so called "non-gaussian" density was developed by Kuhn [35]. By looking at the application of a large field and the almost complete alignment of the chain segments Kuhn worked out a closed form approximation to the integral. We briefly sketch the proof (we follow Yamakawa [62]) by firstly noting the even symmetry of the integrand in equation 2.9. We may set $\xi = kd$ and rewrite the exact answer as,

$$P(\mathbf{R}) = \frac{1}{4i\pi^2 d^2 R} \int_{-\infty}^{+\infty} \xi \exp\left[N f(\xi)\right] d\xi \tag{2.21}$$

$$f(\xi) = ir\xi + \ln\left(\frac{\sin\xi}{\xi}\right), \quad r = \frac{R}{Nd} \tag{2.22}$$

This a typical case of evaluating an integral via the saddle point approximation. The saddle point ξ_0 is given by,

$$f'(\xi_0) = 0 \tag{2.23}$$

and can be shown to be on the imaginary axis $\xi_0 = i\tau$ where τ is a positive and real number (that corresponds to a real force in reduced units like equation 2.15) and it satisfies the following equation,

$$r(\tau) = \mathcal{L}(\tau), \quad \text{with} \quad \mathcal{L}(\tau) \coloneqq \coth\tau - \frac{1}{\tau} \tag{2.24}$$

$\mathcal{L}(\tau)$ is called the Langevin function and is commonly encountered in polymeric and magnetic studies. The above equation is again a relation between a real applied force

τ and the corresponding chain extension r; an equation of state and in the context of saddle point approximation it is a path where the saddle point lies on. Expanding $f(\xi)$ as a power series in the vicinity of ξ_0 and computing the integral yields,

$$P(\mathbf{R}) \sim \exp\left[-N\left(r\mathcal{L}^{-1}(r) - \ln\frac{\sinh\mathcal{L}^{-1}(r)}{\mathcal{L}^{-1}(r)}\right)\right] = \exp\left[-N\int_0^r \mathcal{L}^{-1}(r')dr'\right] \tag{2.25}$$

where

$$\tau(r) = \mathcal{L}^{-1}(r) \tag{2.26}$$

is the inverse of the Langevin function. This is the non-gaussian density and has been useful in free energy calculations of extended polymers (See for example [47]) as well as in the study of magnets [38]. It is a more general relation than equation 2.15 and we recover Hooke's law by taking the small r limit of the $\coth x$ function in equation 2.24,

$$\mathcal{L}(\tau) = -\frac{1}{\tau} + \left(\frac{1}{\tau} + \frac{\tau}{3} + \mathcal{O}(\tau^3)\right) = \frac{\tau}{3} + \mathcal{O}(\tau^3), \quad \tau \to 0 \tag{2.27}$$

by inverting the equation we recover the known result for weak entropic forces,

$$\tau(r) = 3r, \quad r \to 0 \tag{2.28}$$

That shows how the saddle point approximation actually includes the central-limit theory approximation. We will bring all these different approaches under the same theory in the next chapter with the use of large-deviation theory.

The advantage of the non-gaussian density lies on the fact that it is applicable for any r not just for small values of r. Even when the random flight is found extremely far from the origin or the individual links of the chain are fully extended equation 2.24 still holds. Let us remind ourselves that the fact that we have an exact expression for the equation of state lies in the simplicity of the model. For strongly interacting systems contemplated in the thesis we will not have access to an exact expression but we will be able to calculate

the extreme limits exactly. We already saw the weak force limit and by taking the large argument limit $\coth x$ we can work out the complete alignment limit,

$$\mathcal{L}(\tau) = 1 - \frac{1}{\tau} + \mathcal{O}(1), \quad \tau \to \infty \tag{2.29}$$

and in terms of $\tau(r)$,

$$\tau(r) = \frac{1}{1-r} + \mathcal{O}(1), \quad r \to 1 \tag{2.30}$$

where now there is pole at $r = 1$ where the force diverges. Saddle point approximation provides the two extreme limits (equations 2.28 and 2.30) and the strong force limit is usually found in the literature of rubber-like materials where they can deform largely and it is desirable to calculate the free energy of deformation [33] via the reversible work theorem. Interestingly, even in the case of random flights and stiff chains where the equation of state is known, the inverse Langevin function is inconvenient. Simple numerical approximations are being used [33] in order to calculate the force-extension relation and the two extreme limits are used. The polynomial nature of both limits,

$$\tau(r) = \begin{cases} 3r + \mathcal{O}(r^3), & r \to 0 \\ \frac{1}{1-r} + \mathcal{O}(1), & r \to 1 \end{cases} \tag{2.31}$$

suggests the simple Pade-interpolation; A ratio between polynomial functions of r. There is no unique Pade interpolation and numerous answers have been worked out in the literature [11]. We need the Pade function to go to the linear limit for small values and to capture the pole at $r = 1$ when the force is large. At the same time it needs to fulfill the correct symmetry of the equation of state. We saw that the integral of the force is the free energy and $I(\mathbf{R})$ is a function that cannot depend whether we choose $\mathbf{R}$ or $-\mathbf{R}$. That means that the free energy will be a function of even powers of the extension and the derivative of it (force) will be a function of odd powers in r. One example that satisfies

all these conditions up to 3rd power of r is the popular Cohen function [11],

$$\tau(r) = r\frac{3-r^2}{1-r^2}, \quad \text{Pade}[3/2] \tag{2.32}$$

This Pade[3/2] is of course not unique. We can also go to higher powers (it will be useful for the molecular theory we will develop) and develop a Pade[5/2],

$$\tau(r) = \frac{6r-3r^3+r^5}{2(1-r^2)}, \quad \text{Pade}[5/2] \tag{2.33}$$

The reader can verify that both functions go to the correct limits by looking at the two Pade approximations together with the two extremes in the following figure

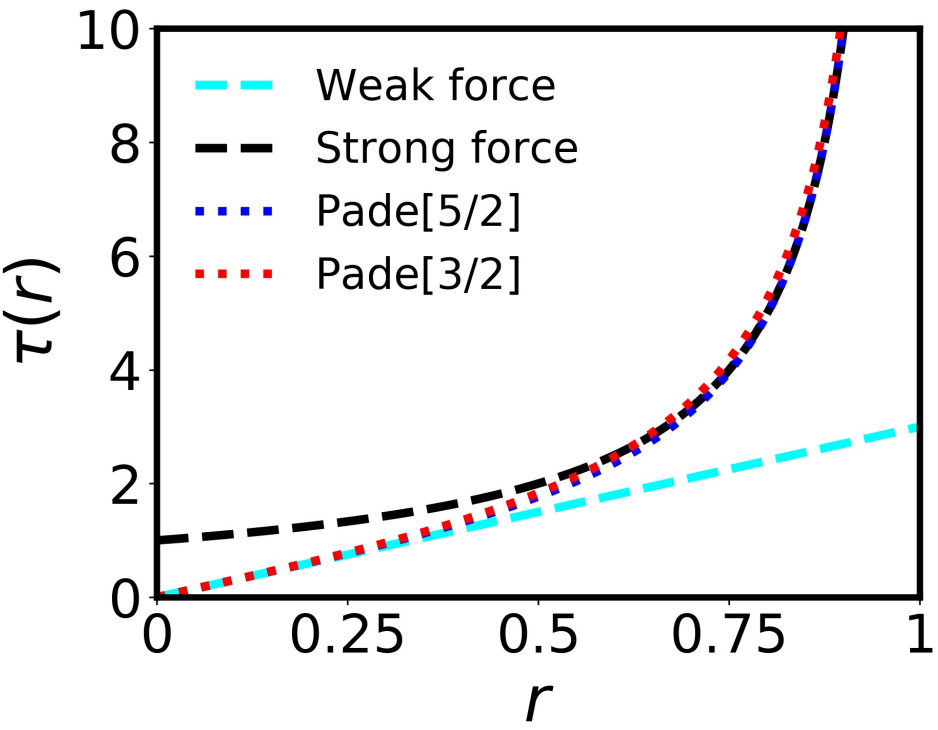

Figure 2.1: The cyan line is the weak force limit (equation 2.28) and the black dashed line is equation 2.30. The blue line is equation 2.33 and the red dotted line is equation 2.32. For weak deformations, both approximations are good and for large deformations the Pade[5/2] is slightly more accurate.

From the reversible work theorem we can work out the free energy per step (or link in

the polymer) for the Pade[5/2]

$$I(\mathbf{R}) = -\ln(1-r^2) + \frac{1}{2}r^2 - \frac{1}{8}r^4 \tag{2.34}$$

and verify that it has the correct even symmetry. Furthermore we see that the pole at $r = 1$ is captured as a logarithmic divergence in the free energy. The corresponding probability density of the reduced deformation is,

$$P(r) \sim r^2\left(1-r^2\right)^N \exp\left(-\frac{N}{2}r^2\right)\exp\left(-\frac{N}{8}r^4\right), \quad \text{for Pade[5/2]} \tag{2.35}$$

This interpolated probability density is fully aware of both the weak-force gaussian limit and the strong-alignment non-gaussian limit. In a computer simulation of a random flight we expect this density to capture sudden and rare fluctuations of the deformation while the gaussian cannot. In this extremely simple example we demonstrated the entire skeleton of the theory that will be developed in the case of liquid crystals. Close to the isotropic/nematic phase transition, the probability distribution $p(s)$ has strong fluctuations and it will be important to go beyond the small-field limit of the central-limit theory.

CHAPTER 3

Large-deviation theory

Large-deviation theory is a very general mathematical framework that has been applied mostly to non-equilibrium problems. The theory has found many applications to glassy systems [10], where the dynamical-activity fluctuations [32] are approximated via large-deviation methods. In the context of dynamical phase transitions, the goal is to describe domain formation in kinetically frustrated spin models such as the FA model [19], [48], the East model [31] but also in atomistic models of glass formers [28]. In equilibrium problems, the probability distribution of some macroscopic variable is usually studied at the central-limit theory level [40, Chapter XII]. This is accurate only when the fluctuations are trivial and breaks down when we approach criticality (The usefulness of the probability distribution fluctuations was recognized by Nigel Goldenfeld in the 60s [24, Chapter 2.9]). One interesting application to equilibrium problems refers to the calculation of the so-called "isometric fluctuations" in systems with broken discrete and continuous symmetry (See for example [38], [39], [61], [21] and [27]). For an exhaustive review of the applications of large-deviation theory see [60].

Large-deviation theory comes from the saddle point approximation that we briefly saw in the previous chapter and can be used in order to formulate a thermodynamic framework that studies strong fluctuations. As we unfold the theory, we will stumble upon classical

thermodynamic ideas like the reversible work theorem and the equation of state. We will use these results in order to study the N-dependence of the probability distribution.

3.1 The large-deviation principle

We are interested in extensive order parameters $\mathbf{A}$ that are sums of N random vectors $\mathbf{x}_j$ where $j = \{1, ..., N\}$.

$$\mathbf{A} = N\mathbf{a} = \sum_{j=1}^{N} \mathbf{x}_j \tag{3.1}$$

In the previous chapter we studied the probability distribution of $\mathbf{A}$, and showed that either central-limit theory approximations or saddle-point approximations give answers of the form,

$$\lim_{N\to\infty} P(\mathbf{A}) \sim \exp\left[-NI\left(\mathbf{a}\right)\right], \quad \int P(\mathbf{A})d\mathbf{A} = 1 \tag{3.2}$$

where I is some positive function that plays the role of free energy per molecule. It turns out that this result is quite general for extensive quantities. The statistical theory that systematically studies scaling laws of that form is called large-deviation theory [60]. The main idea is that as N grows larger, the logarithm of the probability distribution will converge to some positive function, the rate function. This is known as the large-deviation principle,

$$I(\mathbf{a}) = \lim_{N\to\infty} \left(-\frac{1}{N} \ln P(\mathbf{A})\right) \tag{3.3}$$

and we say that $P(\mathbf{a})$ satisfies a large-deviation principle with rate function $I(\mathbf{a})$. The theory provides an entire structure to study probability distributions of variables that are of great interest to thermodynamics. Examples are the magnetization, end-to-end distances in polymers, liquid crystal nematic order and countless other. In the context of thermodynamics the function $I(\mathbf{a})$ corresponds to the Helmholtz free energy (difference) per particle,

$$I(\mathbf{a}) = \beta\frac{\Delta F(\mathbf{a})}{N} \tag{3.4}$$

Getting an expression for the rate function is of primary interest to this study. It includes all the fluctuations of the distribution no matter how strong they are making it more general than the central-limit theorem. If we wish to understand strongly-fluctuating nematic order inside a finite and isotropic medium, developing a method for the full characterization of $I(\mathbf{a})$ is crucial.

3.2 Gaertner-Ellis theorem and classical thermodynamics

The main tool that will be used in order to calculate the rate function is the Gaertner-Ellis theorem (or more precisely its vector version called Sanov's theorem). According to the theorem, we change the focus from the rate function to the (cumulant) generating function of $P(\mathbf{A})$,

$$\exp\left(N\lambda(\mathbf{b})\right) = \left\langle e^{\mathbf{b}\cdot\mathbf{A}} \right\rangle \tag{3.5}$$

$$\Leftrightarrow \lambda(\mathbf{b}) = \lim_{N\to\infty} \frac{1}{N} \ln \left\langle e^{\mathbf{b}\cdot\mathbf{A}} \right\rangle \tag{3.6}$$

where now $\lambda(\mathbf{b})$ is a function of the intensive field variable $\mathbf{b}$ that is conjugate to $\mathbf{A}$. In classical thermodynamic language this is the Gibbs free energy per particle and is the Legendre transform of the Helmholtz free energy per particle. The variable $\mathbf{b}$ can be thought as an external field that we apply to the system in order to get $\mathbf{A}$ to a specific value. In terms of magnetization this could be an external magnetic field that interacts with the all the magnetic moments in the system. Also, in the context of large-deviation theory we make use of the moment-generating function which is a function of a real field as opposed to chapter two where we used the characteristic function that uses an imaginary field variable. The function $\lambda(\mathbf{b})$ is easier to calculate for many problems and that is why we turned our focus to $\lambda(\mathbf{b})$ instead of directly calculating $I(\mathbf{a})$. The Gaertner-Ellis theorem states that the two functions are connected via a Legendre transform (or more

generally Legendre-Fenchel),

$$I(\mathbf{a}) = \mathbf{b} \cdot \mathbf{a} - \lambda(\mathbf{b}) \tag{3.7}$$

where $\mathbf{b}$ is the value that maximizes the rate function and is therefore the solution to

$$\nabla \left[\mathbf{b} \cdot \mathbf{a} - \lambda(\mathbf{b})\right] = 0 \tag{3.8}$$

$$\Leftrightarrow \mathbf{a} = \nabla\lambda(\mathbf{b}) \tag{3.9}$$

Equation 3.9 gives a relation between the force we apply to the system and the conjugate order parameter; it is the multivariate **equation of state**. Inserting 3.9 into equation 3.7 and re-writing λ as a line integral over the vector field $\mathbf{b}$,

$$I(\mathbf{a}) = \mathbf{b}(\mathbf{a}) \cdot \mathbf{a} - \int_C \nabla\lambda(\mathbf{b}) \cdot d\mathbf{b} \tag{3.10}$$

$$\Leftrightarrow I(\mathbf{a}) = \int_C \mathbf{b}(\mathbf{a}) \cdot d\mathbf{a} \tag{3.11}$$

where we used integration by parts and C is some path in thermodynamic state space. What he have here is the equality between the free energy and the work done to the system by some force $\mathbf{b}$ along some path C. By definition this is the work done to the system and the free energy is only equal to the work done to the system only when we integrate along the reversible path $C = C_{rev}$,

$$I(\mathbf{a}) = W_{rev}(\mathbf{a}) \tag{3.12}$$

This is the maximum (or reversible) work theorem [7, p. 103]. From classical thermodynamics we know that for a system in contact with a thermal reservoir, the work delivered by a reversible process is going to be equal to the change in the Helmholtz free energy [7, p. 159]. When we say reversible path we mean that the transformation process along C happens so slowly that the system remains at equilibrium at all times (quasi-static

process, [7, p. 97]).

It is interesting how all these classical results can be expressed in terms of large-deviation theory language. Large-deviation theory however establishes a clear thermodynamic route of evaluating probability distributions of extensive properties. It allows us to establish a clear connection between the equation of state / the reversible work and the probability distribution. To sum up the discussion into one equation,

$$\lim_{N\to\infty} P(N\mathbf{a}) \sim \exp\left[-N\int_{C_{rev}} \mathbf{b}(\mathbf{a})\cdot d\mathbf{a}\right] \tag{3.13}$$

where the probability density is given in terms of a path integral. Although equation 3.13 looks complicated, it will be greatly simplified when dealing with isotropic systems. It is the most important result of this thesis and will be used in order to study the N dependence of the fluctuations of $P(N\mathbf{a})$.

3.3 Spherical symmetry of the free energies

In practical calculations the tensor/vector notation will simplify drastically and only scalars will be needed. This is because for all the time-independent applications in this thesis, the free energy per particle $\lambda(\mathbf{b})$ is spherically symmetric and only depends on the modulus $b = |\mathbf{b}|$,

$$\lambda(\mathbf{b}) = \lambda(b) \tag{3.14}$$

Similarly $I(\mathbf{a})$ will only be a function of the modulus $a = |\mathbf{a}|$ and it is not hard to see that the multivariate equation of state in equation 3.9 will simplify to,

$$a = \frac{\partial\lambda(b)}{\partial b} \tag{3.15}$$

where $a = |\mathbf{a}|$. This makes sense since we can choose the order parameter $\mathbf{a}$ to point the direction of the field that we apply to the system,

$$\mathbf{b} = b\,\hat{\mathbf{b}}, \quad \mathbf{a} = \frac{\partial \lambda(b)}{\partial b}\hat{\mathbf{b}}$$

where $\hat{\mathbf{b}}$ is the direction of the field. This argument will be valid for all the applications of large-deviation theory in this study and will only need to be modified when we consider time-dependent probability distributions with weak-fluctuations in chapter 8. Now, we can drastically simplify our notation since in practice we do not need to deal with vectors/tensors. The Gaertner-Ellis theorem can be written simply as,

$$I(a) = ba - \lambda(b), \quad a = \frac{\partial \lambda(b)}{\partial b} \tag{3.16}$$

The two free energies share the same relation as the Gibbs free energy and the Helmholtz free energy F(x) = xs + G(s) (with x=dG/ds) where G(s) is a function of the intensive pressure variable and F(x) is a function of the conjugate extensive volume variable (See figure 3.1).

As we saw previously, equation 3.16 is equivalent to the **reversible work theorem** from classical thermodynamics (See also [9, Chapter 7.3]).The reversible work theorem can be seen via integration by parts or graphically via the Legendre transformation. In the second case it can be seen as a direct consequence of the Legendre duality between $I(a)$ and $\lambda(b)$. The transformation of $I(a)$ is shown in figure 3.1 if we identify F(x) as $I(a)$ and G(s) as $\lambda(b)$. The slope of $I(a)$ is,

$$\frac{\partial I(a)}{\partial a} = \frac{I(a) + \lambda(b)}{a} \tag{3.17}$$

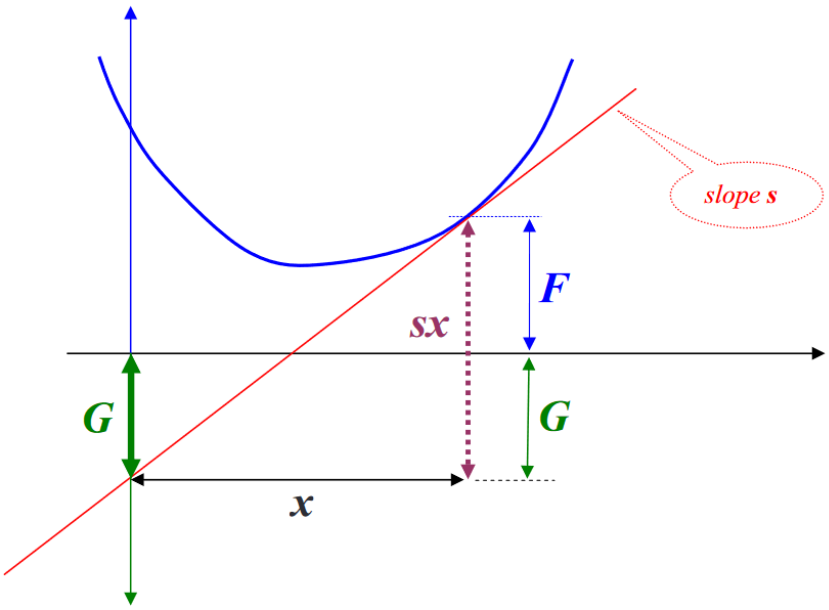

Figure 3.1: The function F that depends on variable x and the Legendre transform G that is a function of the slope. The figure is taken from [64].

inserting the Legendre relation,

$$\frac{\partial I(a)}{\partial a} = \frac{ab(a) - \lambda(b) + \lambda(b)}{a} = b(a) \tag{3.18}$$

or equivalently,

$$I(a) = \int_0^a b(a')da' \tag{3.19}$$

where $b(a)$ is the **(scalar) equation of state**, relating the intensive variable (force) with the extensive variable (order parameter). This is the **(scalar) reversible work theorem**, just like the one we encountered when calculating the elastic free energy of an ideal chain. In chemical systems with non-trivial potential energy interactions, it is almost impossible to know the exact $b(a)$. However it is possible to calculate its extreme limits analytically (Figure 3.2).

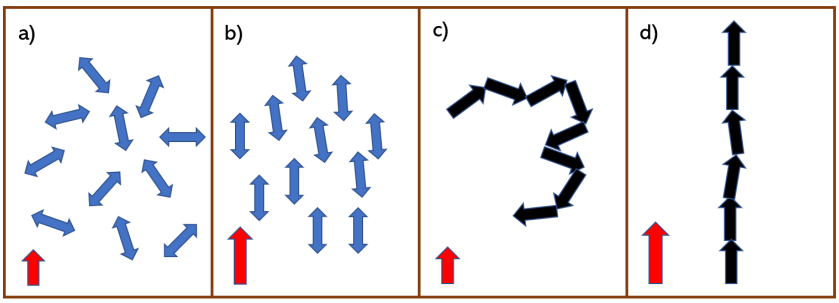

Figure 3.2: Large-deviation theory connects the system's responses to an external field with the probability distribution. The picture shows headless vectors (liquid crystal molecules) and random flights under extreme field limits.

The thermodynamic integral 3.19 suggests a route of calculating free energies just like we saw in the context of random flights; Analytical evaluation of the limits of the equation of state via direct evaluation of the moment generating function, followed by Pade' interpolation between the two limits. Lastly, integration of the interpolated expression for the equation of state $b(a')$ provides the free energy as a function of the order parameter. This is exactly what we will do in the case of strongly interacting liquid crystals where only the limits of the equation of state are known: The weak-field limit that corresponds to the central-limit theorem and the strong-field limit that corresponds to the mean field answer.

3.4 Weak-fluctuations / Central-limit theory

When the fluctuations of $P(N\mathbf{a})$ are small we can think in terms of a weak applied field $\mathbf{b}$ that is coupled to the order parameter $\mathbf{a}$ of the system. The cumulant generating function $\lambda(\mathbf{b})$ can be expanded as a Taylor series in that limit,

$$N\lambda(\mathbf{b}) = \ln \langle \exp(N\mathbf{a}\cdot\mathbf{b})\rangle = N\mathbf{b}\cdot\langle\mathbf{a}\rangle + \frac{1}{2}N^2\mathbf{b}\cdot\langle\delta\mathbf{a}\delta\mathbf{a}\rangle\cdot\mathbf{b} + ... \tag{3.20}$$

where $\delta\mathbf{a} = \mathbf{a} - \langle\mathbf{a}\rangle$. Further manipulation leads to,

$$N\lambda(\mathbf{b}) = N\sum_{j=1}^{N}\langle\mathbf{x}_j\cdot\mathbf{b}\rangle + \frac{1}{2}N\mathbf{b}\cdot\mathcal{X}\cdot\mathbf{b} + ... \tag{3.21}$$

where $\mathcal{X}$ is the susceptibility tensor that is construed by the fluctuation vectors,

$$\mathcal{X} = \left\langle \frac{1}{N}\sum_{j,k}^{N}\delta\mathbf{x}_j\delta\mathbf{x}_k \right\rangle \tag{3.22}$$

When the fluctuations (cumulants) are small we can truncate the power series and only keep the first two terms. Furthermore, for isotropic systems (like the ones we are concerned with in this study), the first term will be identically equal to zero,

$$\langle\mathbf{x}_j\rangle = 0 \tag{3.23}$$

and the susceptibility matrix simplifies,

$$\mathcal{X} = \chi\mathbf{1}, \quad \chi = \left\langle \frac{1}{N}\sum_{j,k=1}^{N}\mathbf{x}_j\cdot\mathbf{x}_k \right\rangle \tag{3.24}$$

where χ is the two-body susceptibility and $\mathbf{1}$ is the unit tensor. It applies even when interactions are very strong and we can extract this quantity from numerical simulation. The cumulant generating function at the central-limit theory level takes the usual parabolic form,

$$\lambda(b) \approx \frac{\chi}{2}b^2, \quad b \to 0 \tag{3.25}$$

and the equation of state the usual linear form,

$$a = \frac{\partial\lambda(b)}{\partial b} = \chi b \tag{3.26}$$

$$\Leftrightarrow b = \frac{1}{\chi}a \tag{3.27}$$

Via the thermodynamic integration

$$I(a) = \int_0^{a'} b(a') = \frac{a^2}{2\chi} \tag{3.28}$$

$$P(\mathbf{A}) \sim \exp\left[-\frac{N}{2\chi}a^2\right] \tag{3.29}$$

we restore the anticipated gaussian density. The central-limit theorem is exact at the limit of weak fluctuations. Lastly, we recover the anticipated result for the second moment of the order parameter a,

$$\langle a^2 \rangle = \frac{\chi}{N} \Leftrightarrow \sqrt{\langle a^2 \rangle} = \sqrt{\frac{\chi}{N}} \tag{3.30}$$

3.5 The central idea of the thesis / Mean-field form of the large-fluctuation limit

In this study we are looking at systems with orientational order and the order parameter $\mathbf{A}$ is the sum of all orientations $\mathbf{x}_j$ that is a vector function that depends on the unit orientations,

$$\mathbf{A} = N\mathbf{a} = \sum_{j=1}^{N} \mathbf{x}_j, \quad \mathbf{x}_j = \mathbf{x}_j(\hat{\Omega}_j) \tag{3.31}$$

In general $\mathbf{x}_j$ does not coincide with $\hat{\Omega}_j$ because of the symmetry of the interactions in the system but for simplicity we will refer to $\mathbf{x}_j$ as the orientations of the molecules. Anisotropic molecules have also center of mass translational coordinates $\mathbf{r}_j$. The hamiltonian of the system in the presence of an external field $\mathbf{b}$ is,

$$\mathcal{H} = \mathcal{K} + \sum_{i,j} U_{ij}(\mathbf{r}_{ij}, \hat{\Omega}_i, \hat{\Omega}_j) - \mathbf{A} \cdot \mathbf{b} \tag{3.32}$$

where $\mathcal{K}$ is the kinetic energy and $\mathbf{r}_{ij} = \mathbf{r}_i - \mathbf{r}_j$. The potential energy term could be the Gay-Berne potential we saw in chapter 1 and is in general a function of both the orientations and the inter-molecular distances. This potential energy term consists of

one-body interactions, two-body interactions and so on and in general it produces very complicated correlations between the molecules. However, in the limit of a very large external field $\mathbf{b}$ the third term in 3.32 will dominate and the orientations of the molecules will be independent from each other. The field will overcome all the inter-molecular correlations and the only orientation-dependent term that will contribute in the potential energy will be the one-body term; the independent-molecule term. In other words, a single molecule will be independent from the rest but it will still feel their presence through an effective mean field. This observation is the foundation of the entire thesis as it provides a relatively simple way of calculating the large-fluctuation limit of $P(\mathbf{A})$ analytically.

In the limit of a strong field $\mathbf{b}$ we can approximate $\mathcal{H}$ with some effective mean field hamiltonian $\mathcal{H}_{mf}$,

$$\mathcal{H} \approx \mathcal{H}_{mf} = \mathcal{K} + \sum_{i,j} V_{ij}(\mathbf{r}_{ij}) - \mathbf{A}\cdot\mathbf{b} - \mathbf{A}\cdot\epsilon \tag{3.33}$$

where V_{ij} only depends on the distances and ϵ is the vector mean field. The cumulant generating function is defined as

$$\exp\left(N\lambda(\mathbf{b})\right) = \frac{\int d\mathbf{\Omega}\exp\left(\mathbf{A}\cdot(\mathbf{b}+\epsilon)\right)}{\int d\mathbf{\Omega}\exp\left(\mathbf{A}\cdot\epsilon\right)} \tag{3.34}$$

where the integration spans over all the orientations $d\mathbf{\Omega} = \prod_{j=1}^{N} d\hat{\Omega}_j$ and the inverse temperature $\beta = \frac{1}{k_B T}$ has been absorbed into the modulus of the vector fields. Taking the fields to be $\mathbf{b} = b\,\hat{b}$, $\epsilon = \epsilon\,\hat{b}$ and remembering the definition for $\mathbf{A}$,

$$\exp\left(N\lambda(\mathbf{b})\right) = \frac{\int \prod_{j=1}^{N} d\hat{\Omega}_j \exp\left((b+\epsilon)\sum_{j=1}^{N}\mathbf{x}_j\cdot\hat{b}\right)}{\int \prod_{j=1}^{N} d\hat{\Omega}_j \exp\left(\epsilon\sum_{j=1}^{N}\mathbf{x}_j\cdot\hat{b}\right)} \tag{3.35}$$

which is a product of N independent integrals because the molecules are independent from

each other at the mean field level of approximation. This allows us to drastically simplify the calculation for $\lambda(\mathbf{b})$

$$\lambda(\mathbf{b}) = \ln \frac{\int d\hat{\Omega}_j \exp\left((b+\epsilon)\,\mathbf{x}_j \cdot \hat{b}\right)}{\int d\hat{\Omega}_j \exp\left(\epsilon\,\mathbf{x}_j \cdot \hat{b}\right)} \tag{3.36}$$

and in terms of the single molecule probability density $\rho(\hat{\Omega}_j)$ defined as

$$\rho(\hat{\Omega}_j) = \frac{\exp\left(\epsilon\,\mathbf{x}_j \cdot \hat{b}\right)}{\int d\hat{\Omega}_j \exp\left(\epsilon\,\mathbf{x}_j \cdot \hat{b}\right)} \tag{3.37}$$

equation 3.36 can be written in the exceptionally simple form

$$\lambda(\mathbf{b}) = \ln \left\langle \exp\left(\mathbf{x}_j \cdot \mathbf{b}\right)\right\rangle_{\rho(\hat{\Omega}_j)} \tag{3.38}$$

We can take the direction of $\mathbf{b}$ to point along any laboratory axis and express the answer in terms of standard analytical functions that are going to be problem-specific. Expression 3.38 for $\lambda(\mathbf{b})$ has **only** been applied to mean field treatments of orientationally ordered phases and has **never** been used as the large fluctuation limit of isotropic systems close to criticality. In order to capture fluctuations we can look at both limits and analytically evaluate them,

$$\lambda(\mathbf{b}) = \begin{cases} \frac{\chi}{2} b^2, & b \to 0 \quad \textbf{central-limit theory} \\ \ln \left\langle \exp\left(\mathbf{x}_j \cdot \mathbf{b}\right)\right\rangle_{\rho(\hat{\Omega}_j)}, & b \to \infty \quad \textbf{mean-field theory} \end{cases} \tag{3.39}$$

and the equation of state in these two extremes is given by $a = \frac{\partial \lambda(b)}{\partial b}$. It is hard to compute $\lambda(\mathbf{b})$ for intermediate values of b but we can use interpolation techniques instead. However, it is not possible to get a simple interpolation applied directly to the cumulant function. Instead applying Pade interpolation to the equation of state produces very simple answers that capture both the weak and the strong-fluctuation limit. Large-deviation theory

provides us with the tools we need in order to connect the equation of state with $P(\mathbf{A})$ and we will do just that in order to study the N-dependence of the fluctuations in a variety of systems. In the next three chapters we will see how this plays out in specific applications to liquid crystals, magnetization and polymer end-to-end distances; problems with order parameters that are defined as sums of individual orientations.

CHAPTER 4

Large-deviation theory perspective on the nematic order of two-dimensional isotropic liquid crystals

4.1 The set up of the problem

We get the two-dimensional order parameter tensor by setting $D = 2$ in the definition 1.2,

$$\mathcal{Q} = \sum_{j=1}^{N} \frac{1}{N}(2\,\hat{\Omega}_j\hat{\Omega}_j - \mathbf{1}) = \begin{pmatrix} Q_1 & Q_2 \\ Q_2 & -Q_1 \end{pmatrix} \tag{4.1}$$

$$Q_1 = Q_{xx} = \frac{1}{N}\sum_{j=1}^{N}\cos 2\theta_j, \quad Q_2 = Q_{xy} = \frac{1}{N}\sum_{j=1}^{N}\sin 2\theta_j \tag{4.2}$$

$$\cos\theta = \hat{\Omega}_j \cdot \hat{x} \tag{4.3}$$

where $\hat{x}$ is a macroscopic axis rather than the unknown director. The low dimensionality of the problem allows us to write the elements Q_1, Q_2 of the tensor as the components of a two-dimensional pseudo-vector,

$$\mathbf{Q}^T = (Q_1, Q_2) \tag{4.4}$$

$$\mathbf{Q} = \frac{1}{N}\sum_{j=1}^{N} \mathbf{q}_j, \quad \mathbf{q}_j^T = (\cos 2\theta_j, \sin 2\theta_j) \tag{4.5}$$

It is not a real vector in the sense that rotation of the axis does not transform the components of the vector in the way one would expect from Cartesian coordinates.

The problem of calculating $P(\mathcal{Q})$ is identical to the calculation of $P(\mathbf{Q})$. Because of the zero trace property of $\mathcal{Q}$, the tensor has two eigenvalues s and λ_2 but the second eigenvalue λ_2 is given by $(s + \lambda_2 = 0 \Leftrightarrow \lambda_2 = -s)$. That means that the only independent variable is s and it coincides with the modulus of the pseudo-vector $Q = |\mathbf{Q}|$. This simple scalar quantity $s = Q$ is actually our order parameter. We can see that by expressing $\mathcal{Q}$ in its eigenvector basis,

$$\mathcal{Q} = \begin{pmatrix} s & 0 \\ 0 & -s \end{pmatrix}, \quad s = \sqrt{Q_1^2 + Q_2^2} = |\mathbf{Q}| = Q \tag{4.6}$$

$$Tr(\mathcal{Q}^2) = 2(Q_1^2 + Q_2^2) = 2s^2 = 2Q^2 \tag{4.7}$$

Equation 4.7 shows that the definition of the vector-order parameter $\mathbf{Q}$ is consistent with the rotational invariance of the problem. The probability distribution and the free energy can only depend on the absolute rotational invariant $Tr(\mathcal{Q}^2)$ which is proportional to Q^2 making the use of the vector $\mathbf{Q}$ equivalent.

The probability distribution of the vector $\mathbf{Q}$ is related to $p(s)$ via a factor that

corresponds to the perimeter of a circle with radius $s = Q$,

$$p(s) = 2\pi s P(\mathbf{Q})_{Q=|\mathbf{Q}|=s} \tag{4.8}$$

This is very convenient since large-deviation theory can be applied to the probability distribution of $P(\mathbf{Q})$ by using the extensive $N\mathbf{Q}$ and the intensive conjugate field $\mathbf{h}$ as ingredients. We start by approximating $P(\mathbf{Q})$ via a large-deviation principle (equation 3.3),

$$P(\mathbf{Q}) \sim \exp\left(-NI(\mathbf{Q})\right) \tag{4.9}$$

where $I(\mathbf{Q})$ is the rate function (free energy per liquid crystal molecule) and will be determined via the Gaertner Ellis theorem from equation 3.7,

$$I(\mathbf{Q}) = \mathbf{h} \cdot \mathbf{Q} - \lambda(\mathbf{h}), \quad \mathbf{Q} = \nabla\lambda(\mathbf{h}) \tag{4.10}$$

$$\lambda(\mathbf{h}) = \lim_{N\to\infty} \frac{1}{N} \ln \left\langle e^{N\mathbf{h}\cdot\mathbf{Q}} \right\rangle \tag{4.11}$$

The relation between the intensive field and the extensive order parameter defines the liquid crystal **equation of state**. The Legendre transform of the rate function $I(\mathbf{Q})$ is the cumulant generating function $\lambda(\mathbf{h})$. Integration by parts as we saw in equation 3.11 recovers the **reversible work theorem**,

$$I(\mathbf{Q}) = \int_0^{\mathbf{Q}} \mathbf{h}(\mathbf{Q}') \cdot d\mathbf{Q}' \tag{4.12}$$

The combination of the large-deviation principle in equation 4.9 and the above expression establish a direct connection between the equation of state and $P(\mathbf{Q})$.

Liquid crystal molecules interact via the Gay-Berne potential discussed in chapter 1. Inter-molecular correlations are strong and complicated making the calculation of the exact $\lambda(\mathbf{h})$ notoriously hard. However, as we saw in previous chapters, it is possible to exactly calculate its extreme limits: The strong- correlations/weak-fluctuation limit where

the central-limit-theorem is used and the weak-correlations/strong-fluctuation limit where the answer is the mean-field. We will be able to calculate its extreme limits exactly and use them in order to get an approximation to the liquid crystal equation of state for the entire range of Q values.

4.2 The strong correlation/weak fluctuation limit: Central-limit theory

We can set aside the limit of N for notational simplicity and write $\lambda(\mathbf{h})$ as

$$N\lambda(\mathbf{h}) = \ln \langle \exp\left(N\mathbf{Q}\cdot\mathbf{h}\right)\rangle \tag{4.13}$$

keeping in mind that this will be progressively more accurate as we go to larger systems. For weak fluctuations and arbitrary strong correlations we may expand $\lambda(\mathbf{h})$ as a series of cumulants (as long as we are not in the immediate vicinity of a critical point),

$$\begin{aligned} N\lambda(\mathbf{h}) &= N\mathbf{h}\cdot\langle\mathbf{Q}\rangle + \frac{1}{2}N^2\mathbf{h}\cdot\langle\delta\mathbf{Q}\delta\mathbf{Q}\rangle\cdot\mathbf{h} + ... \\ &= N\mathbf{h}\cdot\sum_{j=1}^{N}\langle\mathbf{q}_j\rangle + \frac{N^2}{2}\mathbf{h}\cdot\langle\sum_{j,k=1}^{N}\delta\mathbf{q}_j\delta\mathbf{q}_k\rangle\cdot\mathbf{h} + ... \end{aligned} \tag{4.14}$$

where $\delta\mathbf{q}_j = \mathbf{q}_j - \langle\mathbf{q}_j\rangle$ is the molecular fluctuation vector. We can choose the field to point along any macroscopic direction in space so we can choose the most convenient; We can define all the angles θ_j with respect to the axis of the field $\cos\theta_j = \hat{\Omega}\cdot\hat{h}$ and carry out the calculations of the averages that appear in the expansion. Since we are in the isotropic phase the only quantities that survive averaging are the ones that involve angle differences. The rest are all zero

$$\langle\cos 2\theta_j\rangle = \langle\sin 2\theta_j\rangle = \langle\cos 2(\theta_j+\theta_k)\rangle = \langle\sin 2(\theta_j+\theta_k)\rangle = 0 \tag{4.15}$$

That means that first term will be identically zero

$$\langle \mathbf{q}_j \rangle = 0 \tag{4.16}$$

and we write $\lambda(\mathbf{h})$ to second order,

$$\begin{aligned}
\lambda(\mathbf{h}) &= \frac{1}{2N} \left\langle \sum_{j,k}^{N} (\hat{h} \cdot \mathbf{q}_j)(\hat{h} \cdot \mathbf{q}_k) \right\rangle + \mathcal{O}(h^4) \\
&= \frac{h^2}{2N} \frac{1}{2} \left\langle \sum_{j,k}^{N} \mathbf{q}_j \cdot \mathbf{q}_k \right\rangle + \mathcal{O}(h^4) \\
&= \frac{h^2}{4N} \left\langle \sum_{j,k}^{N} \cos 2\theta_j \cos 2\theta_k \right\rangle + \mathcal{O}(h^4), \quad \hat{h} = \hat{x} \\
&= \frac{h^2}{4N} \left\langle \sum_{j,k}^{N} \sin 2\theta_j \sin 2\theta_k \right\rangle + \mathcal{O}(h^4), \quad \hat{h} = \hat{y} \\
&= \frac{h^2}{4N} \left\langle \sum_{j,k}^{N} \cos 2(\theta_j - \theta_k) \right\rangle + \mathcal{O}(h^4) \\
&= \frac{\chi}{4} h^2 + \mathcal{O}(h^4)
\end{aligned} \tag{4.17}$$

where χ is the two-fold/two-body susceptibility

$$\chi = N \left\langle s^2 \right\rangle = \left\langle \frac{1}{N} \sum_{j,k=1}^{N} \cos 2(\theta_j - \theta_k) \right\rangle \tag{4.18}$$

If there are no correlations between the molecules only $j = k$ terms would contribute to the sum and the susceptibility would be $\chi = 1$. It is of course the case that $\lambda(\mathbf{h})$ only depends on the modulus of the field and not on its direction. Consequently the vector-order parameter is also pointing in the direction $\hat{h}$ of the field $\mathbf{h}$ and we can see that by differentiating the spherically symmetric cumulant function. The vector-equation

of state reads,

$$\begin{aligned}\mathbf{Q} &= \nabla\lambda(\mathbf{h}), \quad \nabla_a = \frac{\partial}{\partial h_a} \\ &= \nabla\lambda(h), \quad h = |\mathbf{h}| = \sqrt{h_1^2 + h_2^2} \\ &= \frac{\partial\lambda(h)}{\partial h}\hat{h}\end{aligned} \tag{4.19}$$

$$Q(h) = \frac{\partial\lambda(h)}{\partial h} = \frac{\chi}{2}h + \mathcal{O}(h^3) \Leftrightarrow h(Q) = \frac{2}{\chi}Q + \mathcal{O}(Q^3) \tag{4.20}$$

which means that the vector-equation of state in equation 4.10 simplifies to a scalar one and the determination of the rate function boils down to a simple, one-dimensional reversible work integral

$$\begin{aligned}I(\mathbf{Q}) &= \frac{\partial\lambda(h)}{\partial h}\hat{h}\cdot h\hat{h} - \lambda(\mathbf{h}) \\ &= h\frac{\partial\lambda(h)}{\partial h} - \lambda(h) \\ &= \int_0^Q h(Q')dQ'\end{aligned} \tag{4.21}$$

At the central limit theory level of analysis the expression for $h(Q)$ is given by equation 4.20 and the rate function and the probability distribution are

$$I(\mathbf{Q}) = \frac{Q^2}{\chi} \tag{4.22}$$

$$P(\mathbf{Q}) \sim \exp\left(-NI(\mathbf{Q})\right) = \exp\left(-\frac{N}{\chi}Q^2\right) \tag{4.23}$$

In terms of the largest eigenvalue $s = Q$ of the second rank tensor $\mathcal{Q}$ the probability distribution $p(s)$ is given by equation 4.8,

$$p(s) \sim s\exp\left(-\frac{N}{\chi}s^2\right) \tag{4.24}$$

This is the **central-limit theory** answer for the probability distribution of the order parameter s of two-dimensional isotropic liquid crystals and of course it is a gaussian distribution (technically it is a Maxwellian because of the Jacobian prefactor). With molecular dynamics simulation we can calculate the exact answer for $p(s)$ for Gay-Berne

molecules. From the simulated $p(s)$ we can also calculate χ where $\chi = N\langle s^2 \rangle$. If the liquid crystal molecules do not interact then $\chi = 1$ and

$$p(s) \sim s \exp\left(-Ns^2\right) \tag{4.25}$$

which corresponds to liquid crystals in the gas phase where the distances between the molecules are extremely large (ideal gas).

4.3 The weak correlation/strong fluctuation limit: Mean-field theory

As we saw in chapter 3, when h is large, molecules are independent from each other only interacting with each other via a mean field ϵ. The cumulant function in that limit goes exactly to the mean field answer (see equation 3.38) and it is easy to calculate because we are free to choose $\hat{h}$ to point along any direction. In this case we may say that $\hat{h}$ is parallel to the x-axis,

$$\begin{aligned}
\lambda(\mathbf{h}) &= \ln \left\langle \exp\left(\mathbf{q}_j \cdot \mathbf{h}\right) \right\rangle_{\rho(\hat{\Omega}_j)} \\
&= \ln \frac{\int d\hat{\Omega}_j \exp\left(\left(h+\epsilon\right) \mathbf{q}_j \cdot \hat{h}\right)}{\int d\hat{\Omega}_j \exp\left(\epsilon\, \mathbf{q}_j \cdot \hat{h}\right)}, \quad \mathbf{q}_j \cdot \hat{h} = \cos 2\theta_j \\
&= \ln \frac{\int_0^{2\pi} d\theta_j \exp\left(\left(h+\epsilon\right)\, \cos 2\theta_j\right)}{\int_0^{2\pi} d\theta_j \exp\left(\epsilon\, \cos 2\theta_j\right)} \\
&= \ln \frac{I_0(h+\epsilon)}{I_0(\epsilon)}
\end{aligned} \tag{4.26}$$

$$\text{where} \quad I_0(z) = \frac{1}{2\pi} \int_0^{2\pi} d\theta \exp\left(z \cos 2\theta\right) \tag{4.27}$$

is the zeroth order modified Bessel function of the first kind. The denominator does not affect the thermodynamic formalism and it will eventually be absorbed into the normalization constant of $p(s)$. That means that we can ignore it and by setting $h+\epsilon = z$ we end up with the exceptionally simple expression for the cumulant generator,

$$\lambda(\mathbf{h}) = \ln I_0(z), \quad z = h + \epsilon \tag{4.28}$$

This limit of $\lambda(\mathbf{h})$ captures the spontaneous anisotropy that forms in isotropic liquid crystal systems and will be used in order to incorporate the large fluctuations of $p(s)$ into our formalism. The mean-field limit has extensively been used as a simple model of the nematic phase but has never been used in order to quantify anisotropic deviations in the isotropic phase. As we saw in equation 4.19 the order parameter points in the direction of the field,

$$\mathbf{Q} = \frac{\partial \lambda(z)}{\partial h}\frac{\partial h}{\partial z}\hat{h} = \frac{I_1(z)}{I_0(z)}\hat{h} \tag{4.29}$$

with $I_1(z)$ the modified Bessel function of first order. The modulus of the vector $\mathbf{Q}$ defines the scalar equation of state

$$Q = \frac{I_1(z)}{I_0(z)} \tag{4.30}$$

that saturates at $Q = 1$. Taking the large argument of Bessel functions,

$$Q = \frac{1 - \frac{3}{8z} - \frac{15}{128z^2} + \mathcal{O}(z^{-3})}{1 + \frac{1}{8z} + \frac{9}{128z^2} + \mathcal{O}(z^{-3})} = 1 - \frac{1}{2z} - \frac{1}{8z^2} + \mathcal{O}(z^{-3}) \tag{4.31}$$

Reverting the series yields

$$z = \frac{1}{2(1-Q)} + \frac{1}{4} + \mathcal{O}(1-Q) \tag{4.32}$$

and replacing the value for the field $\mathbf{h}$ we get,

$$h(Q) = \frac{1}{2(1-Q)} + \eta + \mathcal{O}(1-Q) \tag{4.33}$$

where $\eta = \frac{1}{4} - \epsilon$ is the orientational coefficient that we will calculate from a simulation just like the susceptibility χ in the weak-field regime. This divergent term will capture the large fluctuations in the expression for $p(s)$.

4.4 Pade interpolation and a new expression for the free energy

The two limiting behaviors of the equation of state are given by equation 4.20 and equation 4.33

$$h(Q) = \begin{cases} \frac{2}{\chi}Q + \mathcal{O}(Q^3), & Q \to 0 \\ \\ \frac{1}{2(1-Q)} + \eta + \mathcal{O}\left(1-Q\right), & Q \to 1 \end{cases} \tag{4.34}$$

Interestingly, there are no even powers in the equation of state and this has to do with symmetry. This is true because $\lambda(\mathbf{h})$ cannot depend on inversion of the field $\lambda(\mathbf{h}) = \lambda(-\mathbf{h})$ and so it only involves even powers of h which means that its derivative will only involve odd powers. The weak field limit of $Q(h)$ is linear to the field and in the limit of strong fields the order parameter Q is the ratio between $I_1(z)$ (odd) and $I_0(z)$ (even) making it odd overall. Applying the method of Pade interpolation between the linear response regime and the pole at $Q \to 1$ gives a full expression for the equation of state. A minimal Pade interpolant that has the correct symmetry and reproduces the proper limits is the Pade[5/2]

$$h(Q) = \frac{2}{\chi}\frac{Q + AQ^3 + BQ^5}{1 - Q^2} \tag{4.35}$$

$$A = -2 + \frac{\chi}{2}\left(\eta + \frac{9}{4}\right), \quad B = 1 - \frac{\chi}{2}\left(\eta + \frac{5}{4}\right) \tag{4.36}$$

The reader can verify that this simple ratio of polynomials indeed gives the correct limits. Also the denominator is even and reproduces the pole at $Q = 1$ while the numerator is odd giving the correct symmetry overall. The constants A and B are functions of the

microscopic correlation parameters χ and η that we will calculate numerically from a computer simulation. The probability distribution $p(s)$ can now be evaluated analytically from the reversible work theorem in equation 4.21,

$$I(\mathbf{Q}) = \frac{\delta}{2}Q^2 - \frac{B}{2\chi}Q^4 - \frac{1}{2}\ln\left(1-Q^2\right) \tag{4.37}$$

$$P(\mathbf{Q}) \sim \left(1-Q^2\right)^{\frac{N}{2}} \exp\left\{-N\left[\left(\frac{\delta}{2}\right)Q^2 - \left(\frac{1+\delta}{4}\right)BQ^4\right]\right\} \tag{4.38}$$

$$p(s) \sim s\left(1-s^2\right)^{\frac{N}{2}} \exp\left\{-N\left[\left(\frac{\delta}{2}\right)s^2 - \left(\frac{1+\delta}{4}\right)Bs^4\right]\right\} \tag{4.39}$$

$$\delta = \frac{2}{\chi} - 1, \quad -1 \leq \delta \leq 1 \tag{4.40}$$

Notice how the independent limit shows up as probability in the power of N and how there is a new term correcting for the mean field effect. This new probability distribution (equation 4.39) will be proven to be a very powerful tool in analysing large fluctuations. The free energy per liquid crystal molecule we derived with our method (equation 4.37) might seem unfamiliar but in the limit of very small Q we get the familiar Landau-De Gennes expression,

$$I(\mathbf{Q}) = \frac{a}{2}Q^2 + \frac{b}{4}Q^4 + \ldots \quad a = \frac{2}{\chi} \quad \text{and} \quad b = \frac{5}{4} - \delta + \eta \tag{4.41}$$

where the constants a and b are positive and depend on the thermodynamic conditions. This novel approach provides a molecular explanation of the constants. As the system approaches criticality, the fluctuations grow and the free energy starts to feel a logarithmic singularity.

4.5 Similarities with 2D magnetism in the XY model

The problem of characterizing the probability density of nematic order is very closely related to that of magnetism in 2D. Liquid crystal molecules with up and down symmetry

are represented as headless vectors and magnetic moments on a lattice are represented as typical vectors. The probability distribution of the total magnetization and the probability distribution of total nematic order $P(\mathbf{Q})$ share the same cumulant generator and as we will see can be described by the same Pade[5/2] equation of state.

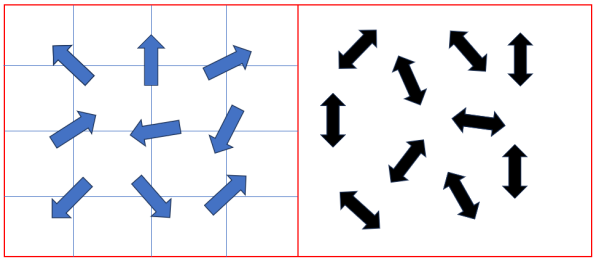

Figure 4.1: On the left we can see magnetic moments lying on lattice sites. On the rights we can see the orientation vectors of anisotropic liquid crystal molecules with up-down symmetry.

Let us imagine a two-dimensional square lattice (See left part of figure 4.1) with a magnetic moment $\mathbf{s}_j$ placed on each lattice site j,

$$\mathbf{s}_j^T = (\cos\theta_j, \sin\theta_j), \quad \left(\mathbf{q}_j^T = (\cos 2\theta_j, \sin 2\theta_j)\right) \tag{4.42}$$

$$\text{for k-fold order} \quad \mathbf{x}_j^T = (\cos k\theta_j, \sin k\theta_j) \tag{4.43}$$

The difference between one-fold (k=1) orientational order (magnetic moments $\mathbf{s}_j$) and two-fold (k=2) orientational order ($\mathbf{q}_j$) will not make a difference in our analysis as we will see later on. Only neighboring spins interact and the spins are able to rotate around (instead of just up and down like the Ising model). The simplest magnetic Hamiltonian we can use is the XY-model Hamiltonian defined as,

$$H = -J \sum_{j,k}^{N} \cos\left(\theta_j - \theta_k\right) \tag{4.44}$$

Depending on the relative orientation of the neighboring magnetic moments the interaction energy varies continuously form -1 to 1, where parallel spins contribute +1 to the sum

and vertical neighbohrs contribute 0. Anti-parallel neighboring spins contribute -1. The magnetization is defined as,

$$\mathbf{M}^T = \frac{1}{N}\sum_{j=1}^{N} \mathbf{s}_j^T = (M_1, M_2) \tag{4.45}$$

$$M_1 = \frac{1}{N}\sum_{j=1}^{N} s_{jx} = \frac{1}{N}\sum_{j=1}^{N} \cos\theta_j, \quad M_2 = \frac{1}{N}\sum_{j=1}^{N} s_{jy} = \frac{1}{N}\sum_{j=1}^{N} \sin\theta_j \tag{4.46}$$

$$\mu = |\mathbf{M}| = \sqrt{M_1^2 + M_2^2} \tag{4.47}$$

The scalar magnetic order parameter μ simplifies to,

$$\mu = \frac{1}{N}\sqrt{\sum_{j,k=1}^{N} \cos\left(\theta_j - \theta_k\right)} \tag{4.48}$$

and goes from $\mu = 0$ (complete isotropy) to $\mu = 1$ (perfect alignment of spins $\mathbf{s}_j$). We wish to describe the probability density $P(\mathbf{M})$ in terms of our large-deviation theory,

$$P(\mathbf{M}) \sim e^{-NI(\mathbf{M})}, \quad \int P(\mathbf{M}) d\mathbf{M} = 1 \tag{4.49}$$

$$P(\mu) = 2\pi\mu P(\mathbf{M}) \tag{4.50}$$

This probability density has been studied before (See for example [3] and [5]) but the large deviations of a strongly interacting system have not been captured. The 2D XY magnet shows a continuous Kosterlitz-Thouless type transition between a high-temperature paramagnetic phase and a low temperature quasi-long range ordered phase. The critical point is located at $1/(\beta_c J) \approx 0.8935$ [30]. There is a finite (not infinite) correlation length that grows as we approach the critical point in the paramagnetic phase similarly to liquid crystals in the isotropic phase close to the isotropic/nematic transition. Although the underlying mechanism has to do with binding-unbinding of vortices [30] instead of disclinations (as is the case for liquid crystals [36]) we expect a non-gaussian profile in the

density $P(\mathbf{M})$ as we approach $1/(\beta_c J)$.

For very weak fluctuations we expect the cumulant expansion to be dominated by the second order term. We start from the definition of $\lambda(\mathbf{h})$ ($\mathbf{h}$ is a magnetic field conjugate to the total magnetic moment $\mathbf{M}$),

$$e^{N\lambda(\mathbf{h})} = \left\langle e^{N\mathbf{M}\cdot\mathbf{h}} \right\rangle \tag{4.51}$$

and expand as a power series,

$$\lambda(\mathbf{h}) \approx \frac{N}{2}\mathbf{h}\cdot\langle\delta\mathbf{M}\delta\mathbf{M}\rangle\cdot\mathbf{h} + ... = \frac{\chi_1}{4}h^2 + O(h^4), \quad h \to 0 \tag{4.52}$$

$$\delta\mathbf{M} = \mathbf{M} - \langle\mathbf{M}\rangle \tag{4.53}$$

Identical answer as in equation 4.17 but with a different susceptibility. Here we have χ_1 which is the one-fold/two-body magnetic susceptibility

$$\chi_1 = \left\langle \frac{1}{N}\sum_{j,k=1}^{N} \cos\left(\theta_j - \theta_k\right) \right\rangle = N\left\langle \mu^2 \right\rangle \tag{4.54}$$

$$\text{for k-fold order} \quad \chi_k = \left\langle \frac{1}{N}\sum_{j,k=1}^{N} \cos k(\theta_j - \theta_k) \right\rangle \tag{4.55}$$

Because the magnetic free energy per particle cannot possibly depend on inversion symmetry of the field,

$$\lambda(\mathbf{h}) = \lambda(-\mathbf{h}) \tag{4.56}$$

the odd terms need to be identically zero. Notice how we get the same result as in the case of liquid crystals. The truncation of $\lambda(\mathbf{h})$ up to second order is exactly true for weak fluctuations regardless of the strength of the correlations between the magnetic moments.

The equation of state now connects the magnetization with the external magnetic field,

$$\mathbf{M} = \nabla\lambda(\mathbf{h}) = \frac{\partial\lambda(h)}{\partial h}\hat{h}, \quad \mu = \frac{\partial\lambda(h)}{\partial h} = \frac{\chi_1}{2}h \tag{4.57}$$

The equation of state between the intensive magnetic field h and the extensive magnetization μ is the same as in the case of liquid crystals (equation 4.19) but with different susceptibility.

The large-field limit is the independent-mean field cumulant function which astonishingly is **exactly** the same as the mean-field answer for liquid-crystals (equation 4.26),

$$\lambda(\mathbf{h}) = \ln\left\langle \exp\left(\mathbf{s}_j \cdot \mathbf{h}\right)\right\rangle_{\rho(\hat{s}_j)}, \quad \mathbf{s}_j \cdot \mathbf{h} = h\cos\theta_j \tag{4.58}$$

where we chose the field **h** to be parallel to the x axis so that we can easily evaluate the integral in terms of Bessel functions. The answer is the same (we ignore the constant term) and involves the mean-field ϵ,

$$\lambda(\mathbf{h}) = \ln I_0(z), \quad z = h + \epsilon \tag{4.59}$$

In fact this is true for any type of k-fold orientational order. The independent k-rotor limit requires the evaluation of ,

$$\lambda(\mathbf{h}) = \ln\left[\frac{1}{2\pi}\int_0^{2\pi}\exp\left(z\cos k\theta\right)d\theta\right] = \ln I_0(z), \quad \forall k \in \{1, 2, 3, ...\} \tag{4.60}$$

where $I_0(z)$ is the zeroth order modified Bessel function. The corresponding equation of state that connects the magnetic field with the magnetization is,

$$\mu = \frac{\partial\lambda(z)}{\partial z} = \frac{I_1(z)}{I_0(z)} \tag{4.61}$$

The same answer as in the case of 2D liquid crystals. In the large field limit the equation

of state,

$$\mu = 1 - \frac{1}{2z} - \frac{1}{8z^2} + ..., \quad h \to \infty \tag{4.62}$$

Similarly to liquid crystals we have the following limits,

$$h(\mu) = \begin{cases} \frac{2}{\chi_1}\mu + O(\mu^3), & \mu \to 0 \\ \\ \frac{1}{2(1-\mu)} + \eta + \mathcal{O}\left(1-\mu\right), & \mu \to 1 \end{cases} \tag{4.63}$$

but with χ_1 in the weak-field limit and $\eta = \frac{1}{4} - \epsilon$ in the strong-field limit. The magnetic equation of state only depends on odd powers of μ and a minimal Pade[5/2] that simultaneously respects the symmetry and correctly reproduces the two limits is (as in equation 4.35),

$$h(\mu) = \frac{2}{\chi_1}\frac{\mu + A_1\mu^3 + B_1\mu^5}{1-\mu^2} \tag{4.64}$$

$$A_1 = -2 + \frac{\chi_1}{2}\left(\eta + \frac{9}{4}\right), \quad B_1 = 1 - \frac{\chi_1}{2}\left(\eta + \frac{5}{4}\right) \tag{4.65}$$

The Gaertner-Ellis theorem dictates that,

$$I(\mathbf{M}) = \mathbf{M}\cdot\mathbf{h} - \frac{\partial\lambda(h)}{\partial h}, \quad \mathbf{M} = \frac{\partial\lambda(h)}{\partial h}\hat{h} \tag{4.66}$$

$$\Leftrightarrow I(\mathbf{M}) = \mu h - \frac{\partial\lambda(h)}{\partial h}, \quad \mu = \frac{\partial\lambda(h)}{\partial h} \tag{4.67}$$

which reduces via integration by parts to the reversible work theorem for the magnetization free energy per spin,

$$I(\mathbf{M}) = \int_0^\mu h(\mu')d\mu' \tag{4.68}$$

Applying the theorem to the Pade equation of state gives us,

$$I(\mathbf{M}) = \frac{\delta_1}{2}\mu^2 - \frac{B_1}{2\chi_1}\mu^4 - \frac{1}{2}\ln\left(1-\mu^2\right) \tag{4.69}$$

$$\delta_1 = \frac{2}{\chi_1} - 1, \quad -1 \leq \delta_1 \leq 1 \tag{4.70}$$

The corresponding probability density of $\mathbf{M}$ is

$$P(\mathbf{M}) \sim \left(1-\mu^2\right)^{\frac{N}{2}} \exp\left\{-N\left[\left(\frac{\delta_1}{2}\right)\mu^2 - \left(\frac{1+\delta_1}{4}\right)B_1\mu^4\right]\right\} \tag{4.71}$$

$$P(\mu) \sim \mu^2\left(1-\mu^2\right)^{\frac{N}{2}} \exp\left\{-N\left[\left(\frac{\delta_1}{2}\right)\mu^2 - \left(\frac{1+\delta_1}{4}\right)B_1\mu^4\right]\right\} \tag{4.72}$$

This expression for the probability distribution of magnetism in 2D is **identical** to the probability distribution of nematic order (equation 4.38). In the results chapter we will show how this equation compares with the gaussian density of the magnetization,

$$P(\mathbf{M}) \sim \exp\left(-\frac{N}{\chi_1}\mu^2\right) \tag{4.73}$$

$$P(\mu) \sim \mu^2 \exp\left(-\frac{N}{\chi_1}\mu^2\right) \tag{4.74}$$

For temperatures close to the critical point, the gaussian density is inaccurate and it is necessary to use equation 4.71 instead.

CHAPTER 5

Large-deviation theory perspective on three-dimensional polymer end-to-end distances

5.1 Large deviations theory set-up of the problem

Before we proceed to three-dimensional liquid crystals, we will discuss an easier three-dimensional problem: end-to-end distance of an interacting chain of stiff bonds. In chapter 2 we studied the random-flight/ideal chain model where there are no correlations between the bond vectors $\hat{\Omega}_l$ and the potential energy between atoms (if we have N bonds that means that we have N+1 atoms) in the idealized polymer was zero. Now, we will study the case where there are arbitrary interactions between the atoms in the chain.

The vector-order parameter of the system is the end-to-end distance as in the random flight case,

$$N\mathbf{r} = \mathbf{R} = \sum_{l=1}^{N} \hat{\Omega}_l, \quad R = |\mathbf{R}| \tag{5.1}$$

where N identical and rigid links of unit length are strongly interacting with each other.

We will derive an expression for the interacting chain from large-deviation theory starting from the intensive/extensive relation between an externally applied field $\mathbf{h}$ and the end-to-end distance $\mathbf{R}$. More specifically we define the scaled cumulant generating function via the relation,

$$e^{N\lambda(\mathbf{h})} = \left\langle e^{\mathbf{h}\cdot\mathbf{R}} \right\rangle \tag{5.2}$$

where the brackets imply averaging over all possible orientations in three-dimensional space. In the limit of large number of polymer links N, large-deviation theory suggests that,

$$P(\mathbf{R}) \sim \exp\left(-NI(\mathbf{r})\right) \tag{5.3}$$

$$I(\mathbf{r}) = \mathbf{h}\cdot\mathbf{r} - \lambda(\mathbf{h}), \quad \mathbf{r} = \nabla_{\mathbf{h}}\lambda(\mathbf{h}) \tag{5.4}$$

Both free energies per bond are spherically symmetric as they will end up being independent from $\hat{h}$, $\lambda(\mathbf{h}) = \lambda(h)$. The two free energies are Legendre transforms of each other (equation 5.4) which implies that they also share that same spherical symmetry. This observation will drastically simplify our calculations as we only need to be concerned with $h = |\mathbf{h}|$ and not $\hat{h}$. Consequently the vector-order parameter $\mathbf{r}$ points in the direction of the field,

$$\begin{aligned} \mathbf{r} &= \nabla_{\mathbf{h}}\lambda(h) \\ &= \frac{\partial\lambda(h)}{\partial h}\hat{h} \\ &= r\,\hat{h}, \quad r = |\mathbf{r}| = \frac{\partial\lambda(h)}{\partial h} \end{aligned} \tag{5.5}$$

and the rate function $I(\mathbf{r})$ in equation 5.4 can be written as

$$I(r) = hr - \lambda(h), \quad r = \frac{\partial\lambda(h)}{\partial h} \tag{5.6}$$

Differentiating both sides with respect to r we get

$$\frac{\partial I(r)}{\partial r} = r\frac{\partial h}{\partial r} + h - \frac{\partial\lambda(h)}{\partial h}\frac{\partial h}{\partial r} = h(r) \tag{5.7}$$

and we recover the reversible work theorem,

$$I(r) = \int_0^r h(r')dr' \tag{5.8}$$

The free energy is equal to the work required to extend the polymer in some reversible manner. The relation $h(r)$ can be obtained by reverting $r = \frac{\partial \lambda(r)}{\partial r}$ and defines a polymer equation of state. Of course we do not know $\lambda(\mathbf{h})$ because it is impossible to solve equation 5.2 analytically for complicated polymer Hamiltonians. Nevertheless the extreme limits of $\lambda(\mathbf{h})$ as we saw in other applications can be evaluated. When the correlations between the bonds are strong and the applied force is weak, we can use central-limit theorem statistics. In that limit we will recover the linear relation between force and response; Hooke's law. When the correlations between the bonds are weak and the applied force is strong, $\lambda(\mathbf{h})$ goes to the mean field answer. The non-linearity of the independent bond limit will capture the strong fluctuations of $P(\mathbf{R})$.

5.2 Central-limit theory of the interacting polymer

In the weak $\mathbf{h}$ limit we may write the generating function as a power series (assuming that we are not close to a critical point and the free energy is an analytic function),

$$\exp\left(N\lambda(\mathbf{h})\right) = \langle \exp\left(F\right) \rangle = \exp\left(\langle F \rangle + \frac{1}{2}\langle (\delta F)^2 \rangle + ... \right) \tag{5.9}$$

$$F = \mathbf{R} \cdot \mathbf{h} = \sum_{l=1}^{N} \hat{\Omega}_l \cdot \mathbf{h} \tag{5.10}$$

Since we are in the isotropic phase the first term averages to zero and because we apply a very weak field, the second term will be dominating over higher order terms. By truncating the series we have,

$$\lambda(\mathbf{h}) = \frac{h^2}{2N} \sum_{l,l'}^{N} \hat{h} \cdot \left\langle \hat{\Omega}_l \hat{\Omega}_{l'} \right\rangle \cdot \hat{h} + \mathcal{O}(h^4) \tag{5.11}$$

The next term in series is going to be proportional to h^4 and not h^3 because all the odd terms are zero. This is a result of the inversion symmetry of the problem since it does not matter whether we define the end-to-end distance vector as $\mathbf{R}$ or $-\mathbf{R}$. The choice of the first atom in the polymer as first and the last atom as last is abstract and thermodynamic potentials do not depend on it.

The second rank tensor in equation 5.11 simplifies because of isotropic symmetry. More specifically, the element μ, ν of the tensor is

$$\left\langle (\hat{\Omega}_l)_\mu (\hat{\Omega}_{l'})_\nu \right\rangle = \frac{1}{3} \left\langle \hat{\Omega}_l \cdot \hat{\Omega}_{l'} \right\rangle \delta_{\mu,\nu} \tag{5.12}$$

The non-diagonal elements will average to zero and the free energy simplifies to,

$$\lambda(h) = \frac{\chi}{6} h^2 + \mathcal{O}(h^4), \quad h \to 0 \tag{5.13}$$

$$\chi = \left\langle \frac{1}{N} \sum_{l,l'=1}^{N} \hat{\Omega}_l \cdot \hat{\Omega}'_l \right\rangle \tag{5.14}$$

The corresponding scalar-equation of state is given by equation 5.7,

$$h(r) = \frac{\partial \lambda(h)}{\partial h} = \frac{3}{\chi} r + \mathcal{O}(r^3), \quad r \to 0 \tag{5.15}$$

As anticipated we recovered the linear strain-stress relation known as Hooke's law (It differs from the random-flight/weak-field answer by a factor of $\frac{1}{\chi}$) The elastic free energy will be given be direct integration of the equation of state (equation 5.8),

$$I(\mathbf{r}) = \int_0^r \left[\frac{3}{\chi} r' + \mathcal{O}(r'^3) \right] dr' = \frac{3}{2\chi} r^2 + \mathcal{O}(r^4) \tag{5.16}$$

and the corresponding probability density is given the large-deviation principle in equation 5.3

$$P(\mathbf{R}) \sim \exp\left[-\frac{3N}{2\chi} r^2 \right] \tag{5.17}$$

We can calculate the corresponding Maxwell density by multiplying with the surface of a three-dimensional sphere

$$P(r) \sim r^2 \exp\left[-\frac{3N}{2\chi} r^2\right] \tag{5.18}$$

This expression for $P(r)$ correctly gives the anticipated scaling for $\langle r^2 \rangle$ (We take $N \to \infty$ in order to extend the upper limit of integration from 1 to ∞),

$$\begin{aligned} \langle r^2 \rangle &= \frac{\int_0^\infty r^4 \exp\left[-ar^2\right]}{\int_0^\infty r^2 \exp\left[-ar^2\right]}, \quad a = \frac{3N}{2\chi} \\ &= \frac{\Gamma(\frac{5}{2})}{\Gamma(\frac{3}{2})} \frac{1}{a}, \quad \Gamma(z) = \int_0^\infty t^{z-1} e^{-t} dt \\ &= \frac{3}{2} \frac{2\chi}{3N} \\ &= \frac{\chi}{N} \end{aligned} \tag{5.19}$$

In the limit of no interactions between the atoms in the polymer, the bond-susceptibility in definition 5.14 becomes $\chi = 1$ since only $l = l'$ terms will contribute to the sum and we get the random-flight gaussian density 2.12 with the corresponding scaling $\sqrt{\langle r^2 \rangle} = 1/\sqrt{N}$. Lastly, we see from 5.17 that $\chi = N\langle r^2 \rangle$ which suggests a route to calculating χ numerically from a simulated $P(r)$.

5.3 The strong-field limit

The central-limit theory answer in equation 5.18 is only accurate when the polymer end-to-end distance stays very small on average. One wonders how the probability distribution would change, if the bonds spent a significant amount of time being aligned. High values of end-to-end distance map to very strong applied forces and as we saw in chapter 3, the cumulant generator goes to the mean-field answer,

$$\lambda(\mathbf{h}) = \ln \left\langle \exp\left(\mathbf{h} \cdot \hat{\Omega}_j\right) \right\rangle_{\rho(\hat{\Omega}_l)}, \quad h \to \infty \tag{5.20}$$

where $\rho(\hat{\Omega}_l)$ is the anisotropic single-bond probability distribution

$$\rho(\hat{\Omega}_l) = \frac{\exp(\epsilon \cdot \hat{\Omega}_l)}{\int d\hat{\Omega}_l \exp(\epsilon \cdot \hat{\Omega}_l)} \tag{5.21}$$

and ϵ is the mean field that a single bond feels. In that limit the field $\mathbf{h}$ is very strong and can be chosen to point along the $\hat{z}$ direction where we can solve the integral exactly. The mean field ϵ also points in that same direction acting as a screening effect,

$$(\mathbf{h} + \epsilon) \cdot \hat{\Omega} = z \cos\theta_l, \quad z = h + \epsilon \tag{5.22}$$

We can calculate 5.20 exactly

$$\lambda(h) = \ln \langle \exp(z \cos\theta_l) \rangle = \ln\left(\frac{\sinh z}{z}\right) \tag{5.23}$$

Notice how this is the real-field version of the single molecule generating function $\psi(k)$ we derived in equation 2.8 for the random flight. Assuming that the bonds have unit length $d = 1$ we can say $z = -ik$ and get $\psi(k)$,

$$\lambda(z) = \ln\left(\frac{\sinh z}{z}\right) = \ln\left(\frac{\sinh(-ik)}{-ik}\right) = \ln\left(\frac{\sin k}{k}\right) = \ln\psi(k) \tag{5.24}$$

The strong-field ($z \to \infty$) implies that the equation of state (equation 5.7),

$$r = \frac{\partial\lambda(h)}{\partial h}\frac{\partial h}{\partial z} = \mathcal{L}(z) \tag{5.25}$$

and for large arguments the Langevin function $\mathcal{L}(z)$ (equation 2.24) takes the simple form

$$\mathcal{L}(z) = \coth z - \frac{1}{z} \to 1 - \frac{1}{z} + \mathcal{O}(1) \tag{5.26}$$

$$\text{because} \quad \lim_{z\to\infty} \coth z = 1 \tag{5.27}$$

where the next correction in the $\coth(z)$ expansion is exponentially small. Putting back the h variable,

$$r(h) = 1 - \frac{1}{h+\epsilon} + \mathcal{O}(1) \tag{5.28}$$

and inverting the equation of state we end up with,

$$h(r) = \frac{1}{1-r} - \epsilon + \mathcal{O}(1-r), \quad r \to 1 \tag{5.29}$$

The strong-field limit of the equation of state provides the non-linearity that will capture the fluctuations of $P(r)$. The pole at $r = 1$ is a result of the saturation that happens when we apply stronger and stronger forces to the polymers; the bonds will align more and more and the end-to-end distance will approach 1 asymptotically. As we saw in other applications the simplicity of 5.29 will allow a simple Pade interpolation that gives us access to intermediate values of h.

5.4 Pade' interpolation between weak- and strong-field limits

Along the same lines with the liquid crystal case and the magnetization of the XY model, we use the variable $\eta = -\epsilon$ for the constant correction at the large field limit. The two limits now read,

$$h(r) = \begin{cases} \frac{3}{\chi} r + O(r^3), & r \to 0 \\ \\ \frac{1}{(1-r)} + \eta + \mathcal{O}(1-r), & r \to 1 \end{cases} \tag{5.30}$$

The simplest Pade interpolant that respects the pole at $r = 1$, has an odd symmetry and successfully goes to the limits in equation 5.30 is,

$$h(r) = \frac{3}{\chi}\frac{r + Ar^3 + Br^5}{1 - r^2} \tag{5.31}$$

$$A + B + 1 = \frac{2\chi}{3} \tag{5.32}$$

$$\frac{3B}{4\chi} = \frac{1}{4}(\delta + \eta - \frac{1}{2}), \quad \delta = \frac{3}{\chi} - 2 \tag{5.33}$$

where δ is the polymer correlation index that goes from -2 (completely correlated) to 1 (completely uncorrelated). The denominator in equation 5.31 is even and at the same time diverges as $r \to 1$ while the numerator is odd and has just enough terms in order to include the constant term η from the ordered limit. Equation 5.31 goes to the random flight Pade[5/2] we calculated in chapter 2 by setting $\delta = 1$ and $\eta = 0$ (equation 2.33)

Application of the reversible work theorem in equation 5.8 gives us the elastic free energy,

$$I(\mathbf{r}) = \int_0^r \frac{3}{\chi}\frac{r' + Ar'^3 + Br'^5}{1 - r'^2}dr' = \frac{\delta}{2}r^2 - \frac{3B}{4\chi}r^4 - \ln(1 - r^2) \tag{5.34}$$

and finally the probability density is,

$$P(\mathbf{R}) \sim (1 - r^2)^N \exp\left(-N\frac{\delta}{2}r^2\right)\exp\left(N\frac{3B}{4\chi}r^4\right) \tag{5.35}$$

and the probability distribution of the reduced end-to-end distance is

$$P(r) \sim r^2(1 - r^2)^N \exp\left(-N\frac{\delta}{2}r^2\right)\exp\left(N\frac{3B}{4\chi}r^4\right) \tag{5.36}$$

For very small end-to-end distances 5.36 goes to the gaussian probability density 5.18 and thus it is a generalization of it,

$$P(r) \sim r^2 \exp\left(-N\frac{3}{2\chi}r^2\right) \tag{5.37}$$

Equation 5.36 is the final large-deviation theory answer for an interacting polymer. It includes two parameters δ and η that physically correspond to the two-body bond correlations and the mean-field interactions between the bonds. We can calculate these two parameters numerically from a computer simulation of $P(r)$. While χ is taken from the second moment of some simulated $P(r)$, we could use information from the first moment $\langle r \rangle$ in order to specify η. This way we have an efficient algorithm of calculating very small probabilities in the tail of the distribution by taking information from the first two moments.

CHAPTER 6

Large-deviation theory perspective on the nematic order of three-dimensional isotropic liquid crystals

6.1 Large-deviation theory order parameter

For three-dimensions, we set $D = 3$ in the definition for the tensor in equation 1.2 and get the 3 by 3 symmetric and traceless matrix

$$\mathcal{Q} = \frac{1}{N}\sum_{j=1}^{N} \mathbf{q}_j = \begin{pmatrix} Q_1 & Q_4 & Q_5 \\ Q_4 & Q_2 & Q_6 \\ Q_5 & Q_6 & Q_3 \end{pmatrix} \tag{6.1}$$

$$Tr(\mathcal{Q}) = Q_1 + Q_2 + Q_3 = 0 \Leftrightarrow (Q_1 + Q_2)^2 = Q_3^2 \tag{6.2}$$

Assuming that the biaxial fluctuations (they correspond to $Tr(\mathcal{Q}^3)$) are small, the only rotational invariant of the tensor is $Tr(\mathcal{Q}^2)$. The probability distribution $P(\mathcal{Q})$ will only depend on $Tr(\mathcal{Q}^2)$ which is equivalent to saying that the probability distribution is spherically symmetric and will only depend on the modulus of the large-deviation theory vector-order parameter. So which vector should we choose? The simplest idea is to use the five independent elements of the matrix directly as ingredients for the vector $\mathbf{Q}^T = (Q_1, Q_2, Q_3, Q_4, Q_5, Q_6)$ just as we did in the case of two-dimensional liquid crystals (See definition 4.4). It is straightforward to see that this is not consistent with our large-deviation theory formalism because the modulus of $\mathbf{Q}$ is not proportional to $Tr(\mathcal{Q}^2)$,

$$\begin{aligned} Q^2 &= Q_1^2 + Q_2^2 + Q_3^2 + Q_4^2 + Q_5^2 + Q_6^2 \\ &= Q_1^2 + Q_2^2 + (Q_1 + Q_2)^2 + Q_4^2 + Q_5^2 + Q_6^2 \\ &= 2(Q_1^2 + Q_2 + Q_1 Q_2) + Q_4^2 + Q_5^2 + Q_6^2 \\ &\not\propto 2(Q_1^2 + Q_2^2 + Q_1 Q_2 + Q_4^2 + Q_5^2 + Q_6^2) = Tr(\mathcal{Q}^2) \end{aligned} \tag{6.3}$$

It turns out that the elements $Q_\alpha, (\alpha = \{1, 2, 4, 5, 6\})$ can be written in terms of complex $l = 2$ spherical harmonics,

$$Y_{2,m} = \frac{1}{N} \sum_{j=1}^{N} y_{2,m}(\hat{\Omega}_j), \quad m = -2, ...2 \tag{6.4}$$

or perhaps more conveniently in terms of their real counterparts (also known as tesseral harmonics [4]),

$$R_{2,m} = \frac{1}{N} \sum_{j=1}^{N} r_{2,m}(\hat{\Omega}_j), \quad m = -2, ...2 \tag{6.5}$$

where we made the distinction between N-body quantities that refer to the entire system and molecular quantities that refer to single molecule j. The Cartesian elements of the

tensor can be written as

$$Q_\alpha = \left(\frac{1}{N} \sum_{j=1}^{N} \mathbf{q}_j(\hat{\Omega}_j) \right)_\alpha = \left(\frac{1}{N} \sum_{j=1}^{N} \frac{3}{2} \hat{\Omega}_j \hat{\Omega}_j - \frac{1}{2} \mathbf{1} \right)_\alpha \tag{6.6}$$

with $Q_1 = Q_{xx}, Q_2 = Q_{yy}, Q_3 = Q_{zz}, Q_4 = Q_{xy}, Q_5 = Q_{xz}, Q_6 = Q_{yz}$. We drop the l part of the harmonic functions for notational clarity,

$$R_2 = \frac{1}{\sqrt{2}}(Y_2 + Y_{-2}) = \sqrt{\frac{5}{12\pi}}(Q_1 - Q_2) \tag{6.7}$$

$$R_1 = \frac{1}{\sqrt{2}}(Y_{-1} - Y_1) = \sqrt{\frac{5}{3\pi}} Q_5 \tag{6.8}$$

$$R_0 = Y_0 = \sqrt{\frac{5}{4\pi}} Q_3 = -\sqrt{\frac{5}{4\pi}}(Q_1 + Q_2) \tag{6.9}$$

$$R_{-1} = \frac{i}{\sqrt{2}}(Y_1 + Y_{-1}) = \sqrt{\frac{5}{3\pi}} Q_6 \tag{6.10}$$

$$R_{-2} = \frac{i}{\sqrt{2}}(Y_{-2} - Y_2) = \sqrt{\frac{5}{3\pi}} Q_4 \tag{6.11}$$

Equations 6.7-6.11 are true for the corresponding molecular quantities $\mathbf{q}_j(\hat{\Omega}_j)$, $y_m(\hat{\Omega}_j)$ and $r_m(\hat{\Omega}_j)$ as well. It is not hard to see now that the modulus of a 5 dimensional vector that consists of either the 5 N-body complex spherical harmonics or the 5 N-body real spherical harmonics is proportional to $Tr(\mathcal{Q}^2)$. However we shall use $R_m(\hat{\Omega}_j)$ because the complex functions lead to technical difficulties and inconsistencies with our theory later on. This happens because the 5 elements of the tensor are real functions and so the more natural basis of the problem is $R_m(\hat{\Omega}_j)$ instead of $Y_m(\hat{\Omega}_j)$. We define the large-deviation theory vector as

$$\mathbf{R} = \{R_m; m = -2, ..., 2\}, \quad R^2 = \mathbf{R} \cdot \mathbf{R} \tag{6.12}$$

$$R_m = \frac{1}{N} \sum_{j=1}^{N} r_m(\hat{\Omega}_j), \quad m = \{-2, ..., 2\} \tag{6.13}$$

where the modulus R is a function of $Tr(\mathcal{Q}^2)$,

$$\begin{aligned} R^2 &= R_{-2}^2 + R_{-1}^2 + R_0^2 + R_1^2 + R_2^2 \\ &= \frac{5}{3\pi}(Q_4^2 + Q_5^2 + Q_6^2) + \frac{5}{4\pi}\left[\frac{1}{3}(Q_1 - Q_2)^2 + (Q_1 + Q_2)^2\right] \\ &= \frac{5}{6\pi}\left[2(Q_4^2 + Q_5^2 + Q_6^2) + \frac{1}{2}(Q_1 - Q_2)^2 + \frac{3}{2}(Q_1 + Q_2)^2\right] \\ &= \frac{5}{6\pi}\left[2(Q_4^2 + Q_5^2 + Q_6^2 + Q_1^2 + Q_2^2 + Q_1 Q_2)\right] \\ &= \frac{5}{6\pi} Tr(\mathcal{Q}^2) \end{aligned} \tag{6.14}$$

The vector $\mathbf{R}$ together with a 5-dimensional vector field $\mathbf{h}$ will be the suitable large-deviation order parameter/conjugate field pair with a dot product,

$$\mathbf{h} \cdot \mathbf{R} = \sum_{m=-2}^{2} h_m R_m \tag{6.15}$$

The goal is to calculate the probability distribution of $\mathbf{R}$ via a large-deviation principle,

$$P(\mathbf{R}) \sim \exp\left(-N I(\mathbf{R})\right), \quad \int P(\mathbf{R}) d\mathbf{R} = 1 \tag{6.16}$$

where $I(\mathbf{R})$ is the free energy per liquid crystal molecule and is can be calculated from the Gaernter Ellis theorem (as the Legendre transform of the cumulant generator),

$$I(\mathbf{R}) = \mathbf{h} \cdot \mathbf{R} - \lambda(\mathbf{h}), \quad \mathbf{R} = \nabla_{\mathbf{h}} \lambda(\mathbf{h}) \tag{6.17}$$

$$\exp\left(N\lambda(\mathbf{h})\right) = \left\langle \exp\left(N \mathbf{h} \cdot \mathbf{R}\right) \right\rangle = \left\langle \exp\left(\sum_{j=1}^{N} \sum_{m=-2}^{2} h_m r_m(\hat{\Omega}_j) \right) \right\rangle \tag{6.18}$$

Because of spherical symmetry and assuming that biaxial fluctuations are small compared to the fluctuations with respect to the director $\hat{n}$, the two molecular free energies $I(\mathbf{R})$ and $\lambda(\mathbf{h})$ are only functions of the modulus of $\mathbf{R}$ and $\mathbf{h}$ respectively. Having that in mind,

the vector-equation of state 6.17 can be simplified,

$$\begin{aligned}
\mathbf{R} &= \nabla_{\mathbf{h}}\lambda(\mathbf{h}) \\
&= \nabla_{\mathbf{h}}\lambda(h) \\
&= \left[\frac{\partial\lambda(h)}{\partial h_{-2}}, \frac{\partial\lambda(h)}{\partial h_{-1}}, \frac{\partial\lambda(h)}{\partial h_0}, \frac{\partial\lambda(h)}{\partial h_1}, \frac{\partial\lambda(h)}{\partial h_2}\right]^T \\
&= \frac{\partial\lambda(h)}{\partial h}\left[\frac{\partial h}{\partial h_{-2}}, \frac{\partial h}{\partial h_{-1}}, \frac{\partial h}{\partial h_0}, \frac{\partial h}{\partial h_1}, \frac{\partial h}{\partial h_2}\right]^T \\
&= \frac{\partial\lambda(h)}{\partial h}\left[\frac{h_{-2}}{h}, \frac{h_{-1}}{h}, \frac{h_0}{h}, \frac{h_1}{h}, \frac{h_2}{h}\right]^T \\
&= \frac{\partial\lambda(h)}{\partial h}\hat{h} \\
&= R\hat{h}, \quad R = \frac{\partial\lambda(h)}{\partial h}
\end{aligned} \tag{6.19}$$

which of course means that the order parameter points in the direction of the field $\hat{h}$. Putting the resulting expression for the vector-order parameter 6.19 into the expression for $I(\mathbf{R})$ (6.17)

$$\begin{aligned}
I(\mathbf{R}) &= \mathbf{h}\cdot\nabla\mathbf{R} - \lambda(\mathbf{h}) \\
&= h\frac{\partial\lambda(h)}{\partial h} - \lambda(h) \\
&= hR - \int_0^h R(h')dh' \\
&= \int_0^R h(R')dR'
\end{aligned} \tag{6.20}$$

where in the last line we used integration by parts and recovered the reversible work theorem as expected. The integration happens over $h(R)$ which will be the scalar equation of state that we will base our theory on. As in other applications in this thesis it will be possible to calculate exactly the limits of $h(R)$ and use Pade interpolation between the two extreme behaviors.

Before we go ahead and calculate the two limits, we need one more piece of information to complete the theory. Let us remind ourselves that what we really need is the probability distribution of the largest eigenvalue $p(s)$. In two-dimensional liquid crystals, we were

lucky and the eigenvalue was just the modulus of the large-deviation vector but in three-dimensions we have $P(\mathbf{R})$ which is the probability distribution of the three eigenvalues of $\mathcal{Q}$. The connection can be established via the methods of random-matrix theory [63].

It is important to uderstand the two types of transformations that took place. First we transformed from the elements of the tensor $\mathcal{Q}$ to the large-deviation vector $\mathbf{R}$ and then we need to transform to the largest eigenvalue ($s \geq \lambda_2 \geq \lambda_3$) of the matrix. The Jacobian of the first transformation J_1 is a constant (and thus we ignore it) and the second Jacobian is $J_2 = (s-\lambda_2)(s-\lambda_3)(\lambda_2-\lambda_3)$, called the Vandermonde determinant in the language of random-matrix theory. Therefore, the connection between $P(\mathbf{R})$ and $p(s)$ is given by,

$$p(s) \sim \int_{-\infty}^{s} d\lambda_2 \int_{-\infty}^{\lambda_2} d\lambda_3 \delta(s+\lambda_2+\lambda_3)(s-\lambda_2)(s-\lambda_3)(\lambda_2-\lambda_3)P(\mathbf{R}) \tag{6.21}$$

We will use large-deviation theory to calculate $P(\mathbf{R})$ and random-matrix theory to calculate $p(s)$ as a cute combination of different statistical mechanical approaches.

6.2 Weak-field limit of the generating function 3D liquid crystals

The strong-correlation/weak-fluctuation limit has been worked out before via random-matrix theory methods by Zhao and Stratt [63]. We will derive the same answer with our theory starting from the usual series expansion of the cumulant generator 6.18,

$$\exp\left(N\lambda(\mathbf{h})\right) = \langle \exp\left(F\right)\rangle = \exp\left(\langle F\rangle + \frac{1}{2}\langle(\delta F)^2\rangle + ...\right) \tag{6.22}$$

$$F = N\mathbf{R}\cdot\mathbf{h} = \sum_{j=1}^{N}\sum_{m=-2}^{2} h_m r_m(\hat{\Omega}_j) \tag{6.23}$$

When the system is isotropic, tesseral harmonics average in the same way that regular spherical harmonics average. The first term is identically zero and so the cumulant

generator is

$$\lambda(\mathbf{h}) = \frac{1}{2N} \sum_{j,k=1}^{N} \sum_{m,m'=-2}^{2} h_m \left\langle r_m(\hat{\Omega}_j) r_{m'}(\hat{\Omega}_k) \right\rangle h_{m'} + \mathcal{O}(h^3) \tag{6.24}$$

Furthermore in the isotropic system the field components are all equal $h_m^2 = h^2/5$ and because the tesseral harmonic form a complete set, the only terms that will survive averaging in equation 6.24 will be the $m = m'$ terms,

$$\lambda(\mathbf{h}) = \frac{h^2}{10N} \sum_{j,k=1}^{N} \sum_{m=-2}^{2} \left\langle r_m(\hat{\Omega}_j) r_m(\hat{\Omega}_k) \right\rangle + \mathcal{O}(h^3) \tag{6.25}$$

We can finish off the weak field limit of the cumulant generator with the assistance of the the tesseral harmonic addition theorem,

$$\sum_{m=-2}^{2} r_m(\hat{\Omega}_j) r_m(\hat{\Omega}_k) = \frac{5}{4\pi} P_2(\hat{\Omega}_j \cdot \hat{\Omega}_k) \tag{6.26}$$

which leads to

$$\lambda(\mathbf{h}) = \frac{h^2}{8\pi} \left\langle \frac{1}{N} \sum_{j,k=1}^{N} P_2(\hat{\Omega}_j \cdot \hat{\Omega}_k) \right\rangle + \mathcal{O}(h^3) = \frac{\chi}{8\pi} h^2 + \mathcal{O}(h^3) \tag{6.27}$$

where χ is the susceptibility. The modulus of the order parameter (equation 6.19) in that limit reads,

$$R = \frac{\partial \lambda(h)}{\partial h} = \frac{\chi}{4\pi} h + \mathcal{O}(h^2) \Leftrightarrow h(R) = \frac{4\pi}{\chi} R + \mathcal{O}(R^2) \tag{6.28}$$

and from the reversible work theorem 6.20

$$I(\mathbf{R}) = \int_0^R h(R') dR' = \int_0^R \left[\frac{4\pi}{\chi} R' + \mathcal{O}(R'^2) \right] dR' = \frac{2\pi}{\chi} R^2 + \mathcal{O}(R^3) \tag{6.29}$$

Now, we can solve with respect to $Tr(\mathcal{Q}^2)$ from the definition in 6.14 and get an expression for $I(\mathbf{R})$ as a function of the three eigenvalues $s \geq \lambda_2 \geq \lambda_3$ of the tensor $\mathcal{Q}$,

$$I(s, \lambda_2) = \frac{5}{3\chi} Tr(\mathcal{Q}^2) = \frac{5}{3\chi}(s^2 + \lambda_2^2 + \lambda_3^2) \tag{6.30}$$

$$\lambda_3^2 = (s + \lambda_2)^2 \tag{6.31}$$

And the corresponding probability distribution for the largest eigenvalues s predicted by the large deviation formalism at the weak field level is,

$$P(s, \lambda_2) \sim \delta(s + \lambda_2 + \lambda_3) \exp\left(-\frac{5N}{3\chi}(s^2 + \lambda_2^2 + \lambda_3^2)\right) \tag{6.32}$$

which can be written in tensor $\mathcal{Q}$ notation simply as,

$$P(\mathcal{Q}) \sim \delta(Tr(\mathcal{Q}) \exp\left(-\frac{5N}{3\chi} Tr(\mathcal{Q}^2)\right) \tag{6.33}$$

This is exactly the anticipated gaussian distribution that is derived via random-matrix theory arguments by Zhao and Stratt [63]. We can integrate expression 6.32 with respect to the two smaller eigenvalues (See equation 6.21) in order to calculate $p(s)$,

$$p(s) = \sqrt{\frac{6a}{\pi}} \left[\exp\left(-6as^2\right) + \exp\left(-\frac{3}{2}as^2\right)\left(\frac{9}{2}as^2 - 1\right)\right], \quad a = \frac{5N}{3\chi} \tag{6.34}$$

and for $\chi = 1$ (uncorrelated liquid crystal molecules) we get the exact answer for a random flight of three-dimensional headless vectors derived almost two decades ago by Doerr, Herman, Mathur and Taylor [15].

Large-deviation theory is capable of reproducing well-known random-matrix theory results in the limit of weak fluctuations but strong correlations. The goal is to go beyond the weak field approach and incorporate the opposite limit in our theory. We will do just that in the next chapter where the system goes to the mean-field answer for

three-dimensional nematics.

6.3 Strong-field limit/Mean-field theory of nematics

In the presence of a strong field, three-dimensional liquid crystal molecules are independent from each other and their orientations are coupled with the field. The inter-molecular correlations coarse grain and a single molecule's orientation only interacts with a mean-field $\epsilon = \beta U_0$ that is parallel to the externally applied field $\mathbf{h}$. U_0 is a constant energy on the order of the average correlation energy. In that limit, the direction of the field can be chosen to be solely along the $\hat{z}$ axis and so the only component of the field that is non-zero is $\mathbf{h} = h_0\hat{z}$ and the only contribution to the sum in the cumulant generator is r_0. The single-molecule generator is simply,

$$\lambda(\mathbf{h}) = \ln \left\langle \exp\left(\sum_{m=-2}^{2} h_m r_m(\hat{\Omega}_j) \right) \right\rangle_{\rho(\hat{\Omega}_j)} = \ln \left\langle \exp\left(h r_0(\hat{\Omega}_l) \right) \right\rangle_{\rho(\hat{\Omega}_l)} \tag{6.35}$$

$$\rho(\hat{\Omega}_j) = \frac{\exp\left(\epsilon r_0(\hat{\Omega}_j)\right)}{\int d\hat{\Omega}_l \exp\left(\epsilon r_0(\hat{\Omega}_j)\right)} \tag{6.36}$$

From the definition in 6.9,

$$h r_0(\hat{\Omega}_j) = h\sqrt{\frac{5}{4\pi}} q_3(\hat{\Omega}_j) = h\sqrt{\frac{5}{4\pi}} P_2(\cos\theta_j) \tag{6.37}$$

where $P_2(x) = \frac{1}{2}(3x^2 - 1)$ is the second Legendre polynomial. Consequently we need to evaluate the following integral,

$$\lambda(\mathbf{h}) = \ln \left\langle \exp\left((h+\epsilon)\sqrt{\frac{5}{4\pi}} P_2(\cos\theta) \right) \right\rangle \tag{6.38}$$

We can work out the integral exactly but before we do so we introduce the re-scaling parameters

$$r = \sqrt{\frac{4\pi}{5}}R, \quad \gamma = \sqrt{\frac{5}{4\pi}}(h+\epsilon) = \sqrt{\frac{5}{4\pi}}h + \epsilon' = H + \epsilon' \tag{6.39}$$

where γ will be used to evaluate the integral and H will be used to simplify the notation during the Pade interpolation,

$$rH = Rh \tag{6.40}$$

The integral can be evaluated in terms of Dawson's function $F(t) = e^{-t^2}\int_0^t e^{x^2}dx$,

$$\begin{aligned} \lambda(\gamma) &= \ln\langle \exp\left(\gamma P_2(\cos\theta)\right)\rangle \\ &= \ln F(t) - \ln t + \frac{2}{3}t^2, \quad t^2 = \frac{3\gamma}{2} \end{aligned} \tag{6.41}$$

With the re-scaled quantities we may say that the scalar equation of state 6.19 transforms to the equivalent form,

$$\begin{aligned} r &= \frac{\partial\lambda(\gamma)}{\partial\gamma} \\ &= \frac{\partial\lambda(\gamma)}{\partial t}\frac{\partial t^2}{\partial\gamma}\frac{\partial t}{\partial t^2} \\ &= \frac{3}{4}\frac{1}{t}\left(\frac{1}{F(t)} - 2t - \frac{1}{t} + \frac{4}{3}t\right), \quad F'(t) = 1 - 2tF(t) \\ &= \frac{3}{4}\left(\frac{1}{tF(t)} - \frac{1}{t^2} - \frac{2}{3}\right) \\ &\to \frac{3}{4}\left(2 - \frac{2}{t^2} - \frac{1}{t^4} + \mathcal{O}(t^{-6}) - \frac{2}{3}\right), \quad F(t) \overset{t\to\infty}{\longrightarrow} \frac{1}{2t} + \mathcal{O}(t^{-3}) \\ &= 1 - \frac{3}{2}\frac{1}{t^2} - \frac{3}{4}\frac{1}{t^4} + \mathcal{O}(t^{-6}) \end{aligned} \tag{6.42}$$

and in the asymptotic limit the equation of state gives the exceptionally simple answer,

$$r = 1 - \frac{1}{\gamma} - \frac{1}{3\gamma^2} + \mathcal{O}\left(\frac{1}{\gamma^3}\right), \quad \gamma \to \infty \tag{6.43}$$

It is simpler to apply Pade interpolation in the reverted series,

$$\gamma(r) = \frac{1}{1-r} + \frac{1}{3} + \mathcal{O}(1-r), \quad r \to 1 \tag{6.44}$$

$$H(r) = \frac{1}{1-r} + \eta + \mathcal{O}(1-r), \quad r \to 1 \tag{6.45}$$

where $\eta = \frac{1}{3} - \epsilon'$ is the constant coefficient that entails the mean-field intermolecular correlations at the asymptotic limit.

6.4 Pade interpolation of the 3D liquid crystalline equation of state

The two limiting extremes of $H(r)$ are given by central-limit theory 6.28 and mean-field theory 6.45

$$H(r) = \begin{cases} \frac{5}{\chi} r + \mathcal{O}(r^2), & r \to 0 \\ \\ \frac{1}{1-r} + \eta + \mathcal{O}(1-r), & r \to 1 \end{cases} \tag{6.46}$$

As we saw in other systems, the simplest and most appropriate technique is Pade interpolation between the two limits. However there is difference here compared to other applications; There is no $\mathbf{h} \Leftrightarrow -\mathbf{h}$ symmetry and so both even and odd powers are included in the equation of state. The simplest Pade that goes to the correct limits is now a Pade[3/1] instead of a Pade[5/2] that we used for two-dimensional liquid crystals and polymers,

$$H(r) = \frac{5}{\chi} \frac{r + Ar^2 + Br^3}{1-r} \tag{6.47}$$

$$A = -2 - \left(\frac{\chi}{5}\right)[-\eta - 3] \tag{6.48}$$

$$B = 1 + \left(\frac{\chi}{5}\right)[-\eta - 2] \tag{6.49}$$

It can be easily verified that this minimal Pade gives the correct weak- and strong-field limits. We can apply the reversible work theorem directly to the variable $H(r)$ instead of $h(R)$ since $Hr = Rh$,

$$I(\mathbf{r}) = \int_0^R h(R')dR' = \int_0^r H(r')dr' \tag{6.50}$$

$$\mathbf{r} = \sqrt{\frac{4\pi}{5}}\mathbf{R} \tag{6.51}$$

Direct integration of 6.47 yields a new free energy per molecule,

$$I(\mathbf{r}) = -\ln(1-r) - r - \frac{1}{2}\left(1 - \frac{5}{\chi}\right)r^2 - \frac{1}{3}\left(\frac{5}{\chi} - \eta - 2\right)r^3 \tag{6.52}$$

where now there is a logarithmic term that captured the fluctuations. This rate function gives us the probability distribution $P(\mathbf{r}) \sim \exp(-NI(\mathbf{r}))$ and $r = \sqrt{\frac{2}{3}(s^2 + \lambda_2^2 + \lambda_3^2)}$. Via random-matrix theory we can establish the connection between $P(\mathbf{r})$ and the desired $p(s)$. Direct application of 6.21 with the rate function given by 6.52 gives us the final answer,

$$p(s) \sim \int_{-\infty}^{s} d\lambda_2 \int_{-\infty}^{\lambda_2} d\lambda_3 \delta(s + \lambda_2 + \lambda_3)(s - \lambda_2)(s - \lambda_3)(\lambda_2 - \lambda_3)\exp(-NI(\mathbf{r})) \tag{6.53}$$

where we can only solve the integral numerically. The expression for $p(s)$ is more general than 6.34 and the two will be compared in the results chapter.

Finally we can make the connection with the Landau free energy. The weak-field limit is,

$$\begin{aligned} I(\mathcal{Q}) &= r + \frac{r^2}{2} - r - \frac{1}{2}\left(1 - \frac{5}{\chi}\right)r^2 - \frac{1}{3}\left(\eta - \frac{7}{3} + \frac{5}{\chi}\right)r^3 + ... \\ &= \left(\frac{5}{\chi}\right)r^2 - \frac{1}{3}\left(\eta - \frac{7}{3} + \frac{5}{\chi}\right)r^3 + ... \\ &= \frac{2}{3}\left(\frac{5}{\chi}\right)Tr(\mathcal{Q}^2) - \left(\frac{2}{3}\right)^{3/2}\left(\frac{\eta}{3} - \frac{7}{9} + \frac{5}{3\chi}\right)\left[Tr(\mathcal{Q}^2)\right]^{3/2} + ... \end{aligned} \tag{6.54}$$

is similar to the Landau form for the free energy per liquid crystal molecule,

$$I(\mathcal{Q}) = \frac{1}{2}aTr(\mathcal{Q}^2) + \frac{1}{3}bTr(\mathcal{Q}^3) + ... \tag{6.55}$$

We are able to give a molecular explanation of the phenomenological coefficients in the Landau form. Moreover it is interesting to notice that there is no $Tr(\mathcal{Q}^3)$ in our equation but this will not be important as biaxial fluctuations are small. We expect that no information is missing from the theory since for very small fluctuations vertical to the director [25] one may say,

$$Tr(\mathcal{Q}^2)^3 = 6Tr(\mathcal{Q}^3)^2 \tag{6.56}$$

which means that information contained in $Tr(\mathcal{Q}^3)$ are given by powers of $Tr(\mathcal{Q}^2)$.

Finally we see that the probability distribution $P(\mathcal{Q})$ takes the anticipated random-matrix theory from for very small fluctuations,

$$P(\mathcal{Q}) \sim \exp\left(-\frac{5N}{3\chi}Tr(\mathcal{Q}^2)\right) \tag{6.57}$$

The value of this thesis is the calculation of a more general function of $Tr(\mathcal{Q}^2)$ not just a gaussian distribution. When the system goes close to the I/N transition, the probability distribution deviates from gaussianity and the free energy starts to feel a logarithmic singularity which is a result of rapid domain growth.

CHAPTER 7

Results

7.1 Results for the 2D XY model

We wish to demonstrate the usefulness of our approach to classical two-dimensional magnetization. The 2D XY model is defined by the Hamiltonian in 4.44 and shows a Kosterlitz-Thouless transition between a high temperature isotropic phase (paramagnetic) and a low temperature (quasi-ferromagnetic) ordered phase. In complete analogy with nematic order in isotropic liquid crystals we want to simulate a system that is close to the critical point $\beta_C J \approx 1.13$ [30] in order to see the non-gaussian profile of the fluctuations. In figures 7.1 and 7.2 we can see the comparison between central-limit theory ("CLT" it refers to equation 4.74), large-deviation theory ("LDT" it refers to equation 4.72) and Monte Carlo simulation ("Simulation"). A small square lattice of 28×28 spins was simulated using the Metropolis algorithm (See Appendix A). The reason why we chose such a small system was to emphasize the difference between our theory and the traditional central-limit theory. Of course one needs to perform more simulations with larger systems in order to demonstrate the faster convergence that large-deviation theory offers. Nevertheless the improved accuracy that our theory provides at calculating high μ configurations is clear even for such a tiny lattice.

We plot the effective free energy per spin ($-\frac{1}{N}\ln P(\mu)$, with μ defined in 4.47) in order to visualize larger fluctuations with small probabilities easier. On figure 7.1 we study thermodynamic conditions that correspond to very high temperatures ($\beta J = 0.01$). This is the paramagnetic region where single vortices dominate and ruin any type of spontaneous magnetization. The fluctuations of $P(\mu)$ are small and both CLT and LDT are very accurate. In fact one may not be able to distinguish between the two curves.

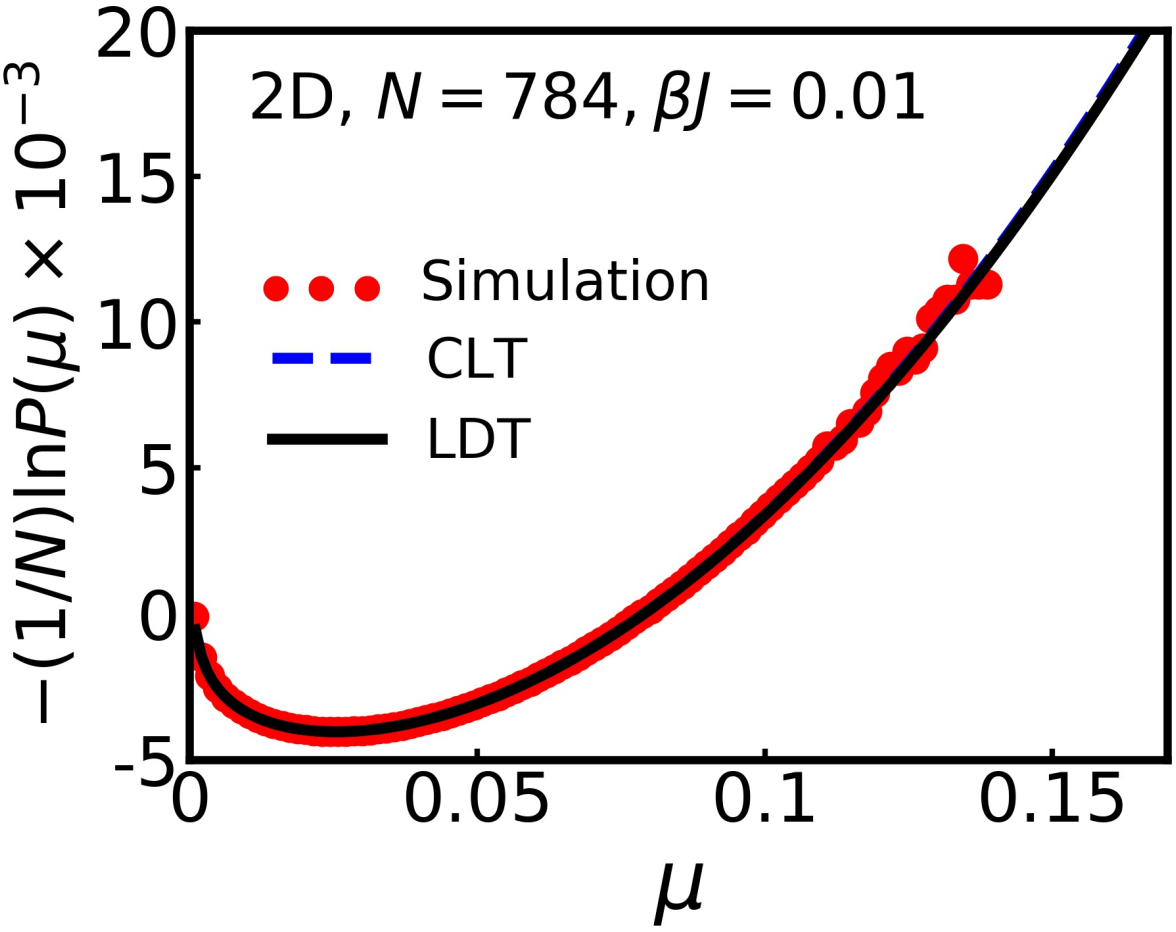

Figure 7.1: The effective rate functions as a function of the order parameter μ for a 2D XY system that consists of $N = 784$ spins deep in the paramagnetic phase where the temperature is really high compared to the ferromagnetic coupling constant J. The dotted line corresponds to a Monte Carlo simulation (Metropolis algorithm) (10^7 configurations); The blue dashed line corresponds to the 2D Central-limit Theory (CLT) approximation; The black solid line corresponds to the 2D Large-deviation Theory (LDT) approach. A very small difference is visible between CLT and LDT for $\mu > 0.12$.

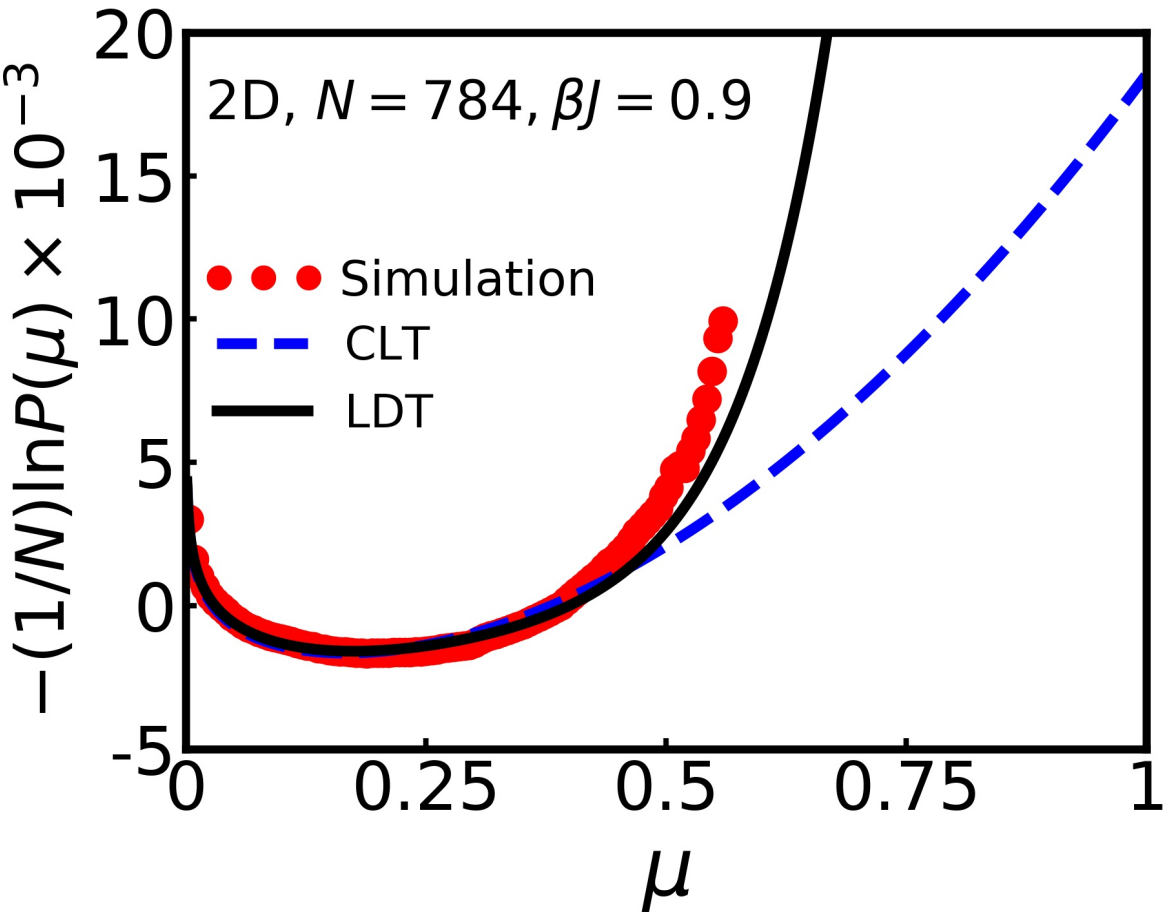

Figure 7.2: The effective rate functions as a function of the order parameter μ for a 2D XY system that consists of $N = 784$ spins in pre-critical paramagnetic conditions under a much lower temperature ($\beta J = 0.9$). The dotted line corresponds to a Monte Carlo simulation (Metropolis algorithm) (10^7 configurations); The blue dashed line corresponds to the 2D Central-limit Theory (CLT) approximation; The black solid line corresponds to the 2D Large-deviation Theory (LDT) approach.

In figure 7.2 we show the fluctuations of a low temperature simulation that corresponds to a 28×28 XY lattice (same size as high temperature simulation). The temperature of the simulation ($\beta J = 0.9$) was chosen to be close to the critical point where vortices will bind and substantial correlations between the spins have formed. Close to the critical point, we can see the non-gaussian profile of the fluctuations; CLT is very inaccurate for values of the magnetization $\mu > 0.5$ as opposed to LDT. Although both of the approaches do well for small deviations around $\langle \mu \rangle$, LDT is more accurate for larger deviations as expected.

Values of μ that are close to the mean correspond to macrostates that are easy to sample. The system visits those configurations multiple times and we get a very accurate estimate of their probabilities. Large deviations however, appear less frequently throughout the Monte Carlo simulation and the sampling of the right tail is poor. By using the LDT approach outlined in chapter 4 we may use information based on $\langle\mu\rangle$ and $\langle\mu^2\rangle$ in order to predict poorly sampled macrostates. The first moment is used to calculate η in the equation for LDT (4.72) and the second moment is used to calculate the two-body magnetic susceptibility $\chi = N\langle\mu^2\rangle$ in the equation for CLT 4.74 and the equation for LDT (4.72). Lastly, imagine an application where we are interested in some probability $P(\mu > 0.6)$. CLT will be a very inaccurate estimate and the simulation won't sample the rare macrostates with $\mu > 0.6$. Or at least it might take a lot of computational power. Instead we can use LDT at a very good approximation by simply taking information from easy-to-sample macrostates close to $\langle\mu\rangle$.

This results section on magnets does not present any kind of finite size scaling analysis. An exhaustive analysis was only performed for two- and three-dimensional Gay-Berne molecules. It simply demonstrates that the Pade probability distribution derived in chapter 4.4 is useful for analyzing magnetization fluctuations close to criticality. The $N = 784$ system seems to be small and future studies would require larger spin systems. Nevertheless the point is hopefully clear and more rigorous analysis will be presented later on for liquid crystals. Finally it is important to mention that the global probability distribution $P(\mu)$ is unaware of the underlying geometry; making it impossible to study vortices. Perhaps the connection between our theory and topological fluctuations might be an interesting pursue.

7.2 Results for two- and three-dimensional isotropic liquid crystals

An exhaustive study of Gay-Berne molecules in two and three dimensions under macroscopically isotropic conditions was performed. We used Molecular Dynamics simulations (See Appendix A for details) in order to calculate the probability distribution of the order parameter $p(s)$ and study the finite-size dependence of the probabilities. The order parameter is defined as the largest eigenvalue of the tensor $\mathcal{Q}$. The sweet spot range of N values (N=128, 242, 450 and 800 for 2D and N=256, 500, 864, 1372 and 2048 for 3D) that was chosen in this study, is able to emphasize the fluctuations due to the proximity to the nematic phase and depict the failure of traditional central-limit approaches.

The simplest system we can test our theory on, is the ideal-gas model. Uncorrelated liquid crystal molecules in 2D and 3D are easy to simulate and demonstrate effectively how both central-limit theory and large-deviations theory predict the N-dependence of the probability distribution. We are studying non-interacting liquid crystals which means that the inter-molecular correlations will be turned off. For the 2D comparison we use equation 4.25 as the CLT (Central-limit theory) and equation 4.39 with $\delta = 1$ and $\eta = 0$ as the LDT (Large-deviation theory answer). For the 3D comparison we use equation 6.34 with $\chi = 1$ for the CLT (Central-limit theory) result and expression 6.53 with $\chi = 1$ and $\eta = 0$ as the LDT (Large-deviation theory) answer. The uncorrelated probability distributions do not exhibit large fluctuations and the convergence to the simulated answer is extremely fast. In figures 7.3 and 7.4 we can see that even for the smallest systems (N=128 and N=256 for 2D and 3D respectively), both CLT and LDT have converged because there are no correlations that could potentially lead to large order parameter fluctuations.

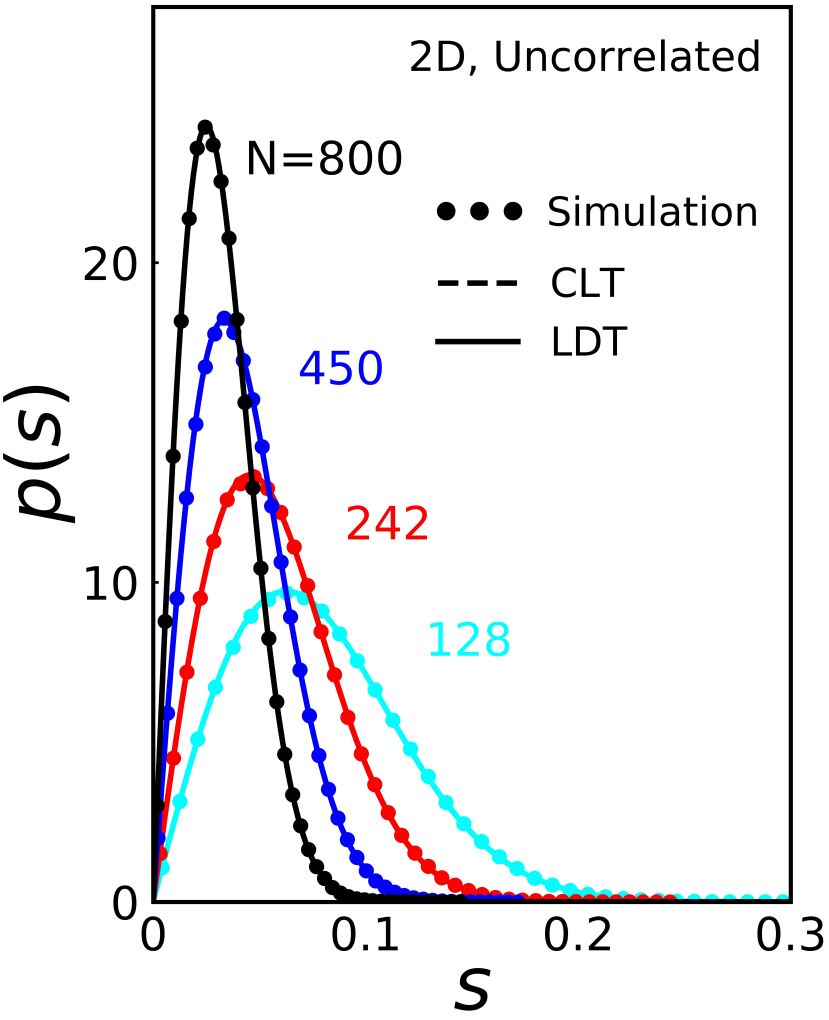

Figure 7.3: Probability distribution of the orientational order parameter s for non-interacting (uncorrelated) molecules in 2D, demonstrating the dependence on the size of the system, N. The dotted line corresponds to a computer simulation over 10^6 configurations; The dashed line corresponds to the Central-limit Theory (CLT) approximation and the solid line corresponds to the Large-deviation Theory (LDT) probability distribution generated from the 2D ideal-gas Pade' equation of state. The CLT and the LDT lines are indistinguishable on that scale shown here.

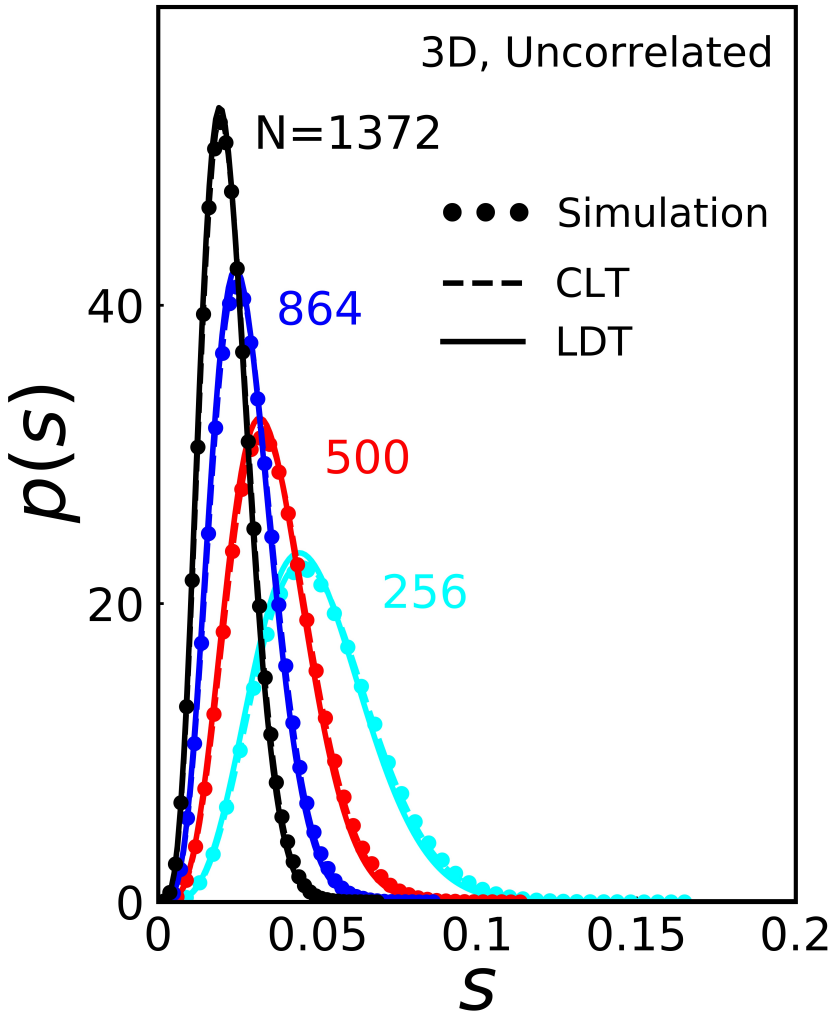

Figure 7.4: Probability distribution of the orientational order parameter s for non-interacting (uncorrelated) molecules in 3D, demonstrating the dependence on the size of the system, N. The dotted line corresponds to a computer simulation of 10^6 configurations; The dashed line corresponds to the Central-limit Theory (CLT) approximation and the solid line corresponds to the Large-deviation Theory (LDT) probability distribution generated from the 3D ideal-gas Pade' equation of state. The CLT and the LDT lines are indistinguishable on the scale of the graph.

7.2.1 Correlated Gay-Berne Molecules/Deep Isotropic Phase

The next step involves the simulation of interacting liquid crystal molecules far from criticality (Deep isotropic phase). For two-dimensional liquid crystals equation 4.24 is used as the central-limit theory answer and the susceptibility χ is calculated from the simulated answer since equation 4.18 ($\chi = N\langle s^2 \rangle$) is true. For the two-dimensional large-deviation

theory answer we use equation 4.39 where again χ is taken from the second moment of the simulated $p(s)$ and η is taken from the first moment of the simulated $p(s)$. This is the simplest way to determine the mean-field orientational correlation coefficient η although it is not unique. The scaling of 4.24, 4.39 and simulated $p(s)$ can be seen in figure 7.5. Both CLT and LDT predict the scaling of the simulated $p(s)$ accurately. We are far from the critical point and the fluctuations are weak, making CLT exact.

In the case of three-dimensional liquid crystals we remind the reader that CLT (central-limit theory) refers to the random-matrix theory results derived by [15] and [63]. The connection was extensively discussed in chapter 6. As CLT we use equation 6.34 and we calculated χ numerically from the simulation. As LDT we use equation 6.53 where χ was also determined numerically and η was taken from the first moment $\langle s \rangle$ of the simulated $p(s)$. As can be seen in figures and 7.6 the lines between the CLT and LDT are identical (or almost identical for the 3D case). Both LDT and CLT predict the N-dependence of the simulated probability distributions under these conditions.

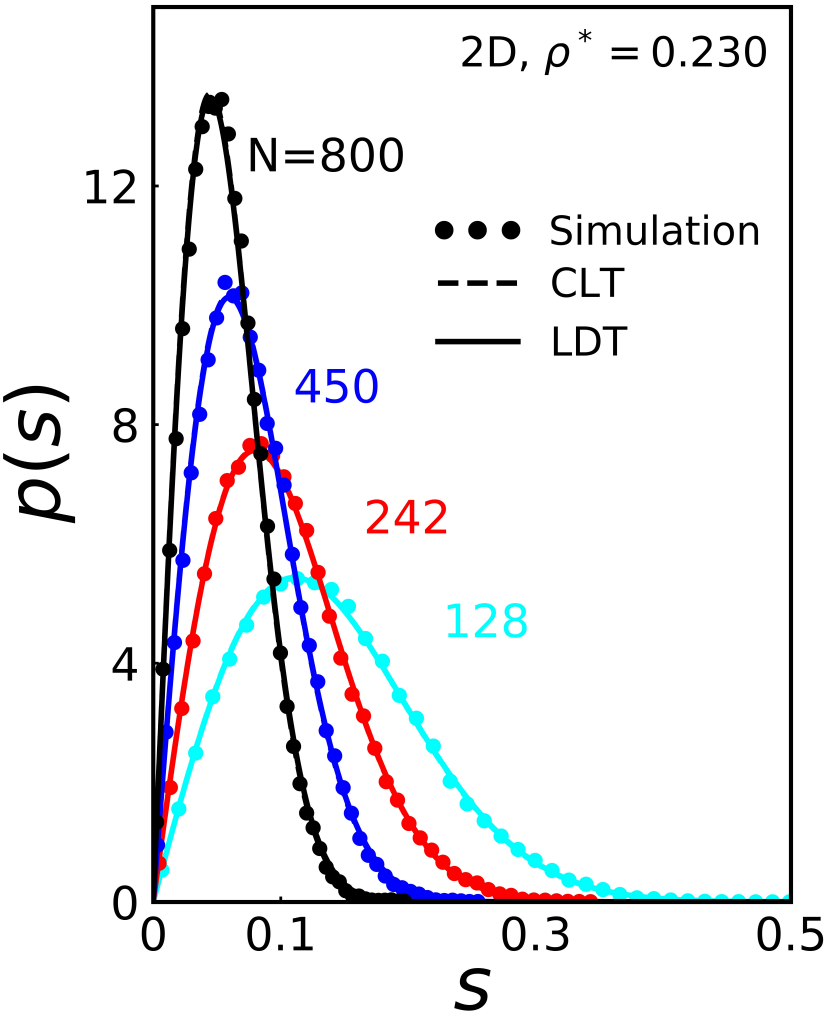

Figure 7.5: Probability distribution of the orientational order parameter s in 2D. The dotted line represents the Molecular Dynamics simulation (3×10^6 configurations) of 2D Gay-Berne molecules under deep isotropic conditions ($\rho^* = 0.230$ and $T^* = 1$); The dashed line is the 2D Central-limit Theory (CLT) approximation with information taken from the deep isotropic simulation; Finally the solid line is the 2D Large-deviation Theory (LDT) answer with information extracted from the same simulation. The CLT and the LDT lines are indistinguishable on the scale of the graph.

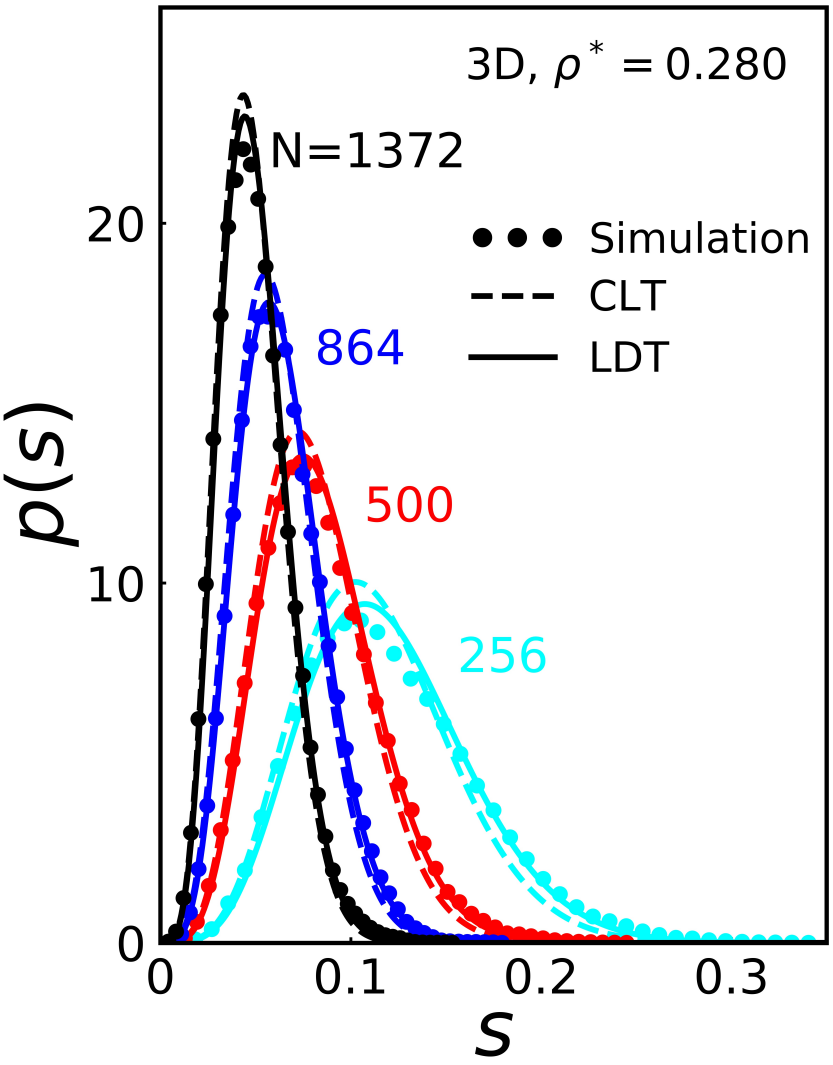

Figure 7.6: Probability distribution of the orientational order parameter s in 3D. The dotted line represents the Molecular Dynamics simulation (3×10^6 configurations) of 3D Gay-Berne molecules at deep isotropic conditions ($\rho^* = 0.280$ and $T^* = 1$); The dashed line is the 3D Central-limit Theory (CLT) approximation with information taken from the deep isotropic simulation; Finally the solid line is the 3D Large-deviation Theory (LDT) answer with information extracted from the same simulation. The difference between CLT and LDT can now be seen on that scale. Moreover it can be seen that for small N, LDT does slightly better than CLT at the tails of the distribution.

In that region of the phase diagram, the number of correlated molecules is a negligible fraction of the total number of molecules in the simulation. It is important that we increase the density and get close to the nematic phase so that correlations really start to impact the fluctuation profile.

7.2.2 Correlated Gay-Berne Molecules/Pre-transitional Isotropic Phase

In two-dimensions, a suitable pre-transitional density was found to be $\rho^* = 0.285$. Under these conditions, the system feels the presence of the critical point that lies on the other side of the Isotropic/Nematic transition line. The correlation length is long and the size of the fluctuations is comparable to the size of the simulated system. It can be seen in figure 7.7 panel (a) how the central limit theorem now converges more slowly to the simulation answer in comparison to our large-deviation theory (panel (b)). For the smallest system (N=242) the improvement is more obvious but even if we go to the larger systems where the CLT does seemingly well, it actually fails to reproduce the large-s tails of the simulated p(s). In order to visualize the large-s tails of the distribution and compare the performance of CLT and LDT we will need compare the logarithms of the probabilities, or the so-called effective rate functions per molecule.

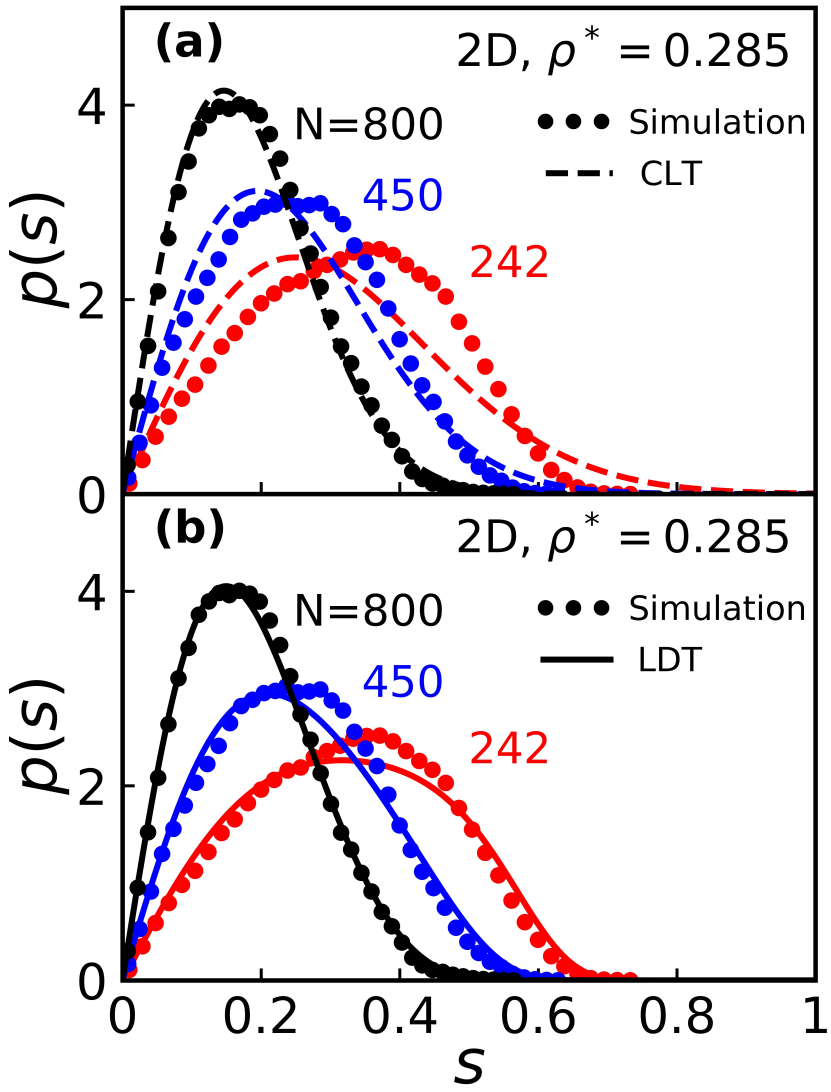

Figure 7.7: (a) The dotted line is the 2D Molecular Dynamics simulation (10^7 configurations) of 2D Gay-Berne molecules in pre-transitional isotropic conditions ($\rho^* = 0.285$, $T^* = 1$). The dashed line is the 2D Central-limit Theory (CLT) approximation with information taken from the same pre-transitional isotropic simulation; (b) The dotted line is the 2D Molecular Dynamics simulation of 2D Gay-Berne molecules in pre-transitional isotropic conditions ($\rho^* = 0.285$, $T^* = 1$); The solid line is the 2D Large-deviation Theory (LDT) answer with information extracted from the same simulation.

By plotting the effective rate functions for only the largest system in 2D (N=800) (figure 7.8), we can easily see that after roughly s=0.4 the CLT starts to diverge from the simulated answer while LDT is significantly more accurate. The crucial point is that, we have used information from well-sampled configurations (just as described in section 7.2.1)

in order to predict atypically large values of s that lie in the tail. The reason why the 2D version is so powerful lies in the very nature of the fluctuations. In lower dimensions, fluctuations are larger and form much easier than higher dimensions. That is why the tails of the simulated distribution reflect fluctuations that sense the extreme order limit s=1, the very limit we have analytically added to our theory and the very limit that CLT is unaware of.

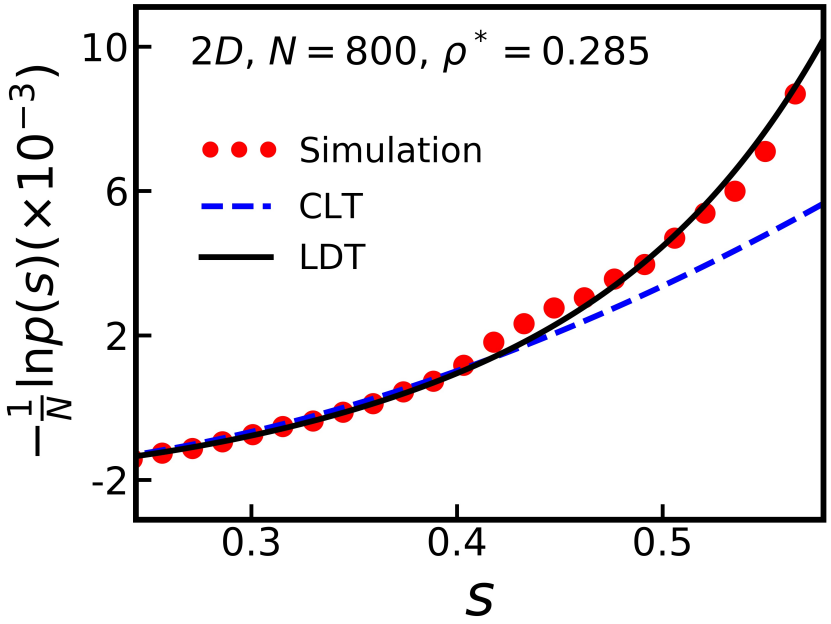

Figure 7.8: The effective rate functions as a function of the order parameter s for a 2D system that consists of $N = 800$ molecules in pre-transitional isotropic conditions ($\rho^* = 0.285$, $T^* = 1$). The dotted line corresponds to a Molecular Dynamics simulation (10^7 configurations) of 2D Gay-Berne molecules; The blue dashed line corresponds to the 2D Central-limit Theory (CLT) approximation with information taken from the simulation; The black solid line corresponds to the 2D Large-deviation Theory (LDT) approach with information taken from the same simulation.

In 3D the situation is much more challenging and interesting. We can immediately see from finite analysis at the pre-transitional density of $\rho^* = 0.300$ (figure 7.9) that CLT converges slower than LDT and the situation at the tails (figure 7.11) follows the same logic as in 2D with only a crucial difference. In 3D the system does not form very highly ordered states with significant probabilities which means that we are noticeably far from s=1. Even so, echoes from the perfectly ordered limit can be seen at the large-s tails of

the distributions by comparing the effective rate functions (subfigure a in figure 7.11). Via the LDT approach we can now compute the tails of the distributions accurately.

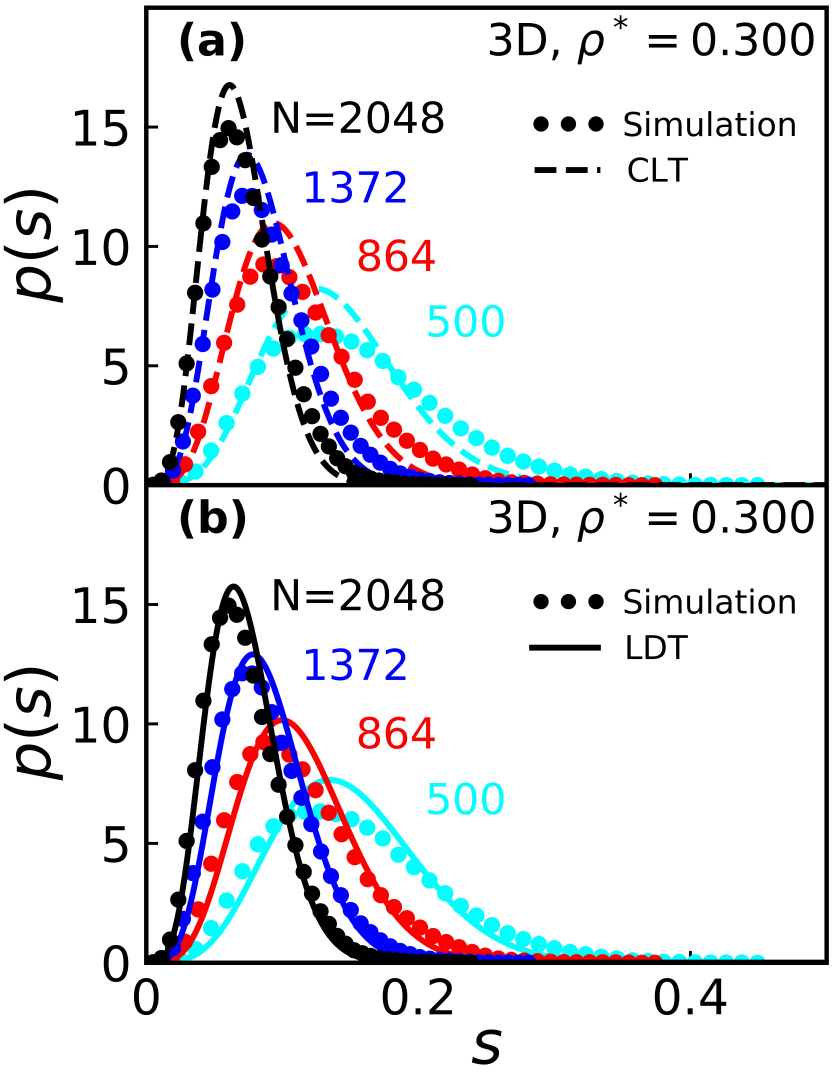

Figure 7.9: (a) The dotted line is the 3D Molecular Dynamics simulation (1.5×10^7 configurations) of 3D Gay-Berne molecules in pre-transitional isotropic conditions ($\rho^* = 0.300$, $T^* = 1$). The dashed line is the 3D Central-limit Theory (CLT) approximation with information taken from the same pre-transitional isotropic simulation; (b) The dotted line is the 3D Molecular Dynamics simulation of 3D Gay-Berne molecules in pre-transitional isotropic conditions ($\rho^* = 0.300$, $T^* = 1$); The solid line is the 3D Large-deviation Theory (LDT) answer with information extracted from the same simulation.

It is enlightening to proceed to even higher densities and see the breakdown of all these approaches. By increasing the density a bit more ($\rho^* = 0.304$), finite size scaling (see figure 7.10) shows how both CLT and LDT converge very slowly to the simulated answer.

It is still true that LDT captures the large-s tails more accurately than CLT (subfigure b in figure 7.11). While under these thermodynamic conditions the fluctuations are too large to be well captured by any theory, we can still see the improvement our approach offers as opposed to traditional central-limit approximations.

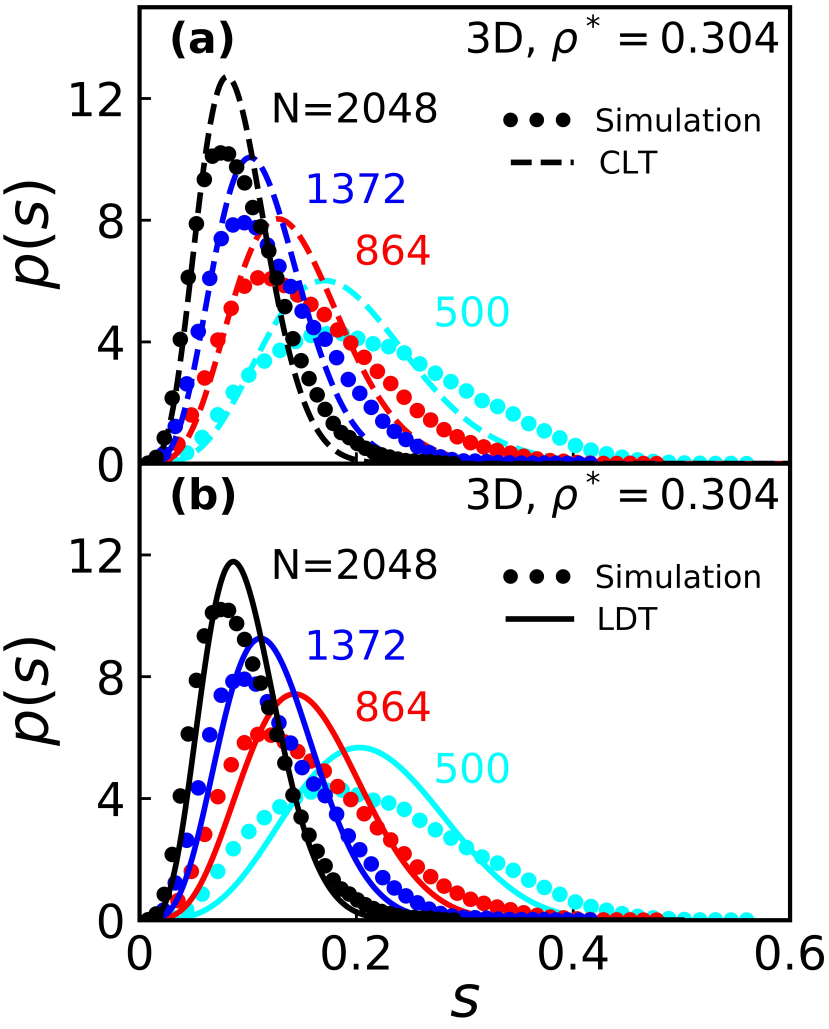

Figure 7.10: (a) The dotted line is the 3D Molecular Dynamics simulation (1.5×10^7 configurations) of 3D Gay-Berne molecules in pre-transitional isotropic conditions extremely close to the nematic phase ($\rho^* = 0.304$, $T^* = 1$). The dashed line is the 3D Central-limit Theory (CLT) approximation with information taken from the same extreme pre-transitional isotropic simulation; (b) The dotted line is the 3D Molecular Dynamics simulation of 3D Gay-Berne molecules in pre-transitional isotropic conditions ($\rho^* = 0.304$, $T^* = 1$); The solid line is the 3D Large-deviation Theory (LDT) answer with information extracted from the same simulation. LDT describes the tails better than CLT as it includes the perfect order limit $s = 1$.

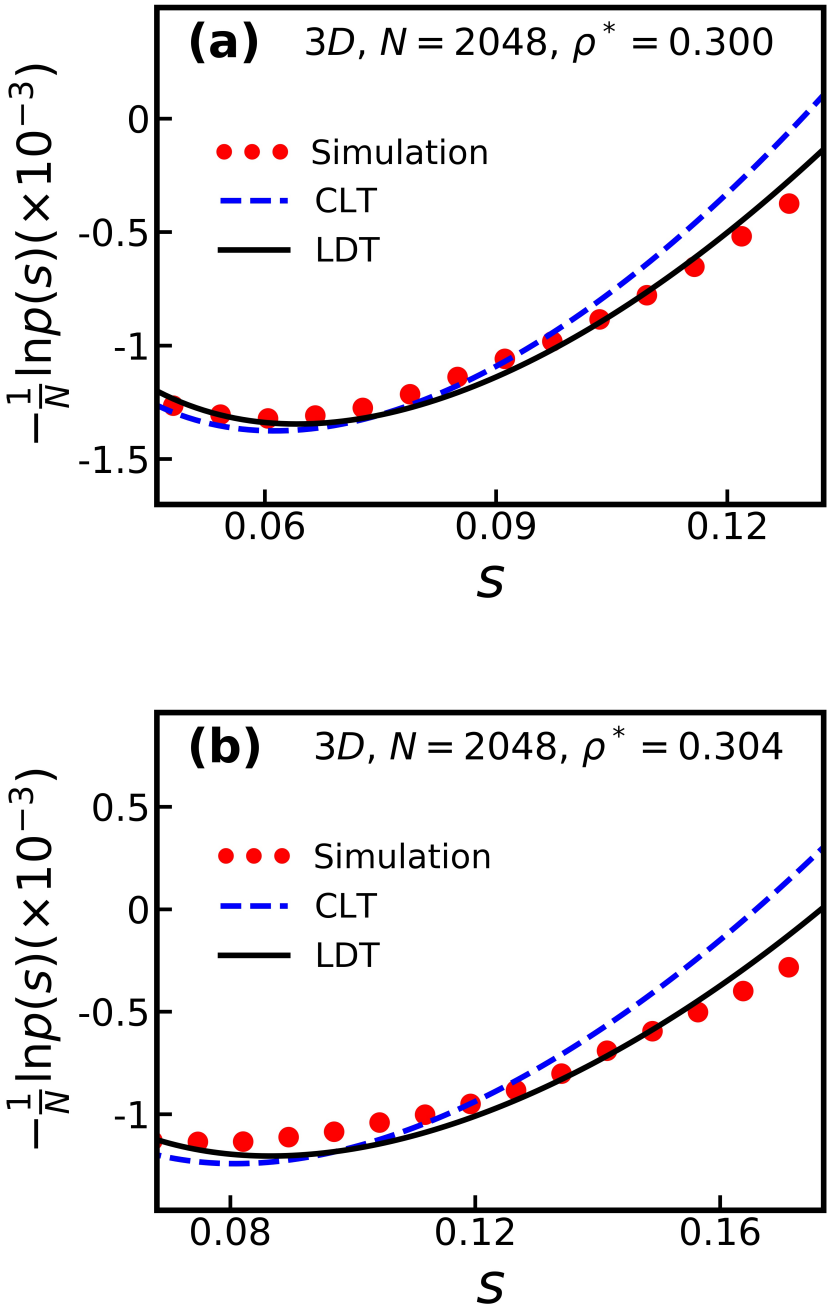

Figure 7.11: The effective rate functions as a function of the order parameter s for a 3D system that consists of $N = 2048$ molecules in (a) pre-transitional isotropic conditions ($\rho^* = 0.300$, $T^* = 1$) and (b) pre-transitional isotropic conditions extremely close to the nematic phase ($\rho^* = 0.304$, $T^* = 1$). For both (a) and (b) sub-figures, the dotted line corresponds to a Molecular Dynamics simulation (1.5×10^7 configurations) of 3D Gay-Berne molecules; The blue dashed line corresponds to the 3D Central-limit Theory (CLT) approximation with information taken from the simulation; The black solid line corresponds to the 3D Large-deviation Theory (LDT) approach with information taken from the same simulation.

CHAPTER 8

Time-dependent large-deviation theory at the weak-fluctuation limit: Three-dimensional isotropic liquid crystals

When the fluctuations are weak, we can generalize our theory and calculate a joint probability distribution of two different times $\tau = 0$ and $\tau = t$. We will have two order parameters whose elements are,

$$\mathcal{Q}_{\mu\nu}(0) = \frac{3}{2N}\sum_{j=1}^{N} q^j_{\mu\nu}(0), \quad q^j_{\mu\nu}(0) = \hat{\Omega}^j_{\mu\nu}(0)\hat{\Omega}^j_{\mu\nu}(0) - \frac{\delta_{\mu\nu}}{3} \tag{8.1}$$

$$\mathcal{Q}_{\mu\nu}(t) = \frac{3}{2N}\sum_{j=1}^{N} q^j_{\mu\nu}(t), \quad q^j_{\mu\nu}(t) = \hat{\Omega}^j_{\mu\nu}(t)\hat{\Omega}^j_{\mu\nu}(t) - \frac{\delta_{\mu\nu}}{3} \tag{8.2}$$

With a joint probability distribution approximated by a large-deviation principle,

$$P(\mathcal{Q}(0), \mathcal{Q}(t)) \sim \exp\left(-N(I(\mathcal{Q}(0), \mathcal{Q}(t))\right) \tag{8.3}$$

$$\int\int d\mathcal{Q}(0)d\mathcal{Q}(t)P(\mathcal{Q}(0),\mathcal{Q}(t)) = 1 \tag{8.4}$$

As we saw in chapter 6, the rate function depends on the large-deviation vector made up of the five tesseral harmonics $\{R_m; m = -2, ..., 2\}$. We can follow the same logic even for a two-time problem and say that the total rate function will take the following general form,

$$I(\mathbf{R}(0), \mathbf{R}(t)) = I(\mathbf{R}(0)) + I(\mathbf{R}(t)) + J(\mathbf{R}(0) \cdot \mathbf{R}(t)) \tag{8.5}$$

The third term makes all the difference. There will be overlap between the two order parameters for finite times, and that overlap will be go to zero at $t \to \infty$,

$$\lim_{t\to\infty} J(\mathbf{R}(0) \cdot \mathbf{R}(t)) = 0 \tag{8.6}$$

That means that the joint rate function will break into the sum of two independent rate functions,

$$\lim_{t\to\infty} I(\mathbf{R}(0), \mathbf{R}(t)) = I(\mathbf{R}(0)) + I(\mathbf{R}(t)) \tag{8.7}$$

and the joint probability distribution will be a sum of two identical densities,

$$P(\mathbf{R}(0), \mathbf{R}(t)) \sim \exp\left(-NI(\mathbf{R}(0))\right) \exp\left(-NI(\mathbf{R}(t))\right) \tag{8.8}$$

Similarly, the generating function will be a function of the large-deviation field at two different times,

$$G(\mathbf{h}(0), \mathbf{h}(t)) = \langle \exp\left(\mathbf{h}(0) \cdot \mathbf{R}(0) + \mathbf{h}(t) \cdot \mathbf{R}(t)\right) \rangle \tag{8.9}$$

and the scaled cumulant generating function will split into sums in the same way that the rate function did,

$$\lambda(\mathbf{h}(0), \mathbf{h}(t)) = \lambda(\mathbf{h}(0)) + \lambda(\mathbf{h}(t)) + \zeta(\mathbf{h}(0) \cdot \mathbf{h}(t)) \tag{8.10}$$

$$\lim_{t\to\infty} \lambda(\mathbf{h}(0), \mathbf{h}(t)) = \lambda(\mathbf{h}(0)) + \lambda(\mathbf{h}(t)) \tag{8.11}$$

At sufficiently long times we expect the terms that involve overlap between two order parameters or overlap between fields at two different times to vanish and recover sums and/or products of independent events.

8.1 Time-dependent scaled cumulant generating function

As a natural extension from a one-time field to a two-time field we define the 10-dimensional 10-dimensional vector $\mathbf{x}$ whose first 5 elements correspond to the field at $\tau = 0$, $\{h_m(0); m = -2, ...2\}$ and the rest of the five elements are the components of the field at time $\tau = t$, $\{h_m(t); m = -2, ...2\}$,

$$\mathbf{x} = \{x_a; a = 1, ..., 10\}, \quad x^2 = \sum_{a=1}^{10} x_a^2 \tag{8.12}$$

The conjugate order parameter $\mathbf{y}$ is also a 10-dimensional vector and is defined in a similar fashion,

$$\mathbf{y} = \{y_a; a = 1, ..., 10\}, \quad y^2 = \sum_{a=1}^{10} y_a^2 \tag{8.13}$$

where the first 5 elements correspond to the five tesseral harmonics at times $\tau = 0$ $\{R_m(0); m = -2, ...2\}$ and the rest of the five elements correspond tesseral harmonics at times $\tau = t$, $\{R_m(t); m = -2, ...2\}$. When the fluctuations at both times are small, we can calculate the cumulant generator exactly. The answer has been worked out via random-matrix theory methods [63] but we can also derive it with our large-deviation theory. The cumulant generator is defined as

$$\exp\left(N\lambda(\mathbf{x})\right) = \langle \exp\left(F\right)\rangle = \exp\left(\langle F\rangle + \frac{1}{2}\langle(\delta F)^2\rangle + ...\right) \tag{8.14}$$

$$F = N\mathbf{y}\cdot\mathbf{x} = \sum_{j=1}^{N}\sum_{m=-2}^{2}\left(r_m(\hat{\Omega}_j(0))h_m(0) + r_m(\hat{\Omega}_j(t))h_m(t)\right) \tag{8.15}$$

When the system is isotropic the tesseral harmonic functions average to zero as we saw in chapter 6 and all the one-body averages will be identically zero. Up to second order, the cumulant generator is,

$$\begin{aligned}\lambda(\mathbf{x}) = &\frac{1}{2N}\sum_{j,k=1}^{N}\sum_{m,m'=-2}^{2} h_m(0)\left\langle r_m(\hat{\Omega}_j(0))r_{m'}(\hat{\Omega}_k(0))\right\rangle h_{m'}(0)\\ &+\frac{1}{2N}\sum_{j,k=1}^{N}\sum_{m,m'=-2}^{2} h_m(t)\left\langle r_m(\hat{\Omega}_j(t))r_{m'}(\hat{\Omega}_k(t))\right\rangle h_{m'}(t)\\ &+\frac{1}{N}\sum_{j,k=1}^{N}\sum_{m,m'=-2}^{2} h_m(0)\left\langle r_m(\hat{\Omega}_j(0))r_{m'}(\hat{\Omega}_k(t))\right\rangle h_{m'}(t)+...\end{aligned} \tag{8.16}$$

The tesseral harmonics are orthogonal to each other so only the terms with m=m' will survive averaging. Also, the isotropic system the field components are all equal $h_m^2(0) = h^2(0)/5, h_m^2(t) = h^2(t)/5$ and $h_m(0)h_m(t) = h(0)h(t)/5$. With these two arguments we can simplify the expression and we get,

$$\begin{aligned}\lambda(\mathbf{x}) = &\frac{h^2(0)}{10N}\sum_{j,k=1}^{N}\sum_{m=-2}^{2}\left\langle r_m(\hat{\Omega}_j(0))r_m(\hat{\Omega}_k(0))\right\rangle\\ &+\frac{h^2(t)}{10N}\sum_{j,k=1}^{N}\sum_{m=-2}^{2}\left\langle r_m(\hat{\Omega}_j(t))r_m(\hat{\Omega}_k(t))\right\rangle\\ &+\frac{2\mathbf{h}(0)\cdot\mathbf{h}(t)}{10N}\sum_{j,k=1}^{N}\sum_{m=-2}^{2}\left\langle r_m(\hat{\Omega}_j(0))r_m(\hat{\Omega}_k(t))\right\rangle+...\end{aligned} \tag{8.17}$$

where

$$h^2(0) = \sum_{m=-2}^{2} h_m^2(0), \quad h^2(t) = \sum_{m=-2}^{2} h_m^2(t), \quad \mathbf{h}(0)\cdot\mathbf{h}(t) = \sum_{m=-2}^{2} h_m(0)h_m(t) \tag{8.18}$$

The last part of the calculation involves the tesseral harmonic addition theorem we used in chapter 6. The theorem states that

$$\sum_{m=-2}^{2} r_m(\hat{\Omega}_j(t_1))r_m(\hat{\Omega}_k(t_2)) = \frac{5}{4\pi}P_2(\hat{\Omega}_j(t_1)\cdot\hat{\Omega}_k(t_2)) \tag{8.19}$$

which leads to

$$\begin{aligned}\lambda(\mathbf{x}) = &\frac{h^2(0)}{8\pi}\left\langle \frac{1}{N}\sum_{j,k=1}^{N} P_2(\hat{\Omega}_j(0)\cdot\hat{\Omega}_k(0))\right\rangle \\ &+\frac{h^2(t)}{8\pi}\left\langle \frac{1}{N}\sum_{j,k=1}^{N} P_2(\hat{\Omega}_j(t)\cdot\hat{\Omega}_k(t))\right\rangle \\ &+\frac{2\mathbf{h}(0)\cdot\mathbf{h}(t)}{8\pi}\left\langle \frac{1}{N}\sum_{j,k=1}^{N} P_2(\hat{\Omega}_j(0)\cdot\hat{\Omega}_k(t))\right\rangle + ...\end{aligned} \tag{8.20}$$

and we can apply it to all three terms in the cumulant generator including the cross term with the dot product. By defining the one-time and two-time susceptibilities

$$\chi = \left\langle \frac{1}{N}\sum_{j,k=1}^{N} P_2(\hat{\Omega}_j(t_1)\cdot\hat{\Omega}_k(t_1))\right\rangle, \quad \chi(t) = \left\langle \frac{1}{N}\sum_{j,k=1}^{N} P_2(\hat{\Omega}_j(t_1)\cdot\hat{\Omega}_k(t_2))\right\rangle \tag{8.21}$$

the scaled cumulant generating function can be written simply as,

$$\lambda(\mathbf{x}) = \frac{\chi}{8\pi}\left(h^2(0) + h^2(t) + 2C(t)\mathbf{h}(0)\cdot\mathbf{h}(t)\right) \tag{8.22}$$

$$C(t) = \frac{\chi(t)}{\chi}, \quad \lim_{t\to\infty} C(t) = 0 \tag{8.23}$$

This is exactly the answer that was derived via random-matrix theory in [63]. We showed that our framework is capable of reproducing the same result. Furthermore we see that the term (in equation 8.10) that depends on the dot product is,

$$\zeta(\mathbf{h}(0)\cdot\mathbf{h}(t)) = C(t)\frac{\chi}{4\pi}\mathbf{h}(0)\cdot\mathbf{h}(t) \tag{8.24}$$

For large times we expect that term to vanish as the two order parameters will be independent from each other,

$$\lim_{t\to\infty}\lambda(\mathbf{x}) = \frac{\chi}{8\pi}h^2(0) + \frac{\chi}{8\pi}h^2(t) = \lambda(\mathbf{h}(0)) + \lambda(\mathbf{h}(t)) \tag{8.25}$$

Finally in the large-deviation theory language we can write the cumulant generator in terms of the vector $\mathbf{x}$ in a very succinct way,

$$\lambda(\mathbf{x}) = \frac{\chi}{8\pi}\mathbf{x}^T\mathcal{M}\mathbf{x} \tag{8.26}$$

where $\mathcal{M}$ is a 10×10 coupling matrix (given in Appendix B, equation B.22) that goes to the 10×10 unit matrix $\mathbf{1}$ for very long times as the fields uncouple,

$$\lim_{t\to\infty} \mathcal{M} = \mathbf{1} \tag{8.27}$$

$$\lambda(\mathbf{x}) = \frac{\chi}{8\pi}x^2, \quad t \to \infty \tag{8.28}$$

It is quite incredible how we can manipulate the cumulant generating function into this extremely simple form. Perhaps one may wonder how far our theory can be stretched. Surprisingly, crucial results and assumptions that we made in the time-independent scenario carry over to time-dependent weak fluctuations albeit with different order parameter and conjugate field.

8.2 Gaertner-Ellis theorem and vector equation of state

The goal is to calculate the rate function $I(\mathbf{y})$ which is the Legendre transform of the cumulant generator $\lambda(\mathbf{x})$. The Gaernter Ellis provides a route of calculating $I(\mathbf{y})$ and without loss of generality we can say

$$\begin{aligned} I(\mathbf{y}) &= \mathbf{x}\cdot\mathbf{y} - \lambda(\mathbf{x}), \quad \mathbf{y} = \nabla_{\mathbf{x}}\lambda(\mathbf{x}) \\ &= \mathbf{x}\cdot\mathbf{y} - \int_0^{\mathbf{x}} \mathbf{y}(\mathbf{x}')\cdot d\mathbf{x}' \\ &= \int_0^{\mathbf{y}} \mathbf{x}(\mathbf{y}')\cdot d\mathbf{y}' \end{aligned} \tag{8.29}$$

where once again we used integration by parts and obtained a reversible work theorem for $I(\mathbf{y})$ in terms of a vector equation of state $\mathbf{x}(\mathbf{y})$. The reversible work theorem does not simplify in a straightforward manner to a one-dimensional integral as in time-independent problems. We will get back to this point later.

Is is interesting that the usual results of our theory generalize to time-dependent problems relatively straightforward.

When the fluctuations are weak for both times, we can calculate the rate function exactly. This can be seen from the vector-equation of state defined in 8.29

$$\mathbf{y} = \nabla\lambda(\mathbf{x}) = \frac{\chi}{4\pi}\mathcal{M}\mathbf{x} \tag{8.30}$$

$$\Leftrightarrow \mathbf{x} = \frac{4\pi}{\chi}\mathcal{M}^{-1}\mathbf{y} \tag{8.31}$$

where $\mathcal{M}^{-1}$ is the inverse (given in Appendix B, equation B.29) of the coupling matrix $\mathcal{M}$

$$\mathcal{M}\mathcal{M}^{-1} = \mathbf{1} \tag{8.32}$$

$$\lim_{t\to\infty}\mathcal{M} = \lim_{t\to\infty}\mathcal{M}^{-1} = \mathbf{1} \tag{8.33}$$

This is the time-dependent analogue of the field being linear to the order parameter. Substituting the expression for $\mathbf{x}$ from equation 8.31 into equation 8.26 we get

$$I(\mathbf{y}) = \frac{4\pi}{\chi}\mathbf{y}^T\mathcal{M}^{-1}\mathbf{y} - \lambda(\mathbf{x}(\mathbf{y})) = \frac{2\pi}{\chi}\mathbf{y}^T\mathcal{M}^{-1}\mathbf{y} \tag{8.34}$$

This can be written in terms of the two 5-dimensional large-deviation vectors which are made out of tesseral harmonics,

$$I(\mathbf{y}) = \frac{2\pi}{\chi}\Delta(t)\left(R^2(0) + R^2(t) - 2C(t)\mathbf{R}(0)\cdot\mathbf{R}(t)\right) \tag{8.35}$$

$$\Delta(t) = \frac{1}{1 - C^2(t)} \tag{8.36}$$

$$\lim_{t\to\infty} \Delta(t) = 1 \tag{8.37}$$

The long-time behavior simplifies,

$$\lim_{t\to\infty} I(\mathbf{y}) = \frac{2\pi}{\chi} y^2 = \frac{2\pi}{\chi} R^2(0) + \frac{2\pi}{\chi} R^2(t) = I(\mathbf{R}(0)) + I(\mathbf{R}(t)) \tag{8.38}$$

Moreover we can express $I(\mathbf{y})$ as a function of the traces of the matrices $\mathcal{Q}(0)$ and $\mathcal{Q}(t)$,

$$Tr(\mathcal{Q}^2(0)) = \frac{6\pi}{5} R^2(0) \tag{8.39}$$

$$Tr(\mathcal{Q}^2(t)) = \frac{6\pi}{5} R^2(t) \tag{8.40}$$

$$Tr(\mathcal{Q}(0)\mathcal{Q}(t)) = \frac{6\pi}{5} \mathbf{R}(0) \cdot \mathbf{R}(t) \tag{8.41}$$

where the term $\mathcal{Q}(0)\mathcal{Q}(t)$ means matrix multiplication between the tensor order parameter at times $\tau = 0$ and the tensor order parameter at times $\tau = t$. Inserting the expressions for the traces into the expression for the rate function in 8.35 we get,

$$I(\mathbf{y}) = \frac{5}{3\chi} \Delta(t) \left(Tr(\mathcal{Q}^2(0)) + Tr(\mathcal{Q}^2(t)) - 2C(t) Tr(\mathcal{Q}(0)\mathcal{Q}(t)) \right) \tag{8.42}$$

$$P(\mathbf{y}) \sim \exp\left(-N I(\mathbf{y})\right) \tag{8.43}$$

This expression has been derived in [63] via random-matrix theory methods. In the limit of large times the third term goes to zero and we get

$$P(\mathbf{y}) = P(\mathcal{Q}(0)) P(\mathcal{Q}(t)) \tag{8.44}$$

which means that the probabilities are independent.

8.3 Scalar equation of state and reversible work theorem

In time independent problems we were able to make a few natural assumptions about the free energy functions as well as the vector equation of state. We were able to choose the order parameter to point parallel to the external field $\mathbf{h}$. Combined with the spherical symmetry of the free energy functions we wrote the rate function as a thermodynamic integral over the scalar equation of state. A natural question rises here: Can we make similar assumptions for the time-dependent problem? The answer is no but there is nevertheless an elegant simplification we can make, at least for the case of weak fluctuations.

Firstly, we observe that for weak fluctuations,

$$\lambda(\mathbf{x}) = \lambda(\sqrt{\mathbf{x}^T \mathcal{M} \mathbf{x}}), \quad I(\mathbf{y}) = I(\sqrt{\mathbf{y}^T \mathcal{M}^{-1} \mathbf{y}}) \tag{8.45}$$

which means that the natural scalar quantities of the problem are,

$$\alpha \equiv \sqrt{\mathbf{x}^T \mathcal{M} \mathbf{x}} \tag{8.46}$$

$$\lim_{t \to \infty} \alpha = x \tag{8.47}$$

$$\beta \equiv \sqrt{\mathbf{y}^T \mathcal{M}^{-1} \mathbf{y}} \tag{8.48}$$

$$\lim_{t \to \infty} \beta = y \tag{8.49}$$

We may assume that the free energy functions of the weak-fluctuation limit are spherically symmetric in the sense that they depend only on the scalar quantities α and β respectively. The two-time scaled cumulant generating function is,

$$\lambda(\alpha) \approx \frac{\chi}{8\pi} \mathbf{x}^T \mathcal{M} \mathbf{x} = \frac{\chi}{8\pi} \alpha^2 \tag{8.50}$$

$$\lim_{t\to\infty} \lambda(\alpha) = \frac{\chi}{8\pi} x^2 \tag{8.51}$$

and the rate function,

$$I(\beta) \approx \frac{2\pi}{\chi} \mathbf{y}^T \mathcal{M}^{-1} \mathbf{y} = \frac{2\pi}{\chi} \beta^2 \tag{8.52}$$

$$\lim_{t\to\infty} I(\beta) = \frac{2\pi}{\chi} y^2 \tag{8.53}$$

with the corresponding large time limits. With the new definitions we can show that it is possible to convert the vector equation of state

$$\mathbf{y} = \nabla_{\mathbf{x}} \lambda(\mathbf{x}) \tag{8.54}$$

into a scalar one by using the newly defined quantities (α and β),

$$\beta = \frac{\partial \lambda(\alpha)}{\partial \alpha} \tag{8.55}$$

Keep in mind that this is not the same as

$$y = \frac{\partial \lambda(x)}{\partial x} \tag{8.56}$$

since 8.56 holds true only for very long times,

$$\lim_{t\to\infty} \left[\beta = \frac{\partial \lambda(\alpha)}{\partial \alpha} \right] \to y = \frac{\partial \lambda(x)}{\partial x} \tag{8.57}$$

The scalar equation of state 8.55 can be derived in the following manner. Starting from the spherical symmetry of $\lambda(\alpha)$ we have,

$$\mathbf{y} = \nabla_{\mathbf{x}} \lambda(\alpha) \tag{8.58}$$

from the definition in 8.46 we can see that,

$$\mathbf{y} = \frac{1}{\alpha}\frac{\partial\lambda}{\partial\alpha}\mathcal{M}\mathbf{x} \tag{8.59}$$

or equivalently,

$$\mathbf{x} = \alpha\frac{1}{\frac{\partial\lambda}{\partial\alpha}}\mathcal{M}^{-1}\mathbf{y} \tag{8.60}$$

By taking the dot product of 8.59 with $\mathbf{x}$ on both sides and equation 8.60 with $\mathbf{y}$ we get the following two equations,

$$\mathbf{x}\cdot\mathbf{y} = \alpha\frac{\partial\lambda}{\partial\alpha} \tag{8.61}$$

$$\mathbf{y}\cdot\mathbf{x} = \alpha\frac{1}{\frac{\partial\lambda}{\partial\alpha}}\beta^2 \tag{8.62}$$

Which of course are equal,

$$\mathbf{x}\cdot\mathbf{y} = \mathbf{y}\cdot\mathbf{x} \tag{8.63}$$

$$\Leftrightarrow \beta = \frac{\partial\lambda(\alpha)}{\partial\alpha}, \quad \text{Q.E.D.} \tag{8.64}$$

In terms of the scalars, the Gaernter-Ellis theorem may be re-written as,

$$I(\mathbf{y}) = \alpha\beta - \lambda(\alpha), \quad \beta = \frac{\partial\lambda(\alpha)}{\partial\alpha} \tag{8.65}$$

which means that it can be written as a reversible work type of integral over the the equation of state just as we did in the time-independent case,

$$I(\mathbf{y}) = \int_0^\beta \alpha(\beta')d\beta' \tag{8.66}$$

Which is a generalization of the scalar reversible work theorem but for a joint rate function. As in the case of the equation of state 8.57

$$\lim_{t\to\infty}\left[\int_0^\beta \alpha(\beta')d\beta' = \int_0^y x(y')dy'\right] \tag{8.67}$$

Finally we can verify that equation 8.66 is true in the weak fluctuation limit. The inverse of the equation of state is,

$$\beta = \frac{\partial \lambda}{\partial \alpha} = \frac{\chi}{4\pi}\alpha \tag{8.68}$$

$$\text{or} \quad \alpha = \frac{4\pi}{\chi}\beta \tag{8.69}$$

providing the correct rate function,

$$I(\beta) = \int_0^\beta \alpha(\beta')d\beta' = \int_0^\beta \frac{4\pi}{\chi}\beta' d\beta' = \frac{2\pi}{\chi}\beta^2 \tag{8.70}$$

It is impressive that the theory of large-deviations gives a very simple answer for the joint-probability distributions in the limit of weak fluctuations. When time-dependence is considered, the large-deviation theory vector $\mathbf{y}$ does not point parallel to $\mathbf{x}$. Instead we have,

$$\mathbf{y} \parallel \mathcal{M}\mathbf{x} \tag{8.71}$$

This result is exactly true for weak fluctuations and it led to a reversible work theorem expression albeit with an unusual form,

$$I(\mathbf{y}) = \int_0^\beta \alpha(\beta')d\beta', \quad \beta = \frac{\partial \lambda(\mathbf{x})}{\partial \alpha} \tag{8.72}$$

$$\alpha \equiv \sqrt{\mathbf{x}^T \mathcal{M}\mathbf{x}} \tag{8.73}$$

$$\beta \equiv \sqrt{\mathbf{y}^T \mathcal{M}^{-1}\mathbf{y}} \tag{8.74}$$

In other words, we have articulated in very succinct mathematics the case of two-time probability distributions with gaussian fluctuations. However, the focus of this study is to go beyond weak fluctuations and analytically include strong fluctuations in the picture. This thesis has reached its chronological limit and any investigation of the strongly-fluctuating limit and the possible application of Pade interpolation remains an open question.

CHAPTER 9

Concluding remarks

In this thesis we have developed a novel theory for the calculation of rare configurations in finite disordered systems. Many physical problems require the calculation of the probability distribution of an orientational order parameter. However, standard techniques like the central-limit theorem suffice when the fluctuations are weak but fail in the vicinity of a critical point. There, the fluctuations of the orientational order parameter are large and their direct simulation is subject to numerical noise and poor sampling. According to large-deviation theory, we are able to move our attention to the thermodynamic integration of the equation of state of the system. Analytical evaluation of the exact limits of the equation of state, and direct interpolation between them provides us with a new way of evaluating the probability distribution. In the low field limit, the correlations are strong but the fluctuations are easy to simulate while in the strong field limit the opposite is true. We exploited the analytical simplicity of the strong field limit in order to calculate it based on configurations that are easy to sample. The re-direction of rare-configuration calculation to some easily obtained computational information is the core of the theory.

Large-deviation theory directed us into thinking in terms of a conjugate field but in practice we never applied such a field to any of our simulations. For all the applications that were presented in the thesis, the equation of state was evaluated analytically via

Pade' interpolation. Would it be the same if we could simulate directly the equation of state by applying an external field to our system? For liquid crystals, it would not be the same for two reasons. Firstly, the application of strong alignment fields might take us to regions in the phase diagram that we do not wish to go. The system might transition to the solid phase instead of the pre-transitional isotropic phase that we want. Secondly, the very existence of domains and long correlation lengths implies that numerical evaluation of the equation of state will be noisy and the resulting rate function inaccurate. The case described in this thesis is possibly a rare occasion where analytical manipulations are actually easier than direct numerical computations.

Moreover, it is important to comment on our approach to three-dimensional liquid crystals. The absolute invariants of the problem according to random matrix theory are,

$$Tr(\mathcal{Q}^2) \quad \text{and} \quad Tr(\mathcal{Q}^3)$$

since higher order traces are functions of these two objects. In our theory however we assumed that the probability distribution will be a function of just $Tr(\mathcal{Q}^2)$,

$$P(\mathcal{Q}) \sim f(Tr(\mathcal{Q}^2))$$

ignoring the effects coming from the other invariant. This assumption is exactly true for two-dimensional systems but it is not for the three-dimensional case. The second invariant $Tr(\mathcal{Q}^3)$ represents the fluctuations perpendicular to the director and are usually found to be small, making our assumption justified. More specifically we see in Appendix A that, $\langle Tr(\mathcal{Q}^2)\rangle$ is approximately two orders of magnitude bigger than $\langle Tr(\mathcal{Q}^3)\rangle$ for a typical pre-transitional simulation. The probability distribution $P(\mathcal{Q})$ will be dominated by $Tr(\mathcal{Q}^2)$ and our assumption is reasonable. We do not expect crucial information to be missing from our theory.

Lastly, an interesting lesson that we ought to take from this study is the following:

The two-dimensional liquid crystal case is surprisingly easier than the three-dimensional counterpart. One might have expected the opposite because of the low-dimensionality topological complications (disclinations) and the inherently strong fluctuation profile of two-dimensions. It was shown that the underlying geometry is not pertinent to the discussion of the global probability distribution. Furthermore, the large deviations in two-dimensional liquid crystals brought the system closer to the perfect order limit, the very limit we implemented analytically.

Appendix A: Simulation details

Monte Carlo simulation of the 2D XY model

Monte Carlo simulations have been used extensively to study the XY model in two-dimensions since the 1970s [59]. The XY model (or planar rotor) is the simplest model to exhibit a Kosterlitz-Thouless continuous transition between a paramagnetic phase and quasi-ferromagnetic phase. In this study we used the standard Metropolis Monte Carlo (MC) algorithm under canonical conditions (NAT - constant number of spins N, constant area A and constant temperature T). We used a square lattice of dimensions 28×28 and each of the $N = 28^2 = 784$ spins lies on a site of the lattice. Periodic boundary conditions were employed which means that the spins lie on the surface of a torus. See figure 9.1 for a pictorial representation of the lattice we simulated.

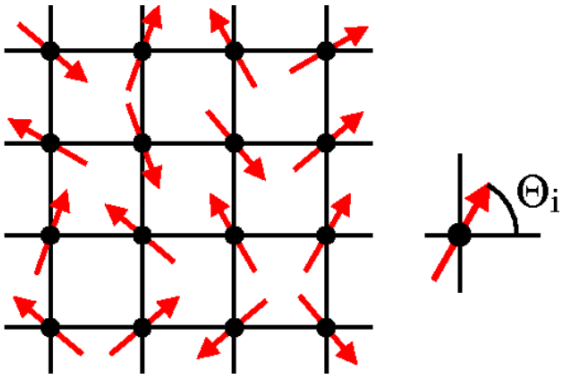

Figure 9.1: A typical configuration of the 2DXY lattice simulation. The figure is taken from [52]

Working similarly to 2D liquid crystals, we simulate the crystal under different temperatures in order to understand the fluctuation profile of $P(\mu)$. The conditions are specified via the dimensionless constant ("temperature"),

$$\beta J = \frac{J}{k_B T} \tag{9.1}$$

which is the ratio between the ferromagnetic coupling constant J and the thermal energy $k_B T$. As $\beta J \to 0$ the spins are disordered and when $\beta J \to \beta_C J$ the system approaches the Kosterlitz-Thouless transition and order grows.

Parameter	**Value**
Number of spins	$N = 784$
Dimensionality	$D = 2$
Temperature	$\beta J = 0.01$
Relaxation MC moves	10^5
Data collection MC moves	10^7

Table 9.1: Monte Carlo simulation of the 2DXY model under high-temperature conditions. We relaxed the system sufficiently and then proceeded to data collection where for every 10 Monte Carlo moves, we calculated μ.

Parameter	**Value**
Number of spins	$N = 784$
Dimensionality	$D = 2$
Temperature	$\beta J = 0.9$
Relaxation MC moves	10^6
Data collection MC moves	10^8

Table 9.2: Monte Carlo simulation of the 2DXY model under low-temperature conditions. The system is close to the critical point $\beta_C J \approx 1.13$ ([30]). After enough relaxation we started calculating μ every 10 moves.

In tables 9.1 and 9.2 the exact conditions and parameters for the two simulations are shown. The high-temperature paramagnetic phase is useful because it shows us that in that limit the fluctuations are gaussian; truncating the cumulant generating function is exact in that limit. Interestingly, when we cool the system down to a temperature that is very close to criticality, correlations between the spins are important and the fluctuations

are intrinsically non-gaussian. The approach we developed can be used to describe the probability distribution of the magnetization when fluctuations dominate and central-limit theory fails.

Molecular dynamics simulation of the Gay-Berne liquid

We performed standard Molecular Dynamics simulations where Newton's classical equations of motion are propagated numerically in time. All the quantities in the simulation are expressed in terms of the fundamental energy ϵ_0 scale, length scale σ_0 and time scale τ_0. The simulations are performed using microcanonical conditions with tetragonal and cubic periodic boundary conditions for 2D and 3D systems respectively. We follow similar initialization and relaxation protocols that are described in previous work [63]. Via Molecular Dynamics simulations we generate equilibrium ensembles of liquid crystal configurations that are used in order to calculate the elements of the tensor $\mathcal{Q}$. For each configuration we diagonalize the tensor and get the largest eigenvalue s (order parameter). Before we unfold the exact simulation protocol we remind the reader about reduced temperature and density units,

$$T^* = \frac{k_B T}{\epsilon_0}, \quad \rho^* = \rho\sigma_0^2 \quad (2D) \quad \text{and} \quad \rho^* = \rho\sigma_0^3 \quad (3D) \tag{9.2}$$

and the time-step of the simulation is,

$$\delta t = 0.001\tau_0, \quad \tau_0 = \sqrt{\frac{m\sigma_0^2}{\epsilon_0}} \tag{9.3}$$

Initialization

For the initialization of the simulation we set the center-of-mass positions of the Gay-Berne molecules in the sites of square (2D) and cubic (3D) lattices respectively. The initial density is very low $\rho^* = 0.05$ so that we make sure that there are no overlaps

between molecules. The initial orientations of all the molecules were initialized using the structure described by Allen and Tildesley [1, p. 169]. The initial velocities and angular velocities were selected from the Maxwell-Boltzmann distribution. Moreover, we made use of square and cubic periodic boundary conditions for two- and three-dimensional simulations respectively. We used the velocity Verlet algorithm [1, Chapter 3] for the propagation of the equations of motion.

Relaxation and data collection

In order to equilibrate the 2D and the 3D systems we run the following protocol:

1. **Melting**: We sample the initial velocities and angular velocities from a high-temperature ($T^* = 5.00$) distribution, and allow the system to relax for $25\tau_0$. This step is used in order to melt the initial crystal.

2. **Compression**: We compress the system by increasing the density in small steps. ($\rho^*_{new} = \rho^*_{old} + \Delta\rho^*$) Every $0.1\tau_0$ we increase the density, until the final density is reached. During this time, we rescale the velocities and angular velocities to $T^* = 3.00$ so that the system's temperature will not increase in an uncontrollable manner upon compression. The compression steps for the 2D systems are,

$$\Delta\rho^*_{242} = 0.002 \tag{9.4}$$

$$\Delta\rho^*_{450} = 0.002 \tag{9.5}$$

$$\Delta\rho^*_{800} = 0.001 \tag{9.6}$$

and for the 3D systems the optimal values were found to be

$$\Delta\rho^*_{256} = 0.002 \tag{9.7}$$

$$\Delta\rho^*_{500} = 0.002 \tag{9.8}$$

$$\Delta\rho^*_{864} = 0.001 \tag{9.9}$$

$$\Delta\rho^*_{1372} = 0.001 \tag{9.10}$$

$$\Delta\rho^*_{2048} = 0.0005 \tag{9.11}$$

3. **Cooling**: We rescale the velocities and angular velocities every $1\tau_0$ in small temperature increments $T^*_{new} = T^*_{old} - 0.1$ until the desired temperature ($T^* = 1$ for all simulations in this study) is reached. We continue to rescale the velocities and angular velocities to the desired temperature for another $20\tau_0$ and then we allow the system to relax for $60\tau_0$. We repeat the cycle of rescaling and equilibrating one more time.

4. **Relaxation**: Allow the system to relax for $200\tau_0$. We run a significant amount of steps before data collection to make sure the system is sufficiently relaxed.

5. **Data collection**: After the system has finished equilibrating, configurations are sampled every $0.01\tau_0$ (corresponds to 10 time steps). We propagate the system for enough steps so that we can get decent sampling of rare deviations. We use different amount of averaging for different systems and the exact number is mentioned in the caption of each figure.

We can visualize each step of the simulation by plotting the total, translational kinetic, rotational kinetic and potential energy per particle. In figure 9.2 we see the different energies as the simulation time progresses.

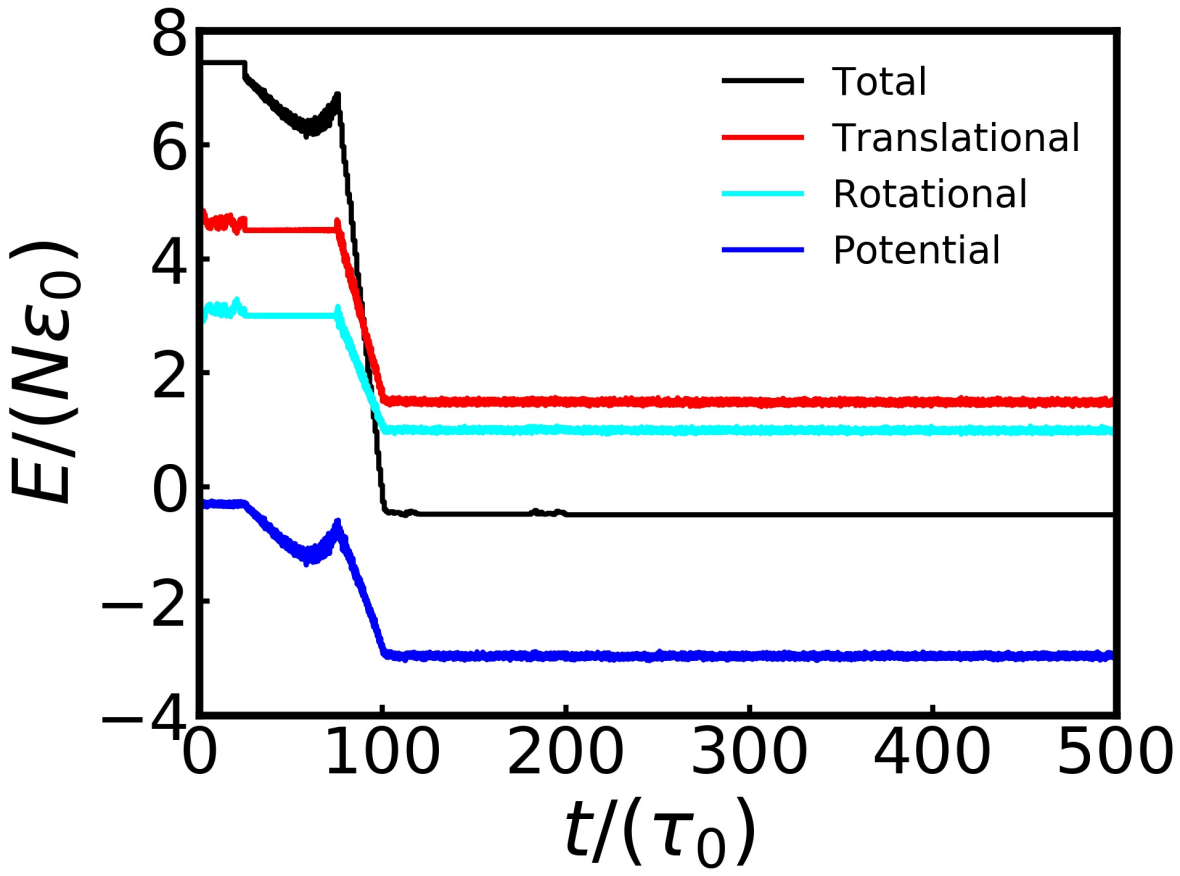

Figure 9.2: The total, translational, rotational and potential energy per particle for a three-dimensional simulation of $N = 2048$ Gay-Berne molecules under pre-transitional isotropic conditions $\rho^* = 0.30$ and $T^* = 1$.

In figure 9.2 we show the total, rotational, translational and potential energy during melting-compression-cooling and relaxation. Indeed our system's energy has relaxed and at the same time we can verify that equipartition of energy holds. This can be used as a diagnostic tool of the simulation. In terms of simulation units, each degree of freedom contributes on average 1/2. The rotational degrees of freedom are 2 (in three-dimensions), so the average rotational energy is 1 and the translational energy is 3/2 since there are 3 degrees of freedom for translation (again, in three-dimensions). The means with the standard deviations of the means for the different energies in the simulation shown in

figure 9.2 are (up to 3 decimal places),

$$\langle E_{total}/(N\epsilon_0)\rangle = -0.488 \pm 0.000 \tag{9.12}$$

$$\langle E_{translational}/(N\epsilon_0)\rangle = 1.486 \pm 0.021 \tag{9.13}$$

$$\langle E_{rotational}/(N\epsilon_0)\rangle = 0.991 \pm 0.019 \tag{9.14}$$

$$\langle E_{potential}/(N\epsilon_0)\rangle = -2.964 \pm 0.021 \tag{9.15}$$

which verifies that the equipartition theorem and the conservation of energy are true.

After reaching equilibrium we proceed to the data collection where a plethora of configurations is produced and for each configuration we calculate the elements of the tensor $\mathcal{Q}$ and we diagonalize it in order to calculate the three eigenvalues s, λ_2 and λ_3 ($s \geq \lambda_2 \geq \lambda_3$). For the diagonalization we use Eigen library's Francis QR algorithm [26] and the instantaneous eigenvalues are shown in figure 9.3.

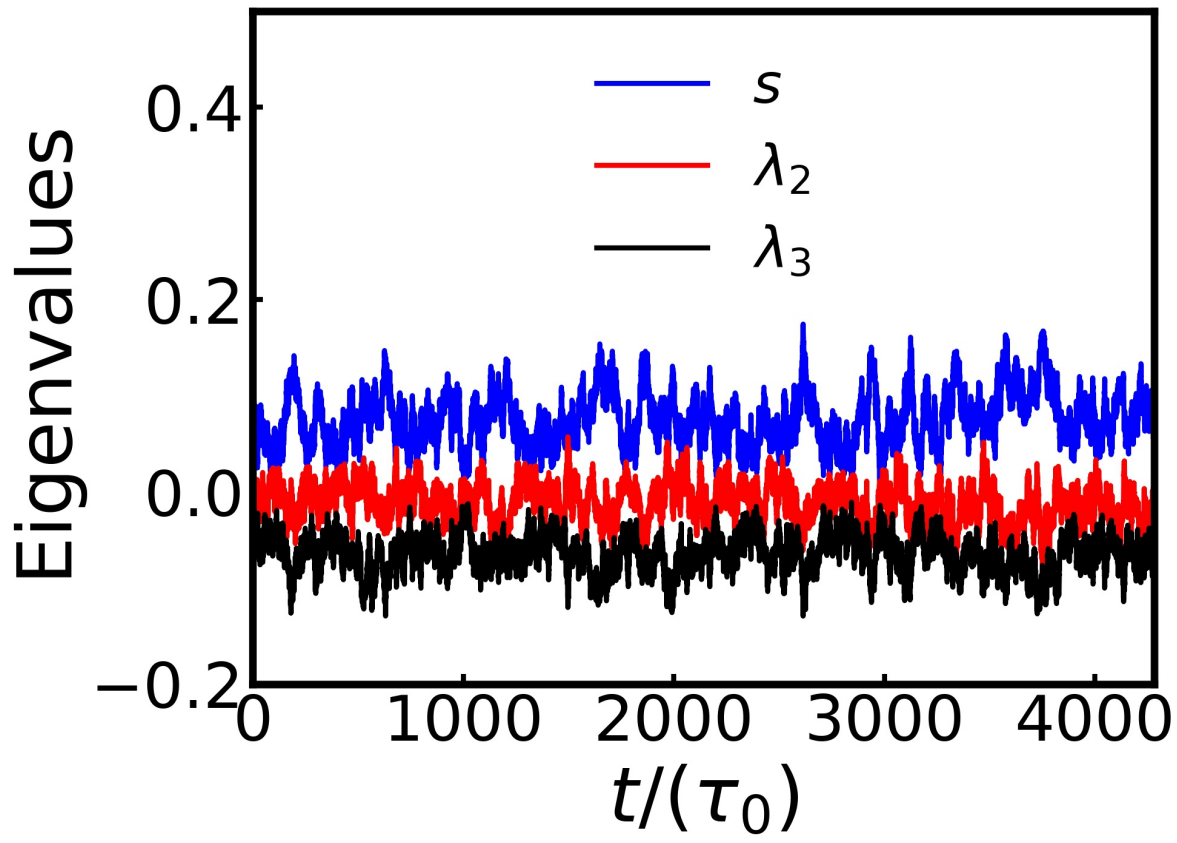

Figure 9.3: The three instantaneous eigenvalues of the tensor $\mathcal{Q}$ for a three-dimensional simulation of $N = 2048$ Gay-Berne molecules under pre-transitional isotropic conditions $\rho^* = 0.30$ and $T^* = 1$. This is the data collection process of the same simulation shown in figure 9.2.

with,

$$\langle s \rangle = 0.077 \pm 0.028 \tag{9.16}$$

$$\langle \lambda_2 \rangle = -0.011 \pm 0.019 \tag{9.17}$$

$$\langle \lambda_3 \rangle = -\langle s \rangle - \langle \lambda_2 \rangle \tag{9.18}$$

The largest eigenvalue s is our order parameter, the second largest eigenvalue is λ_2 and the third eigenvalue is λ_3. Another useful calculation involves the absolute rotational invariants of the tensor $\mathcal{Q}$. These are defined in terms of the eigenvalues,

$$Tr(\mathcal{Q}^2) = s^2 + \lambda_2^2 + \lambda_3^2 \tag{9.19}$$

$$Tr(\mathcal{Q}^3) = s^3 + \lambda_2^3 + \lambda_3^3 \tag{9.20}$$

and can be evaluated for each configuration. It is useful to see the relative magnitude of the two traces and for the system shown in figure 9.3 we can calculate that

$$\frac{\langle Tr(\mathcal{Q}^2)\rangle}{\langle Tr(\mathcal{Q}^3)\rangle} \sim \mathcal{O}(10^2) \tag{9.21}$$

which means that $Tr(\mathcal{Q}^2)$ is two orders of magnitude bigger than $Tr(\mathcal{Q}^3)$ on average and it will dominate the probability distribution of $P(\mathcal{Q})$ for three-dimensional liquid crystals.

Appendix B: Definition of $\mathcal{M}$ and calculation of $\mathcal{M}^{-1}$

When discussing time-dependent weak fluctuations we derived the expression for the cumulant generator in equation 8.26. The expression involves the 10 by 10 matrix $\mathcal{M}$ defined as,

$$\mathcal{M} = \begin{pmatrix} 1 & 0 & 0 & 0 & 0 & C(t) & 0 & 0 & 0 & 0 \\ 0 & 1 & 0 & 0 & 0 & 0 & C(t) & 0 & 0 & 0 \\ 0 & 0 & 1 & 0 & 0 & 0 & 0 & C(t) & 0 & 0 \\ 0 & 0 & 0 & 1 & 0 & 0 & 0 & 0 & C(t) & 0 \\ 0 & 0 & 0 & 0 & 1 & 0 & 0 & 0 & 0 & C(t) \\ C(t) & 0 & 0 & 0 & 0 & 1 & 0 & 0 & 0 & 0 \\ 0 & C(t) & 0 & 0 & 0 & 0 & 1 & 0 & 0 & 0 \\ 0 & 0 & C(t) & 0 & 0 & 0 & 0 & 1 & 0 & 0 \\ 0 & 0 & 0 & C(t) & 0 & 0 & 0 & 0 & 1 & 0 \\ 0 & 0 & 0 & 0 & C(t) & 0 & 0 & 0 & 0 & 1 \end{pmatrix} \tag{B.22}$$

or in terms of elements

$$\mathcal{M}_{ij} = \delta_{ij} + C(t)\delta_{i,\alpha}, \quad \alpha = \mod_{10}(j+5) \tag{B.23}$$

The matrix $\mathcal{M}$ might be high dimensional and cumbersome to handle but in reality it can be very simply written as a 2 by 2 block matrix

$$\mathcal{M} = \begin{pmatrix} \mathbf{1} & C(t)\mathbf{1} \\ C(t)\mathbf{1} & \mathbf{1} \end{pmatrix} \tag{B.24}$$

where $\mathbf{1}$ is the 5 by 5 unit matrix. The rate function 8.34 is expressed in terms of the inverse of $\mathcal{M}$. We can do the inversion of $\mathcal{M}$ by using the block inversion formula [45],

$$\begin{pmatrix} \mathcal{A} & \mathcal{B} \\ \mathcal{C} & \mathcal{D} \end{pmatrix}^{-1} = \begin{pmatrix} \mathcal{A}^{-1} + \mathcal{A}^{-1}\mathcal{B}\mathcal{S}^{-1}\mathcal{C}\mathcal{A}^{-1} & -\mathcal{A}^{-1}\mathcal{B}\mathcal{S}^{-1} \\ -\mathcal{S}^{-1}\mathcal{C}\mathcal{A}^{-1} & \mathcal{S}^{-1} \end{pmatrix} \tag{B.25}$$

where $\mathcal{S}$ is called the Schur complement of $\mathcal{A}$ and is defined as,

$$\mathcal{S} = \mathcal{D} - \mathcal{C}\mathcal{A}^{-1}\mathcal{B} \tag{B.26}$$

In our case we have the following 5 by 5 matrices $\mathcal{A} = \mathbf{1}$, $\mathcal{B} = C(t)\mathbf{1}$, $\mathcal{C} = \mathbf{1}$, $\mathcal{D} = C(t)\mathbf{1}$. Applying B.25 to B.24 we get,

$$\mathcal{M}^{-1} = \Delta(t) \begin{pmatrix} \mathbf{1} & -C(t)\mathbf{1} \\ -C(t)\mathbf{1} & \mathbf{1} \end{pmatrix} \tag{B.27}$$

$$\Delta(t) = \frac{1}{1 - C^2(t)} \tag{B.28}$$

which means that $\frac{1}{\Delta(t)}\mathcal{M}^{-1}$ is

$$\frac{\mathcal{M}^{-1}}{\Delta(t)} = \begin{pmatrix} 1 & 0 & 0 & 0 & 0 & -C(t) & 0 & 0 & 0 & 0 \\ 0 & 1 & 0 & 0 & 0 & 0 & -C(t) & 0 & 0 & 0 \\ 0 & 0 & 1 & 0 & 0 & 0 & 0 & -C(t) & 0 & 0 \\ 0 & 0 & 0 & 1 & 0 & 0 & 0 & 0 & -C(t) & 0 \\ 0 & 0 & 0 & 0 & 1 & 0 & 0 & 0 & 0 & -C(t) \\ -C(t) & 0 & 0 & 0 & 0 & 1 & 0 & 0 & 0 & 0 \\ 0 & -C(t) & 0 & 0 & 0 & 0 & 1 & 0 & 0 & 0 \\ 0 & 0 & -C(t) & 0 & 0 & 0 & 0 & 1 & 0 & 0 \\ 0 & 0 & 0 & -C(t) & 0 & 0 & 0 & 0 & 1 & 0 \\ 0 & 0 & 0 & 0 & -C(t) & 0 & 0 & 0 & 0 & 1 \end{pmatrix} \tag{B.29}$$

and in terms of elements

$$\mathcal{M}^{-1}_{ij} = \Delta(t)\left[\delta_{ij} - C(t)\delta_{i,\alpha}\right], \quad \alpha = \mod_{10}(j+5) \tag{B.30}$$

Bibliography

[1] M. P. Allen and D. J. Tildesley. *Computer Simulation of Liquids*. Clarendon Press, Oxford [England], 1987.

[2] D. Andrienko. Introduction to liquid crystals. *Journal of Molecular Liquids*, 267: 520–541, 2018. Special Issue Dedicated to the Memory of Professor Y. Reznikov.

[3] S. T. Banks and S. T. Bramwell. Temperature-dependent fluctuations in the twodimensional xy model. *J. Phys. A: Math. Gen.*, 38:5603, 2005.

[4] M. A. Blanco, M. Flórez, and M. Bermejo. Evaluation of the rotation matrices in the basis of real spherical harmonics. *Journal of Molecular Structure: THEOCHEM*, 419(1):19–27, 1997.

[5] S. T. Bramwell, J.-Y. Fortin, P. C. W. Holdsworth, S. Peysson, J.-F. Pinton, B. Portelli, and M. Sellitto. Magnetic fluctuations in the classical XY model: The origin of an exponential tail in a complex system. *Phys. Rev. E*, 63:041106, Mar 2001.

[6] A. Calderón-Alcaraz, J. Munguía-Valadez, S. I. Hernández, A. Ramírez-Hernández, E. J. Sambriski, and J. A. Moreno-Razo. A bidimensional gay-berne calamitic fluid: Structure and phase behavior in bulk and strongly confined systems. *Frontiers in Physics*, 8, 2021.

[7] H. B. Callen. *Thermodynamics and an Introduction to Thermostatistics*. John Wiley & Sons, New York, 2nd edition, 1960.

[8] H. Cang, J. Li, and M. Fayer. Short time dynamics in the isotropic phase of liquid crystals: the aspect ratio and the power law decay. *Chemical Physics Letters*, 366(1): 82–87, 2002.

[9] D. Chandler. *Introduction to Modern Statistical Mechanics*. Oxford University Press, 1987.

[10] D. Chandler and J. P. Garrahan. Dynamics on the way to forming glass: Bubbles in space-time. *Annual review of physical chemistry*, 61:191–217, 2010.

[11] A. Cohen. A padé approximant to the inverse langevin function. *Rheologica Acta*, 30 (3):270–273, May 1991.

[12] P. De Gennes. Phenomenology of short-range-order effects in the isotropic phase of nematic materials. *Physics Letters A*, 30(8):454–455, 1969.

[13] E. De Miguel, L. F. Rull, M. K. Chalam, and K. E. Gubbins. Liquid crystal phase diagram of the gay-berne fluid. *Molecular Physics*, 74(2):405–424, 1991.

[14] I. Dierking and S. Al-Zangana. Lyotropic liquid crystal phases from anisotropic nanomaterials. *Nanomaterials (Basel)*, 7(10), Oct. 2017.

[15] T. Doerr, D. Herman, H. Mathur, and P. Taylor. Randomness in nanoscopic liquid-crystal droplets—how small is too small? *EPL (Europhysics Letters)*, 59(3):398, 2002.

[16] J. Dutka. On the problem of random flights. *Archive for History of Exact Sciences*, 32(3/4):351–375, 1985.

[17] A. Einstein. Über die gültigkeitsgrenze des satzes von thermodynamischen gleichgewicht und über die möglichkeit einer neuen bestimmung der elementarquanta. *Annalen der Physik*, 22:569–572, 1907.

[18] R. Eppenga and D. Frenkel. Monte carlo study of the isotropic and nematic phases of infinitely thin hard platelets. *Molecular Physics*, 52(6):1303–1334, 1984.

[19] G. H. Fredrickson and H. C. Andersen. Kinetic ising model of the glass transition. *Physical review letters*, 53(13):1244, 1984.

[20] L. R. O. F.R.S. Xxxi. on the problem of random vibrations, and of random flights in one, two, or three dimensions. *The London, Edinburgh, and Dublin Philosophical Magazine and Journal of Science*, 37(220):321–347, 1919.

[21] P. Gaspard. Fluctuation relations for equilibrium states with broken discrete symmetries. *Journal of Statistical Mechanics: Theory and Experiment*, 2012(08):P08021, aug 2012.

[22] J. G. Gay and B. J. Berne. Modification of the overlap potential to mimic a linear site–site potential. *The Journal of Chemical Physics*, 74(6):3316–3319, 03 1981.

[23] P.-G. d. Gennes and J. Prost. *The physics of liquid crystals*. Oxford science publications. Clarendon Press ; Oxford University Press, Oxford, New York, 2nd ed edition, 1993.

[24] N. Goldenfeld. *Lectures On Phase Transitions And The Renormalization Group*. CRC Press, Boca Raton, 1st edition edition, 1992.

[25] E. F. Gramsbergen, L. Longa, and W. H. de Jeu. Phys. rep. 135:195, 1986.

[26] G. Guennebaud, B. Jacob, et al. Eigen v3. http://eigen.tuxfamily.org, 2010.

[27] J. Guioth and D. Lacoste. Thermodynamic bounds on equilibrium fluctuations of a global or local order parameter. *Europhysics Letters*, 115(6):60007, nov 2016.

[28] L. O. Hedges, R. L. Jack, J. P. Garrahan, and D. Chandler. Dynamic order-disorder in atomistic models of structural glass formers. *Science*, 323(5919):1309–1313, 2009.

[29] K. Hoffman and R. Kunze. *Linear Algebra*. Prentice-Hall, Englewood Cliffs, 1971.

[30] Y.-D. Hsieh, Y.-J. Kao, and A. W. Sandvik. Finite-size scaling method for the

berezinskii-kosterlitz-thouless transition. *Journal of Statistical Mechanics: Theory and Experiment*, 2013(9):P09001, 2013.

[31] R. L. Jack and P. Sollich. Large deviations of the dynamical activity in the east model: Analysing structure in biased trajectories. *Journal of Physics A: Mathematical and Theoretical*, 47(1):015003, 2013.

[32] R. L. Jack, L. O. Hedges, J. P. Garrahan, and D. Chandler. Preparation and relaxation of very stable glassy states of a simulated liquid. *Physical review letters*, 107(27):275702, 2011.

[33] R. Jedynak. Approximation of the inverse langevin function revisited. *Rheologica Acta*, 54(1):29–39, Jan 2015.

[34] H. Kelker and B. Scheurle. A liquid-crystalline (nematic) phase with a particularly low solidification point. *Angewandte Chemie International Edition*, 8(11):884, 1969.

[35] W. Kuhn and F. Grün. Beziehungen zwischen elastischen konstanten und dehnungs-doppelbrechung hochelastischer stoffe. *Kolloid-Zeitschrift*, 101:248–271, 1942.

[36] P. Kundu, P. Mishra, A. Jaiswal, and J. Ram. Structures and phase transition in a two-dimensional system of gay-berne molecules. *Journal of Molecular Liquids*, 296: 111769, 2019. ISSN 0167-7322.

[37] P. Kundu, J. Saha, and P. Mishra. Long-range decay of pair correlations and nematic ordering in a two-dimensional system of gay-berne mesogens. *Fluid Phase Equilibria*, 549:113224, 2021.

[38] D. Lacoste and P. Gaspard. Isometric fluctuation relations for equilibrium states with broken symmetry. *Phys. Rev. Lett.*, 113:240602, Dec 2014.

[39] D. Lacoste and P. Gaspard. Fluctuation relations for equilibrium states with broken discrete or continuous symmetries. *Journal of Statistical Mechanics: Theory and Experiment*, 2015(11):P11018, 2015.

[40] L. D. Landau and E. M. Lifshitz. *Statistical Physics, vol. 1.* Pergamon, Oxford, 1980.

[41] P. A. Lebwohl and G. Lasher. Nematic-liquid-crystal order—a monte carlo calculation. *Phys. Rev. A*, 6:426–429, Jul 1972.

[42] J. Li, H. Cang, H. C. Andersen, and M. D. Fayer. A mode coupling theory description of the short- and long-time dynamics of nematogens in the isotropic phase. *The Journal of Chemical Physics*, 124(1):014902, 2006.

[43] J. Li, I. Wang, and M. D. Fayer. Three homeotropically aligned nematic liquid crystals: Comparison of ultrafast to slow time-scale dynamics. *The Journal of Chemical Physics*, 124(4):044906, 2006.

[44] J. D. Litster and T. W. S. Stinson III. Critical slowing of fluctuations in a nematic liquid crystal. *Journal of Applied Physics*, 41(3):996–997, 1970.

[45] T.-T. Lu and S.-H. Shiou. Inverses of 2×2 block matrices. *Computers & Mathematics with Applications*, 43(1–2):119–129, 2002.

[46] N. D. Mermin and H. Wagner. Absence of ferromagnetism or antiferromagnetism in one- or two-dimensional isotropic heisenberg models. *Phys. Rev. Lett.*, 17:1133–1136, Nov 1966.

[47] V. Morovati and R. Dargazany. Improved approximations of non-gaussian probability, force, and energy of a single polymer chain. *Phys Rev E*, 99(5-1):052502, May 2019.

[48] T. Nemoto, R. L. Jack, and V. Lecomte. Finite-size scaling of a first-order dynamical phase transition: Adaptive population dynamics and an effective model. *Physical review letters*, 118(11):115702, 2017.

[49] L. Onsager. The effects of shape on the interaction of colloidal particles. *Ann. N. Y. Acad. Sci.*, 51:627–659, 1949.

[50] E. Priestley. *Introduction to Liquid Crystals.* Springer, 1976.

[51] M. Rubinstein and R. H. Colby. Polymer physics. pages 72–73, Oxford, 2003. Oxford University Press.

[52] A. W. Sandvik. Quantum spin systems - models and computational methods. Summer School on Computational Statistical Physics, NCCU, Taipei, Taiwan, August 4-11 2010.

[53] K. P. Sokolowsky and M. D. Fayer. Dynamics in the isotropic phase of nematogens using 2d ir vibrational echo measurements on natural-abundance ^{13}cn and extended lifetime probes. *The Journal of Physical Chemistry B*, 117(48):15060–15071, 2013.

[54] K. P. Sokolowsky, H. E. Bailey, and M. D. Fayer. Length scales and structural dynamics in nematogen pseudonematic domains measured with 2d ir vibrational echoes and optical kerr effect experiments. *The Journal of Physical Chemistry B*, 118 (28):7856–7868, 2014.

[55] K. P. Sokolowsky, H. E. Bailey, and M. D. Fayer. New divergent dynamics in the isotropic to nematic phase transition of liquid crystals measured with 2d ir vibrational echo spectroscopy. *The Journal of Chemical Physics*, 141(19):194502, 2014.

[56] K. P. Sokolowsky, H. E. Bailey, D. J. Hoffman, H. C. Andersen, and M. D. Fayer. Critical slowing of density fluctuations approaching the isotropic nematic transition in liquid crystals: 2d ir measurements and mode coupling theory. *The Journal of Physical Chemistry B*, 120(28):7003–7015, 2016.

[57] J. J. Stankus, R. Torre, C. Marshall, S. Greenfield, A. Sengupta, A. Tokmakoff, and M. Fayer. Nanosecond time scale dynamics of pseudo-nematic domains in the isotropic phase of liquid crystals. *Chemical Physics Letters*, 194(3):213–216, 1992.

[58] T. W. Stinson III and J. D. Litster. Pretransitional phenomena in the isotropic phase of a nematic liquid crystal. *Phys. Rev. Lett.*, 25:503–506, Aug 1970.

[59] J. Tobochnik and G. V. Chester. Monte carlo study of the planar spin model. *Physical*

Review B, 20(9):3761–3769, 1979.

[60] H. Touchette. The large deviation approach to statistical mechanics. *Physics Reports*, 478(1-3):1–69, 2009.

[61] H. Vroylandt, K. Proesmans, and T. R. Gingrich. Isometric uncertainty relations. *Journal of Statistical Physics*, 178(4):1039–1053, Feb 2020.

[62] H. Yamakawa. Modern theory of polymer solutions. pages 14–15, 1971.

[63] Y. Zhao and R. M. Stratt. Measuring order in disordered systems and disorder in ordered systems: Random matrix theory for isotropic and nematic liquid crystals and its perspective on pseudo-nematic domains. *The Journal of chemical physics*, 148(20):204501, 2018.

[64] R. K. P. Zia, E. F. Redish, and S. R. McKay. Making sense of the Legendre transform. *American Journal of Physics*, 77(7):614–622, 07 2009.